

การปรับปรุงการเร่งปฏิกิริยาการเติมหมู่ไฮดรอกซิลบนฟินอลด้วยเหล็กรองรับ
ด้วย ZSM-5

นางสาวมัสดิกา พิมพ์สุตะ

วิทยานิพนธ์นี้เป็นส่วนหนึ่งของการศึกษาตามหลักสูตรปริญญาวิทยาศาสตรมหาบัณฑิต
สาขาวิชาเคมี
มหาวิทยาลัยเทคโนโลยีสุรนารี
ปีการศึกษา 2555

**IMPROVEMENT OF CATALYTIC PERFORMANCE FOR
PHENOL HYDROXYLATION BY IRON SUPPORTED ON
ZSM-5**

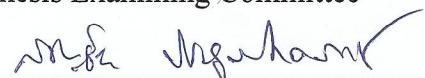
Mustika Pimsuta

**A Thesis Submitted in Partial Fulfillment of the Requirements for the
Degree of Master of Science in Chemistry
Suranaree University of Technology
Academic Year 2012**

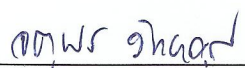
**IMPROVEMENT OF CATALYTIC PERFORMANCE FOR
PHENOL HYDROXYLATION BY IRON SUPPORTED ON ZSM-5**

Suranaree University of Technology has approved this thesis submitted in partial fulfillment of the requirements for a Master's Degree.

Thesis Examining Committee


(Asst. Prof. Dr. Sanchai Prayoonpokarach)

Chairperson


(Assoc. Prof. Dr. Jatuporn Wittayakun)

Member (Thesis Advisor)


(Asst. Prof. Dr. Visit Vao-soongnern)

Member


(Dr. Rapee Gosalawit-Utke)

Member


(Prof. Dr. Sukit Limpijumnong)

Vice Rector for Academic Affairs


(Assoc. Prof. Dr. Prapun Manyum)

Dean of Institute of Science

มัสติกา พิมพ์สุตะ : การปรับปรุงการเร่งปฏิกิริยาการเติมหมู่ไฮดรอกซิลบนฟีนอล
ด้วยเหล็กรองรับด้วย ZSM-5 (IMPROVEMENT OF CATALYTIC
PERFORMANCE FOR PHENOL HYDROXYLATION BY IRON SUPPORTED
ON ZSM-5) อาจารย์ที่ปรึกษา : รองศาสตราจารย์ ดร.จตุพร วิทยาคุณ, 126 หน้า.

ในวิทยานิพนธ์นี้ ได้สังเคราะห์ซีโอไลต์ NaZSM-5 ซึ่งเป็นวัสดุไมโครพอร์ส โดยใช้แหล่งซิลิกาจากแคลบข้าว แล้วทำการดัดแปรด้วยการกำจัดซิลิเกตออกจากโครงสร้างซีโอไลต์ทำให้เกิดมีโซพอร์ โดยไม่ทำลายโครงสร้างของซีโอไลต์ เมื่อนำซีโอไลต์ก่อนและหลังการดัดแปร (NaZSM-5 และ NaZSM-5(D)) ไปเป็นตัวรองรับสำหรับการเตรียมตัวเร่งปฏิกิริยาเหล็ก (Fe) ด้วยการทำให้เอิบชุ่มแบบเปียกพอดี้ แล้วนำไปเร่งปฏิกิริยาการเติมหมู่ไฮดรอกซิลบนฟีนอล การเพิ่มมีโซพอร์จะช่วยในการแพร่ของสารและทำให้การเร่งปฏิกิริยาดีขึ้น

เมื่อเปลี่ยน NaZSM-5 และ NaZSM-5(D) ให้อยู่ในรูปโปรตอน (HZSM-5 และ HZSM-5(D)) แล้วสมบัติทางกายภาพและเคมีไม่แตกต่างจากรูปเดิมอย่างมีนัยสำคัญ เมื่อนำซีโอไลต์ทั้งหมดไปเป็นตัวรองรับของ Fe ด้วยการทำให้เอิบชุ่มแบบเปียกพอดี้เช่นเดิม พบว่าการเร่งปฏิกิริยาของ Fe/HZSM-5(D) เกิดเร็วกว่า Fe/NaZSM-5(D) แสดงว่าการดูดซับของสารเกิดได้ดีกว่า อย่างไรก็ตาม การเลือกเกิดผลิตภัณฑ์ยังไม่ดีขึ้น อาจเป็นผลจากการเตรียมตัวเร่งปฏิกิริยาแบบเอิบชุ่ม ที่ทำให้เหล็กมีการกระจายตัวแบบลุ่ม ดังนั้น ในส่วนต่อไปจึงศึกษาผลของการเตรียมตัวเร่งปฏิกิริยา

ส่วนสุดท้าย คือการเตรียมตัวเร่งปฏิกิริยา Fe บน HZSM-5 และ HZSM-5(D) โดยการแลกเปลี่ยนไอออนในของเหลว (LS) และในของแข็ง (SS) พบว่าการเตรียมแบบ LS จะให้ค่าการแปลงผันของฟีนอลที่น้อยกว่าตัวเร่งปฏิกิริยาที่เตรียมแบบทำให้เอิบชุ่ม แต่ให้ค่าการเลือกเกิดผลิตภัณฑ์เหมือนเดิม การเตรียมโดยวิธี SS ให้การกระจายตัวของเหล็กไม่ดี ซึ่งดูได้จากการลดลงของพื้นที่ผิวและผลการเร่งปฏิกิริยา พบว่า $Fe_{SS}/HZSM-5$ ไม่สามารถผลิตสารผลิตภัณฑ์ ในขณะที่ $Fe_{SS}/HZSM-5(D)$ ให้สารผลิตภัณฑ์ที่เป็นแคทคอลลอยด์เดี่ยวแต่การดูดซับของฟีนอลต่ำ

MUSTIKA PIMSUTA : IMPROVEMENT OF CATALYTIC
PERFORMANCE FOR PHENOL HYDROXYLATION BY IRON
SUPPORTED ON ZSM-5. THESIS ADVISOR : ASSOC. PROF. JATUPORN
WITTAYAKUN, Ph.D. 126 PP.

PHENOL HYDROXYLATION/RICE HUSK SILICA/ZSM-5/ IRON/
DESILICATION

In this thesis NaZSM-5, a microporous material was synthesized by using rice husk silica source and modified by desilication to generate mesopores without destroying the zeolite structure. The modified and non-modified zeolites (NaZSM-5 and NaZSM-5(D)) were used as supports for preparation of Fe catalysts by incipient wetness impregnation. The catalysts were tested for phenol hydroxylation. The presence of mesopores could improve diffusion of reactants and thus, catalytic performance.

When NaZSM-5 and NaZSM-5(D) were converted to proton form, HZSM-5 and HZSM-5(D), respectively, physical and chemical properties of the proton forms did not change significantly from those of the parents. When all zeolites were used as the supports for Fe, also prepared by incipient wetness impregnation, the reaction on Fe/HZSM-5(D) was faster than Fe/NaZSM-5(D) likely because the higher adsorbed amount of reactants. However, the product selectivity was not improved probably because Fe species prepared by impregnation were in random positions. Consequently, effect of catalyst preparation method was studied.

Finally, Fe on HZSM-5 and HZSM-5(D) were prepared by liquid-state ion exchange (LS) and solid-state ion exchange (SS). The catalysts prepared by LS gave a

ACKNOWLEDGEMENT

I would like to thank everybody that helped me throughout my studies. First of all, I would like to thank my advisor, Assoc. Prof. Dr. Jatuporn Wittayakun, for sharing his knowledge with me, supporting in term of the finance, guiding me and editing my thesis. He taught me not only the subject matter, but also life lessons and this I appreciate very much. His encouragement, understanding and instruction are invaluable and I will treasure it. I am also thankful to the thesis examining committee, including Asst. Prof. Dr. Sanchai Prayoonpokarach, Asst. Prof. Dr. Visit Vao-soongnern, and Dr. Rapee Gosalawit-Utke for their helpful and valuable comments and suggestions during my thesis defense.

I would like to acknowledge the scholarship, Science Achievement Scholarship of Thailand, (SAST), from the Thai government and Synchrotron Light Research Institute. I would like to thank Asst. Prof. Dr. Arthit Nermittagapong from the Department of Chemical Engineering, Khon Kaen University, for his help with a gas chromatograph.

Finally, I would like to thank my family for their enduring love, support and encouragement. I would like to thank all of the friends in my catalysis group and my friend at Suranaree University of Technology, Mr. Chanintorn Ruangudomsakul, for their inspiration and Miss Talita Momsen for helping me to improve my English writing.

Mustika Pimsuta

CONTENTS

	Page
ABSTRACT IN THAI.....	I
ABSTRACT IN ENGLISH.....	II
ACKNOWLEDGEMENT.....	IV
CONTENTS.....	V
LIST OF TABLES.....	IX
LIST OF FIGURES.....	XI
LIST OF SCHEMES.....	XIV
CHAPTER	
I INTRODUCTION.....	1
1.1 Introduction.....	1
1.2 References.....	6
II LITERATURE REVIEW.....	8
2.1 Fe catalysts for phenol hydroxylation.....	8
2.2 Synthesis and modification of ZSM-5.....	14
2.3 Preparation of Fe/ZSM-5.....	17
2.4 References.....	19
III PHYSICOCHEMICAL PROPERTIES AND CATALYTIC PERFORMANCE OF IRON ON TYPICAL AND HIERACHICAL NaZSM-5 ON PHENOL HYDROXYLATION.....	23

CONTENTS (Continued)

		Page
3.1	Abstract.....	23
3.2	Introduction	24
3.3	Experimental	25
	3.3.1 Extraction of rice husk silica (RHS) and characterization.....	25
	3.3.2 Synthesis and desilication of NaZSM-5.....	26
	3.3.3 Preparation of supported Fe catalysts.....	28
	3.3.4 Catalytic testing for phenol hydroxylation.....	29
3.4	Results and discussion.....	31
	3.4.1 Characterization of rice husk silica (RHS).....	31
	3.4.2 Determination of the Si/Al of NaZSM-5 and NaZSM-5(D)....	33
	3.4.3 Catalysts characterization by XRD, ICP-MS and XANES.....	33
	3.4.4 Characterization by TEM.....	36
	3.4.5 Characterization by N ₂ adsorption-desorption.....	37
	3.4.6 Catalytic testing for phenol hydroxylation.....	41
3.5	Conclusions.....	44
3.6	References.....	44
IV	CHARACTERIZATION AND PERFORMANCE IN PHENOL	
	HYDROXYLATION OF IRON CATALYSTS SUPPORTED ON	
	HZSM-5 AND HZSM-5(D).....	47

CONTENTS (Continued)

		Page
4.1	Abstract.....	47
4.2	Introduction.....	48
4.3	Experimental.....	50
	4.3.1 Alkali treatment and conversion of NaZSM-5 to HZSM-5 by ion exchange.....	50
	4.3.2 Preparation of supported Fe catalysts.....	50
	4.3.3 Catalytic testing for phenol hydroxylation.....	51
4.4	Results and discussion.....	51
	4.4.1 Analysis by ICP-MS.....	51
	4.4.2 Analysis by XRD and XANES.....	51
	4.4.3 Analysis by TEM.....	55
	4.4.4 Analysis by N ₂ adsorption-desorption.....	59
	4.4.5 Catalytic performance for phenol hydroxylation.....	62
4.5	Conclusions.....	65
4.6	References.....	65
V	PREPARATION OF IRON CATALYSTS BY ION EXCHANGE FOR PHENOL HYDROXYLATION.....	68
5.1	Abstract.....	68
5.2	Introduction.....	69
5.3	Experimental.....	70

CONTENTS (Continued)

	Page
5.3.1 Preparation of ZSM-5 and Fe catalysts.....	70
5.4 Results and discussion.....	71
5.4.1 Analysis by XRD and ICP-MS.....	71
5.4.2 Analysis by TEM.....	74
5.4.3 Analysis by N ₂ adsorption-desorption.....	77
5.4.4 Catalytic testing for phenol hydroxylation.....	79
5.5 Conclusions.....	82
5.6 References.....	82
VI CONCLUSIONS AND RECOMMENDATION.....	84
APPENDICES.....	86
APPENDIX A Si/Al RATIOS AND THE AMOUNT OF Fe CATALYSTS ANALYZED BY ICP-MS.....	87
APPENDIX B DETERMINATION OF PRODUCTS AND REACTANTS FOR PHENOL HYDROXYLATION.....	97
APPENDIX C DATA FROM N ₂ ADSORPTION-DESORPTION.....	112
APPENDIX D THESIS OUTPUT.....	125
CURRICULUM VITAE.....	126

LIST OF TABLES

Table		Page
2.1	Examples of Fe catalysts, conditions, percent conversion of phenol, and percent selectivity for phenol hydroxylation.....	9
3.1	Composition of rice husk silica measured by XRF analysis.....	32
3.2	Percent of Fe species in calcined Fe/NaZSM-5 and Fe/NaZSM-5(D) analyzed by linear combination fit in Athena program.....	36
3.3	Results from N ₂ adsorption-desorption analysis.....	40
3.4	Product selectivity of Fe/NaZSM-5 and Fe/NaZSM-5 (D).....	43
4.1	Percent of Fe species in calcined Fe/HZSM-5 and Fe/HZSM-5(D) analyzed by linear combination fit in Athena program.....	55
4.2	Results from N ₂ adsorption-desorption analysis.....	61
4.3	Product selectivity of Fe/HZSM-5 and Fe/HZSM-5 (D).....	65
5.1	Results from N ₂ adsorption-desorption analysis.....	79
5.2	Product selectivity of all Fe catalysts.....	81
C-1	N ₂ adsorption-desorption of NaZSM-5.....	113
C-2	N ₂ adsorption-desorption of Fe/NaZSM-5.....	114
C-3	N ₂ adsorption-desorption of NaZSM-5(D).....	115
C-4	N ₂ adsorption-desorption of Fe/NaZSM-5(D).....	116
C-5	N ₂ adsorption-desorption of HZSM-5.....	117
C-6	N ₂ adsorption-desorption of Fe/HZSM-5.....	118
C-7	N ₂ adsorption-desorption of HZSM-5(D).....	119

LIST OF TABLES (Continued)

Table		Page
C-8	N ₂ adsorption-desorption of Fe/HZSM-5(D).....	120
C-9	N ₂ adsorption-desorption of Fe _{LS} /HZSM-5.....	121
C-10	N ₂ adsorption-desorption of Fe _{LS} /HZSM-5(D).....	122
C-11	N ₂ adsorption-desorption of Fe _{SS} /HZSM-5.....	123
C-12	N ₂ adsorption-desorption of Fe _{SS} /HZSM-5(D).....	124

LIST OF FIGURES

Figure		Page
3.1	XRD spectrum of rice husk silica.....	32
3.2	XRD patterns of NaZSM-5, Fe/NaZSM-5, NaZSM-5(D), and Fe/NaZSM-5(D).....	34
3.3	XANES spectra of (a) Fe standards: Fe foil, FeO, Fe ₃ O ₄ , Fe ₂ O ₃ , and (b) Fe catalysts: Fe/NaZSM-5, Fe/NaZSM-5(D) showing form of Fe as Fe ₂ O ₃	35
3.4	TEM micrographs of (a) NaZSM-5, (b) Fe/NaZSM-5, (c) NaZSM-5(D), and (d) Fe/NaZSM-5(D).....	37
3.5	N ₂ adsorption-desorption isotherm of NaZSM-5, Fe/NaZSM-5, NaZSM- 5(D), and Fe/NaZSM-5(D).....	39
3.6	BJH pore size distribution of NaZSM-5, Fe/NaZSM-5, NaZSM-5(D), and Fe/NaZSM-5(D).....	41
3.7	Phenol conversions of NaZSM-5, Fe/NaZSM-5, NaZSM-5(D), and Fe/NaZSM-5 (D).....	42
4.1	XRD patterns of HZSM-5, Fe/HZSM-5, HZSM-5(D), and Fe/HZSM- 5(D).....	52
4.2	XANES spectra of (a) Fe standards: Fe foil, FeO, Fe ₃ O ₄ , Fe ₂ O ₃ , and (b) Fe catalysts: Fe/HZSM-5 and Fe/HZSM-5(D) showing form of Fe as Fe ₂ O ₃	54

LIST OF FIGURES (Continued)

Figure	Page
4.3	TEM micrographs of (a) HZSM-5, (b) Fe/HZSM-5, (c) HZSM-5(D), and (d) Fe/HZSM-5(D)..... 57
4.4	TEM micrographs of Fe/HZSM-5(D) at 50 nm..... 58
4.5	TEM micrographs of sample Fe/HZSM-5(D) at 100 nm..... 58
4.6	TEM micrographs of Fe/HZSM-5(D) at 200 nm..... 59
4.7	N ₂ adsorption-desorption isotherms of HZSM-5, Fe/HZSM-5, HZSM-5(D), and Fe/HZSM-5(D)..... 60
4.8	BJH pore size distribution of HZSM-5, Fe/HZSM-5, HZSM-5(D), and Fe /HZSM-5(D)..... 62
4.9	Phenol conversions of HZSM-5, HZSM-5(D), Fe/HZSM-5, and Fe/HZSM-5 (D)..... 63
5.1	XRD patterns of (a) supports and Fe catalysts by liquid-state ion exchange (LS), (b) supports and Fe catalysts by solid-state ion exchange (SS)..... 73
5.2	TEM micrographs of Fe _{LS} /HZSM-5..... 75
5.3	TEM micrographs of Fe _{LS} /HZSM-5(D)..... 76
5.4	TEM micrographs (a) and (b) of Fe _{SS} /HZSM-5; (c) and (d) of Fe _{SS} /HZSM-5(D)..... 77
5.5	N ₂ adsorption-desorption isotherms of Fe _{LS} /HZSM-5, Fe _{LS} /HZSM-5(D), Fe _{SS} /HZSM-5, and Fe _{SS} /HZSM-5(D)..... 78

LIST OF FIGURES (Continued)

Figure	Page
5.6	Phenol conversions of Fe _{LS} /HZSM-5, Fe _{LS} /HZSM-5(D), Fe _{SS} /HZSM-5, and Fe _{SS} /HSZM-5(D)..... 80
A-1	External calibration curve of Fe standard measured by ICP-MS..... 91
A-2	External calibration curve of Si standard measured by ICP-MS..... 92
A-3	External calibration curve of Al standard measured by ICP-MS..... 93
B-1	Internal standard calibration curve of phenol for phenol hydroxylation.....106
B-2	Internal standard calibration curve of catechol for phenol hydroxylation.....107
B-3	Internal standard calibration curve of hydroquinone for phenol hydroxylation.....108
B-4	Internal standard calibration curve of para-benzoquinone for phenol hydroxylation.....109

LIST OF SCHEMES

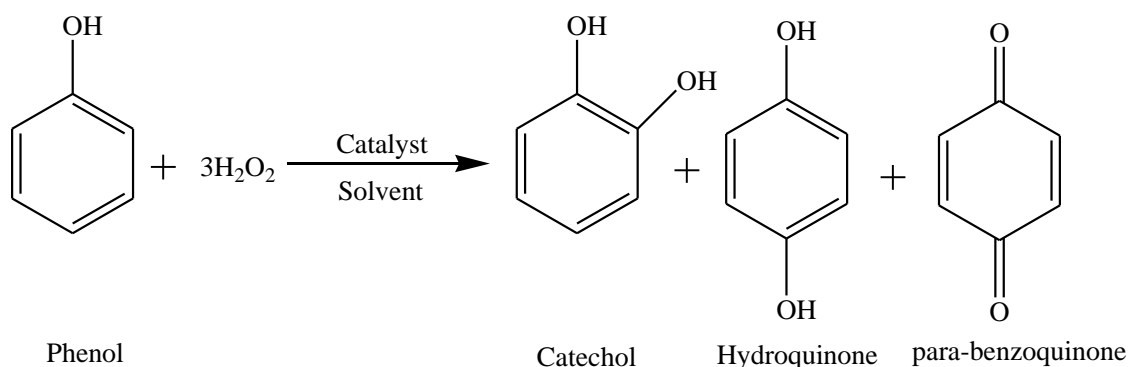
Scheme	Page
1.1 Phenol hydroxylation reaction to produce catechol (CAT), hydroquinone (HQ), and para-benzoquinone (PBQ).....	1
2.1 Mechanism of phenol hydroxylation to produce CAT on 10Fe/Al-MCM-41.....	11
2.2 Proposed mechanism of phenol hydroxylation with H ₂ O ₂ over 4Fe/MCM-41.....	12
2.3 The pore structure of ZSM-5 zeolite along xz and yz plane of (a) and (b), respectively; (c) the schematic diagram of 3D channels in ZSM-5.....	15
3.1 Proposed mechanism of desilication from zeolite framework by alkaline treatment (0.2 M NaOH solution).....	24
3.2 Apparatus setup for catalytic testing.....	30
4.1 Metal dispersed over the untreated (A) and alkali-treated (B) in HZSM-5 zeolite.....	49

CHAPTER I

INTRODUCTION

1.1 Introduction

Phenol hydroxylation is a reaction between phenol (C_6H_5OH) and hydrogen peroxide (H_2O_2). This reaction is ecologically friendly and can be achieved by the presence of a catalyst (Yu et al., 1999). The main products from this reaction are dihydroxybenzene isomers: catechol (CAT) and hydroquinone (HQ) as shown in Scheme 1.1. In addition, para-benzoquinone (PBQ) is produced from over-oxidation. CAT and HQ are used in such diverse applications as photographic chemicals, pesticide, antioxidants, flavoring agents, polymerization inhibitors, and starting materials for pharmaceuticals which are medicine, perfume, and many fine chemicals (Kannan et al., 2005).



Scheme 1.1 Phenol hydroxylation reaction to produce catechol (CAT), hydroquinone (HQ), and para-benzoquinone (PBQ).

CAT and HQ can be synthesized by several processes such as Rhône-Poulenc and Hamilton process in homogeneous system (Choi et al., 2006). In homogeneous catalysis, the catalyst, reactants and products are in the same phase, mainly in a solvent. Thus, the process is not suitable for a continuous operation due to difficulty in catalyst separation and recovery. Such problem could be avoided by using heterogeneous catalysis in which the catalyst and substrates are in different phases (Rothenberg et al., 2008).

In phenol hydroxylation Fe is widely used as a heterogeneous catalyst providing high phenol conversion and product selectivity. The reaction mechanism has been proposed by several researchers. Choi et al. (2006) suggested a mechanism involving $\text{Fe}^{3+}/\text{Fe}^{2+}$ redox pair to produce OH radical from H_2O_2 . Oxidation states of a transition metal in zeolite framework can be changed between +2 and +3. For phenol hydroxylation, the induction period of Fe-containing catalysts was usually about 5-15 mins before reaching the steady state due to depletion of H_2O_2 .

The performance of Fe catalysts depended on loading and type of support. Adam et al. (2010) studied an effect of Fe^{3+} loading on non-uniform mesoporous material, rice husk (RH) with various amount in the range of 5-20 wt.%. The results showed that 10 wt.% of the Fe supported on RH gave the highest conversion at 95.2% and selectivity for CAT and HQ at 61.3 and 38.7%, respectively. However, high amount of Fe (20 wt.%) resulted in pore blocking which lowered the reaction rate. Preethi et al. (2008) prepared 10 wt.% Fe on mordenite zeolite (MOR), a microporous materials but the 10Fe/MOR gave only 20.0% phenol conversion with only CAT as a product. Kulawong et al. (2011) further increased the conversion on Fe/MOR to 60.0% by generating mesopores in the support and only used 5wt.% Fe but another

by-product, PBQ was obtained along with CAT and HQ. Choi et al. (2006) used uniform mesoporous MCM-41 as a support for Fe particles and Fe₂O₃ nanoparticles with 0.5-4 wt.% of Fe. The catalytic testing of 4Fe/MCM-41 for phenol hydroxylation showed that 60.0% phenol conversion was obtained in 10 min and selectivity for CAT and HQ were 68.0 and 32.0%, respectively. Thus, the optimum Fe loading should be around 4-5 wt.% and the suitable support should contain mesopores.

Product selectivity could be improved by changing support to zeolite because its specific pore shape and size only allows molecules with similar shape and size to pass through. ZSM-5 is interesting as a support material for metal catalysts because it contains medium pore size of ~0.55 nm and pore network composes of straight and zigzag channels. The narrow pores of ZSM-5 are necessary for formation of CAT and HQ. Such property could improve the product selectivity (Song et al., 2004).

There was a report on using ZSM-5 as a support for Fe. Villa et al. (2005) reported that phenol hydroxylation over 1.47Fe/ZSM-5 gave a conversion of 32.9% in 4 h and selectivity for CAT and HQ at 60.5 and 39.5%, respectively. However, slow diffusion of reactants would result in adsorption in active sites of catalyst and subsequently polymerization which could block the pores and deactivate the catalyst. The diffusion of reactants to the metal active sites in the zeolite could be improved by generating mesopores in zeolite by desilication to remove some silicate in the framework by base. The resulting material is called hierarchical zeolite which combines micro- and mesoporosity. By desilication, surface area of the zeolite is increased, large pores are created and subsequently, the mass transport is improved (Abelló et al., 2009). Ogura et al. (2001) reported that creation of mesopores in ZSM-5

by a treatment with NaOH improved the adsorptive and diffusive properties for cracking of cumene.

In general, the metal species can be loaded on zeolite in proton form (H-form) by interacting with Brønsted acid sites. Song et al. (2009) prepared Pt on modified HZSM-5 desilicated with NaOH. For n-hexane isomerization, they observed an increase of dimethyl butanes (DMB), isomer products with the creation of mesopores. Desilication allowed a better accessibility to Al and thus, increased strength of Lewis acid sites. Higher loading of Pt was also possible after the zeolite desilication. Li et al. (2009) desilicated NaZSM-5 with NaOH and transformed to proton form before loaded with Zn by liquid state ion exchange and wet impregnation. The desilicated ZSM-5 had more Lewis acid site than the parent; the resulting catalysts had good metal dispersion and gave high products yield for 1-hexane aromatization. Because desilication can improve metal loading on zeolite, it is used in zeolite modification in this thesis.

The goal of this thesis was to improve catalytic performance of Fe supported on ZSM-5 for phenol hydroxylation. The ZSM-5 in sodium form (NaZSM-5) was synthesized by hydrothermal method using rice husk silica (RHS). Some of NaZSM-5 was transformed to proton form (HZSM-5) and some was modified by desilication with NaOH solution to generate mesopores. The obtained sample will be referred to as NaZSM-5(D). After desilication, the NaZSM-5(D) was transformed to proton form and referred to as HZSM-5(D). The presence of the mesopores in the zeolite was expected to facilitate diffusion of the starting reagents to active sites and improve catalytic performance for phenol hydroxylation. The ZSM-5 in various forms as

NaZSM-5, NaZSM-5(D), HZSM-5, and HZSM-5(D) were used as supports for Fe catalyst.

In addition, effect of Fe loading method including ion exchange and incipient wetness impregnation methods were studied. In ion exchange, Fe ion could replace zeolite charge-balancing ion at exchange position (Ertl et al., 1997). In incipient wetness impregnation, Fe ion can exchange with the charge-balancing ion in a similar manner as in ion exchange and with proton of OH groups in the zeolite channels (Kinger et al., 2000).

Properties of all ZSM-5 zeolites and catalysts were investigated by several techniques including X-ray diffraction (XRD) to confirm structure and crystallinity of the ZSM-5 zeolite and phase of supported Fe; X-ray fluorescence (XRF) to determine the elemental composition; inductively coupled plasma-mass spectrometry (ICP-MS) to determine Si/Al ratio; X-ray absorption near edge structure (XANES) to determine the oxidation number of the iron supported on ZSM-5 zeolite; and transmission electron microscopy (TEM) to observe the intracrystalline mesoporosity from the desilication and Fe metal clusters in catalysts. In addition, the samples were analyzed by nitrogen (N₂) adsorption-desorption to obtain adsorption isotherms, surface area and pore dimension.

Finally, all the ZSM-5 and supported Fe catalysts were tested for phenol hydroxylation in a batch reactor. The influences of desilication, forms of support for Fe loading and method of Fe loading on catalytic performance in phenol hydroxylation were investigated.

1.2 References

- Abelló, S., Bonilla, A., and Pérez-Ramírez, J. (2009). Mesoporous ZSM-5 zeolite catalysts prepared by desilication with organic hydroxides and comparison with NaOH leaching. **Appl. Catal. A: Gen.** 364: 191-198.
- Adam, F., Andas, J., and Rahman, I. A. (2010). A study on the oxidation of phenol by heterogeneous iron silica catalyst. **Chem. Eng. J.** 165: 658-667.
- Choi, J-S., Yoon, S-S., Jang, S-H., and Ahn, W-S. (2006). Phenol hydroxylation using Fe-MCM-41 catalysts. **Catal. Today.** 111: 280-287.
- Ertl, G., Knözinger, H., and Weitkamp, J. (1997). **Handbook of Heterogeneous Catalysis (vol.1)**. (pp. 191-194). Germany: VCH Verlagsgesellschaft mbH.
- Kannan, S., Dubey, A., and Knozinger, H. (2005). Synthesis and characterization of CuMgAl ternary hydrotalcites as catalysts for the hydroxylation of phenol. **J. Catal.** 231: 381-392.
- Kinger, G., Lugetein, A., Swagera, R., Ebel, M., Jentys, A., and Vinek, H. (2000). Comparison of impregnation, liquid- and solid-state ion exchange procedures for the incorporation of nickel in HMFI, HMOR and HBEA. **Micropor. Mesopor. Mat.** 39: 307-317.
- Kulawong, S., Prayoonpokarach, S., Neramittagapong, A., and Wittayakun, J. (2011). Mordenite modification and utilization as supports for iron catalyst in phenol hydroxylation. **J. Ind. Eng. Chem.** 17: 346-351.
- Li, Y., Liu, S., Xie, S., and Xu, L. (2009). Promoted metal utilization capacity of alkali-treated zeolite: Preparation of Zn/ZSM-5 and its application in 1-hexene aromatization. **Appl. Catal. A: Gen.** 360: 8-16.

- Ogura, M., Shinomiya, S-y., Tateno, J., Nara, Y., Nomura, M., Kikuchi, E., and Matsukata, M. (2001). Alkali-treatment technique-new method for modification of structure and acid-catalytic properties of ZSM-5 zeolite. **Appl. Catal. A: Gen.** 219: 33-43.
- Preethi, M. E. L., Revathi, S., Sivakumar, T., Manikandan, D., Divakar, D., Rupa, A. V., and Palanichami, M. (2008). Phenol hydroxylation using Fe/Al-MCM-41 catalysts. **Catal. Lett.** 120: 56-64.
- Rothenberg, G. (2008). **Catalysis Concepts and Green Applications.** (pp. 66-67). Germany: WILEY-VCH Verlag GmbH & Co. KGaA.
- Song, W., Justice, R. E., Jones, C. A., Grassian, V. H., and Larsen, S. C. (2004). Synthesis, characterization, and adsorption properties of nanocrystalline ZSM-5. **Langmuir.** 20: 8301-8306.
- Song, Y-Q., Feng, Y-L., Lui, F., Kang, C-L., Zhou, X-L., Xu, L-Y., and Yu, G-X. (2009). Effect of variations in pore structure and acidity of alkali treated ZSM-5 on the isomerization performance. **J. Mol. Catal. A: Chem.** 310: 130-137.
- Villa, A. L., Caro, C. A., and de Correa, C. M. (2005). Cu- and Fe-ZSM-5 as catalysts for phenol hydroxylation. **J. Mol. Catal. A: Chem.** 228: 233-240.
- Yu, R., Xiao, F-S., Wang, D., Sun, J., Liu, Y., Pang, G., Feng, S., Qiu, S., Xu, R., and Fang, C. (1999). Catalytic performance in phenol hydroxylation by hydrogen peroxide over a catalyst of V-Zr-O complex. **Catal. Today.** 51: 39-46.

CHAPTER II

LITERATURE REVIEW

This chapter provides literature reviews on three aspects: Fe catalysts for phenol hydroxylation, synthesis and modification of ZSM-5, and preparation of Fe/ZSM-5.

2.1 Fe catalysts for phenol hydroxylation

Fe is widely used as a heterogeneous catalyst in phenol hydroxylation, providing a high phenol conversion and product selectivity. The reaction depends on type of support materials. Preethi et al., 2008 prepared 10 wt.%Fe on mesoporous material (Al-MCM-41) and microporous material (MOR) at the same condition. 10Fe/Al-MCM-41 gave a higher phenol conversion than 10Fe/MOR but 10Fe/MOR showed selectivity to CAT only. With the same reaction condition, type of support has influence on phenol conversion and product selectivity.

Table 2.1 shows Fe catalysts on various supports for phenol hydroxylation (Liu et al., 2006; Adam et al., 2010; Chumee et al., 2009; Choi et al., 2006; Preethi et al., 2008; Kulawong et al., 2011; Liu et al., 1996; Villa et al., 2005). Homogeneous $\text{Fe}(\text{phen})_3^{2+}$ catalyst was compared with heterogeneous 4Fe/MCM-41 at similar reaction condition (Liu et al., 1996 and Choi et al., 2006). The result showed that 4Fe/MCM-41 gave higher phenol conversion than $\text{Fe}(\text{phen})_3^{2+}$ and water was the best solvent. The active species $\cdot\text{OH}$ and OH^- in reaction system could be produced and

dispersed in water more easily than in organic solvents including cyclohexane, acetone, and acetonitrile.

Many researchers investigated phenol hydroxylation over homogeneous and heterogeneous Fe catalyst on different supports. The reaction condition under high temperature and high mole ratio of H₂O₂ was interesting because it gave high phenol conversion. Over Fe/ZSM-5, the lowest amount of Fe was used and low conversion.

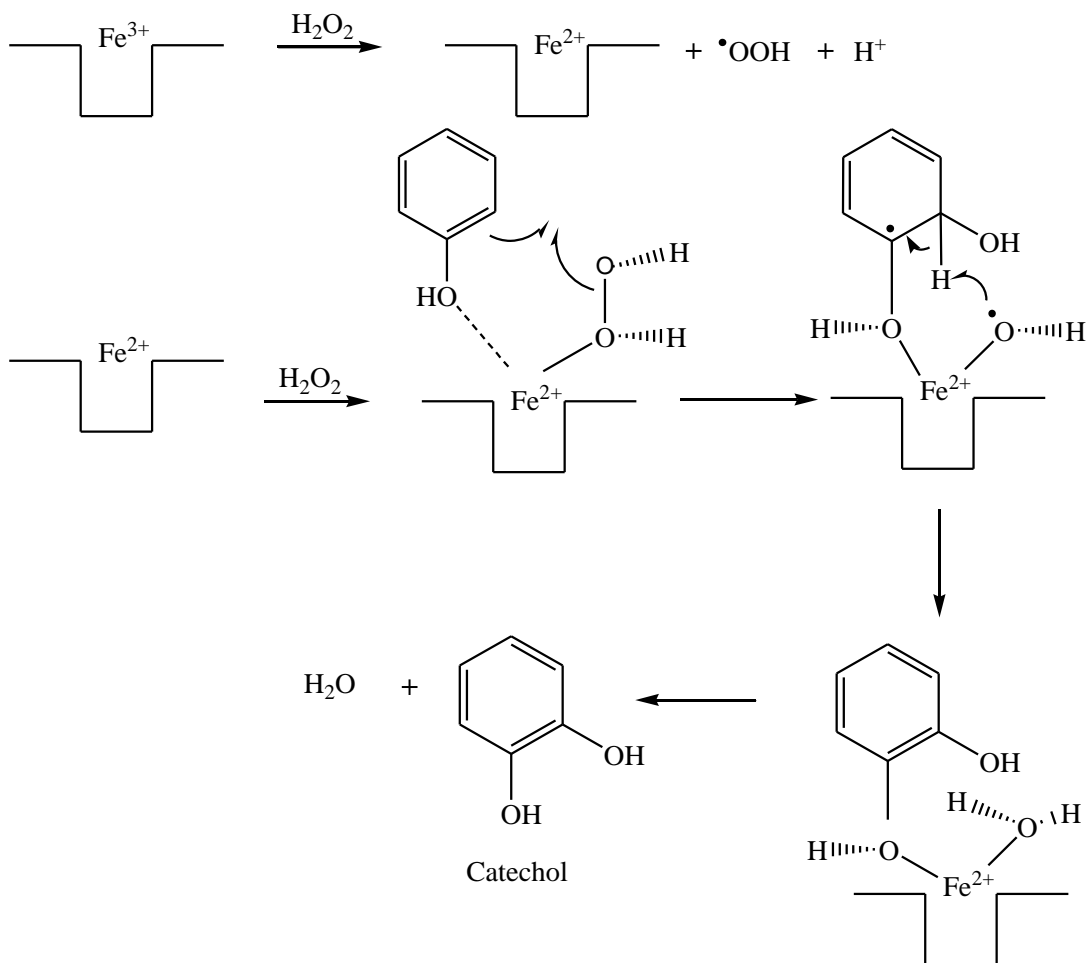
Table 2.1 Examples of Fe catalysts, conditions, percent conversion of phenol, and percent selectivity for phenol hydroxylation.

Catalyst	Temperature, solvent	Phenol:H ₂ O ₂	% Conversion of phenol	% Selectivity			Reference
				CAT	HQ	PBQ	
Fe(phen) ₃ ²⁺	40°C, water	1:1	29.5	70.0	28.2	1.8	Liu et al. (1996)
4Fe/MCM-41	50°C, water	1:1	60.0	68.0	32.0	0.0	Choi et al. (2006)
10Fe/Al-MCM-41	40°C, water	1:3	58.5	38.9	61.1	0.0	Preethi et al. (2008)
10Fe/MOR	40°C, water	1:3	20.7	100.0	0.0	0.0	Preethi et al. (2008)
5Fe/ABMOR	70°C, water	1:3	60.0	57.5	42.5	0.0	Kulawong et al. (2011)
5Fe0.5Pt/RH-MCM-41	70°C, water	2:3	47.0	54.6	46.4	0.0	Chumee et al. (2009)
10Fe/RH	70°C, water	1:2	95.2	61.3	38.7	0.0	Adam et al. (2010)
2.7Fe/HMS	84°C, water	3:1	20.6	61.0	37.7	1.3	Liu et al. (2006)
1.47Fe/ZSM-5	80°C, water	3:1	32.9	60.5	39.5	0.0	Villa et al. (2005)

The reaction time, reaction temperature, the nature of the solvent and molar ratio of phenol: H_2O_2 were found to be major factors for phenol conversion and product selectivity (Yu et al., 1999).

Preethi et al. (2008) synthesized Al-MCM-41 with Si/Al ratios of 25, 50, 75, and 100 by hydrothermal method and loaded with 10 wt.%Fe by wet impregnation. Liquid phase hydroxylation with the phenol: H_2O_2 ratio in range of 1:1 to 1:5 and optimum condition over highly acidic Fe/Al-MCM-41(25) was 1:3 at 40°C. Higher selectivity to hydroquinone over all Fe/Al-MCM-41 catalysts suggests preferential adsorption of H_2O_2 on Fe^{3+} site leaving more phenol in the unadsorbed state which was a requirement for parahydroxylation. Fe/Al-MCM-41 was more hydrophilic than MCM-41 and favored both chemisorption of H_2O_2 and phenol on the active site. Because $\cdot\text{OH}$ radical is highly polar and small, it could be chemisorbed on Fe/Al-MCM-41. The reaction between free phenol and adsorbed hydroxyl radical could yield HQ selectively. This result has different from the result of Choi et al. (2006) which studied the same reaction over Fe/MCM-41 by hydrothermal method. The products were selective to CAT higher than HQ.

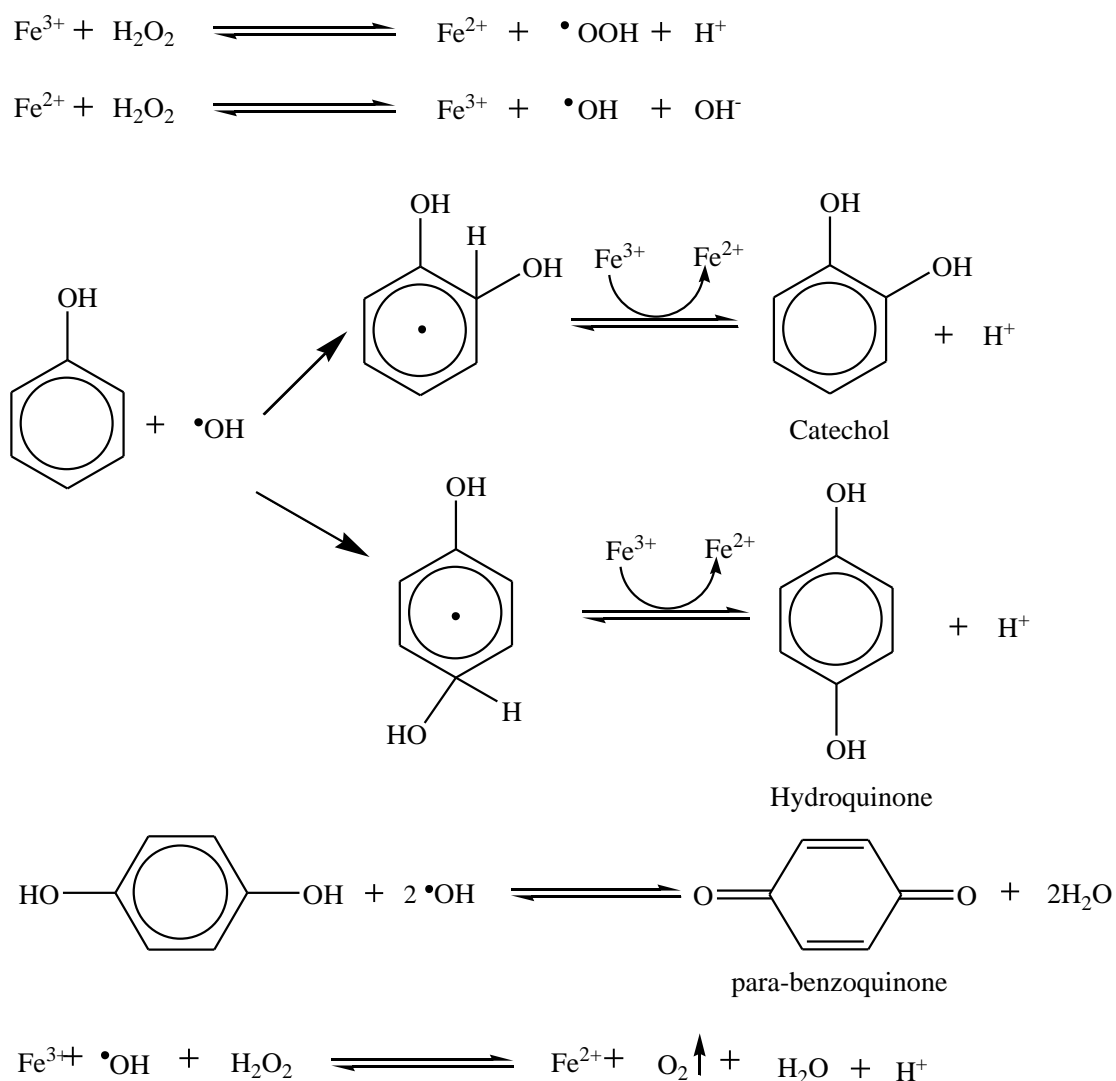
The activity followed the order of acidity: Fe/Al-MCM-41 (25) > Fe/Al-MCM-41 (50) > Fe/Al-MCM-41 (75) > Fe/Al-MCM-41 (100). They proposed the mechanism of CAT which favored CAT formation do to thermodynamic. Both phenol and H_2O_2 adsorbed on the same active site as described in Scheme 2.1. This Scheme provides understanding in mechanism of phenol hydroxylation to produce CAT over highly acidic catalyst.



Scheme 2.1 Mechanism of phenol hydroxylation to produce CAT on 10Fe/Al-MCM-41 (Preethi et al., 2008).

Choi et al. (2006) synthesized highly ordered Fe-containing MCM-41 with 0.5-4 mol% Fe by hydrothermal method. The Fe-MCM-41 exhibited high catalytic activity in phenol hydroxylation using H_2O_2 as an oxidant. The amount of Fe species gave phenol conversion in a shorter reaction time because of the decomposition of H_2O_2 and phenol adsorbed on the Fe species (Li et al., 2011). The mechanism of phenol hydroxylation was proposed as shown in Scheme 2.2. In this case, HQ selectivity was lower than CAT. H_2O_2 decomposed to hydroxyl radicals ($\cdot\text{OH}$) with Fe^{2+} or Fe^{3+}

redox pairs. The reaction between $\cdot\text{OH}$ and phenol leads to the formation of CAT and HQ. The $\cdot\text{OH}$ can further react with HQ to produced PBQ; the condensation of PBQ can also lead to a tarry by-product. However, this mechanism did not illustrate the phenol and H_2O_2 adsorption on Fe catalyst.



Scheme 2.2 Proposed mechanism of phenol hydroxylation with H_2O_2 over 4Fe/MCM-41 (Choi et al., 2006).

Comparing between the work of Chumee et al. (2009) and Kulawong et al. (2011), different phenol:H₂O₂ mole ratio between 2:3 and 1:3 had no significant effect on conversion and product selectivity.

At high temperature and high the amount of Fe loading on rice husk silica; Liu et al. (2006) synthesized Fe-incorporated in hexagonal mesoporous silica (Fe/HMS). After calcination, most of the Fe³⁺ ions remained in the tetrahedral coordinated framework and only a small part of Fe species migrated to the extraframework. Its catalytic performance for phenol hydroxylation with H₂O₂ was studied in a fix-bed reactor. The mesoporous pore size of Fe/HMS is much larger than that of dihydroxybenzene, so the pores of Fe/HMS have non-shape selectivity. As a result, an excess of CAT was observed on Fe/HMS catalyst which was thermodynamically isomer.

Adam et al. (2010) synthesized Fe-incorporated in rice husk (Fe/RH) with various the amount of Fe in the range of 5-20 wt.% and explained the role of solvents as water, acetonitrile, methanol, and dioxane. The water was the best solvent. When Fe³⁺ loading more than 10 wt.% resulted in smaller pore size and more extraframework Fe³⁺ in the catalyst and low activity in phenol hydroxylation. The liquid phase hydroxylation with the phenol: H₂O₂ ratio of 1:2 was studied. They studied reaction temperature in the range of 30-80°C and found that 70°C gave high phenol conversion. When the temperature was more than 70°C, the phenol conversion did not change significantly. At this condition benzoquinone was not observed.

From literature review, the reaction was done at various temperatures and phenol:H₂O₂ ratios. The conversion of phenol over Fe/ZSM-5 could be improved by increasing Fe loading or changing catalyst preparation method.

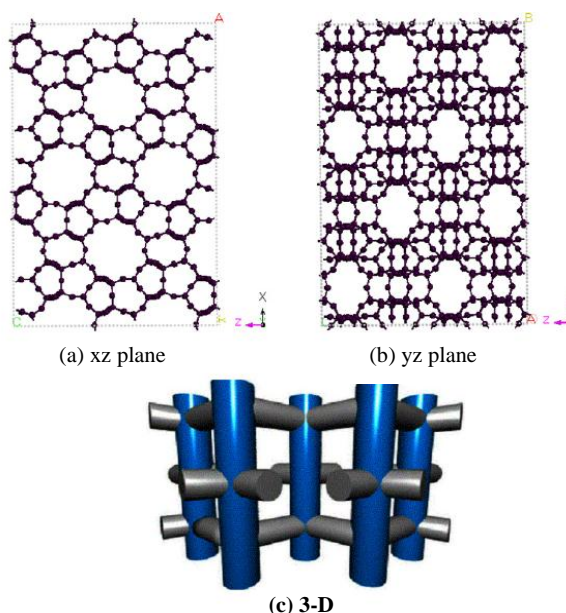
Villa et al. (2005) synthesized Fe catalysts on ZSM-5 by hydrothermal method with ammonium fluoride (NH_4F) as a mineralizing agent in the synthesis gel. The Fe content was varied between 0 and 1.8 wt.%. The Fe containing ZSM-5 had Fe^{3+} in the zeolite framework. The highest CAT was obtained over low Si/Fe loaded on ZSM-5. However, the most active Fe/ZSM-5 catalyst contained extraframework Fe and the presence of Al was required to obtain high phenol conversion.

Mesoporous materials (RHS and MCM-41) have large pore sizes which allow phenol to diffuse and adsorb more easily than microporous materials (MOR and ZSM-5). However, selectivity in phenol hydroxylation could be improved by using ZSM-5 because the pore size of ZSM-5 matched well with the molecular size of reactants and products for phenol hydroxylation.

2.2 Synthesis and modification of ZSM-5

The ZSM-5 is widely used as a heterogeneous catalyst in various reactions such as catalytic cracking, alkylation, isomerization and phenol hydroxylation (Abelló et al., 2009) because it has both Lewis and Brønsted acid sites. ZSM-5 is one example of MFI framework type. Furthermore, The ZSM-5 is interesting as a support material for Fe catalysts for phenol hydroxylation because it contains medium pore size of ~ 0.55 nm and a pore network composed of straight and zigzag channels. The most stable of extraframework mononuclear Fe species was in the straight and zigzag channels (Li et al., 2011). A straight channel has dimension of 0.53 nm x 0.56 nm along the xz plane as shown in Scheme 2.3 (a). The zigzag channel has of dimension of 0.51 nm x 0.55 nm along the yz plane as in Scheme 2.3 (b). In addition, the

schematic diagram of the ZSM-5 channels is shown in Scheme 2.3 (c) (Chen et al., 2007).



Scheme 2.3 The pore structure of ZSM-5 zeolite along xz and yz plane of (a) and (b), respectively; (c) the schematic diagram of 3D channels in ZSM-5 (Chen et al., 2007).

ZSM-5 can be synthesized by using several raw materials such as lignite fly ash from the Mae-Moh Powder Plant, rice husk ash (RHA) and rice husk silica (RHS) (Chareonpanich et al., 2004). Parameters in the synthesis included factors of $\text{SiO}_2/\text{Al}_2\text{O}_3$ mole ratio, temperature, pressure, and time.

Kim et al. (1998) synthesized ZSM-5 by using colloidal silica as a silica source and temperature at 100°C and atmospheric pressure in a batch reactor for 72 h. The crystallinity was 70% and average BET surface area was $371 \text{ m}^2/\text{g}$.

Kulkarni et al. (2002) prepared seeding gel for synthesis of ZSM-5 and using tetraethoxysilane as a silica source in autoclave under high pressure (40-60 atm) with various solvents including methanol, acetonitrile, isopropanol and water. The

resulting ZSM-5 synthesized by using water as a solvent had the highest surface area and crystallinity of 83%.

Rice husk was utilized as an alternative silica source for the synthesis of ZSM-5 because it has high silica content. Kordatos et al. (2008) synthesized ZSM-5 by using RHA which was prepared at 700°C for 5 h as a silica source. They mixed RHA with the organic template, TPABr at 110°C under atmospheric pressure for 11 days to produce ZSM-5.

Panpa and Jinawath (2009) synthesized ZSM-5 using RHS under hydrothermal treatment at 150°C with a short reaction time (4-24 h) and varied SiO₂/Al₂O₃ gel molar ratios in the range of 30-2075. The maximum zeolite yield was 84% with SiO₂/Al₂O₃ molar ratio of 80 but a transition of ZSM-5 to silicalite occurred when the SiO₂/Al₂O₃ molar ratio was higher than 200. The product from the SiO₂/Al₂O₃ molar ratio of 80 had BET surface area of 306 m²/g.

Diffusion of reactants to metal active sites in zeolites could be improved by generating mesopores by desilication. The resulting materials are often called “hierarchical zeolites” which combine microporosity and mesoporosity. When mesopores were created in ZSM-5 by desilication, the surface area of the zeolite was increased (Ogura et al., 2001; Groen et al., 2004).

Abelló et al. (2009) created mesopores in NaZSM-5 by desilication using tetrapropylammonium hydroxide (TPAOH), tetrabutylammonium hydroxide (TBAOH) and NaOH. The TPAOH was effective to generate mesoporous zeolite without changing the structure and increase mesopore surface areas from 60 to 160 m²/g. The catalytic performance of benzene alkylation with ethylene in liquid-phase was improved.

Groen et al. (2004), Abelló et al. (2009) and Caicedo-Realpe et al. (2010) created mesopores in the framework of ZSM-5 in ammonium form ($\text{NH}_4\text{-ZSM-5}$) with $\text{SiO}_2/\text{Al}_2\text{O}_3$ ratio in range of 37-42 by using 0.2 M NaOH at 65°C for 30 min and then converted to proton form. The results showed that silicate was dissolved fast in NaOH solution and the surface area of ZSM-5 increased after desilication. Pore size of ZSM-5 after desilication was around 10 nm.

Li et al. (2009) desilicated NaZSM-5 with Si/Al ratio of 27.1 by using 0.5 M NaOH at 75°C for 2 h and then converted to proton form. The non-treated and treated NaZSM-5 were used as supports for Zn catalyst by liquid-state ion exchange (LS) and incipient wetness impregnation (IMP) methods. Comparison between non-treated and treated NaZSM-5, treated NaZSM-5 exhibited higher Zn-loading in LS, better metal distribution and more Lewis acid sites in IMP, owing to the location of Zn species in the created mesopores. The majority of pore size distribution was at about 10 nm. So the counter cation (NH_4^+ , Na^+) had a minor influence to formation of mesopores in ZSM-5 by desilication.

From all literature reviews, this thesis aimed to synthesize ZSM-5 by using RHS and modify the zeolite by desilication to generate mesopores.

2.3 Preparation of Fe/ZSM-5

Catalytic performance in phenol hydroxylation can be improved by loading Fe on the support. Fe/ZSM-5 could be prepared by several methods; each method has effect on the amount and location of Fe species. High amount of Fe could improve phenol conversion and product selectivity.

In this work, NaZSM-5, NaZSM-5(D), HZSM-5, and HZSM-5(D) were loaded with Fe by IMP. Only the proton form, HZSM-5, HZSM-5(D) were used as support for Fe loading by LS from $\text{Fe}(\text{NO}_3)_3 \cdot 9\text{H}_2\text{O}$, and SS from FeCl_3 .

Long and Yang (2001) prepared Fe catalysts with Si/Al ratio of 10 for selective catalytic reduction (SCR) with ammonia by using four different methods: LS from $\text{FeCl}_2 \cdot 4\text{H}_2\text{O}$, improved aqueous-exchange (IA) from $\text{FeCl}_2 \cdot 4\text{H}_2\text{O}$, SS from $\text{FeCl}_2 \cdot 4\text{H}_2\text{O}$, and chemical vapor ion-exchange (CVD) from FeCl_3 . All of the Fe/ZSM-5 catalysts showed very high activities which were ranged in the following sequence: Fe/ZSM-5 (IA) > Fe/ZSM-5 (LS), Fe/ZSM-5 (SS) > Fe/ZSM-5 (CVD). ESR results indicated that Fe^{3+} ions with tetrahedral coordination are the active sites for SCR.

Guzmán-Vargas et al. (2005) studied the influence of preparation method of Fe/ZSM-5 with Si/Al ratio of 15 for the SCR of NO_x by *n*-decane. The catalysts were prepared by CVD and SS method from FeCl_3 , ligand exchange (LE) from iron acetylacetonate in toluene, and IMP or LS with iron nitrate in water. The amounts of Fe content were in the following order: SS (4.4 wt.%) > LE (4.2 wt.%) > IMP (3.9 wt.%) > CVD (3.8 wt.%) > IE (1.6 wt.%). The catalysts prepared by CVD from FeCl_3 and by LE from iron acetylacetonate in toluene were the most efficient for SCR of NO_x by *n*-decane.

Because the method for Fe loading on ZSM-5 had influence on Fe content, Fe was loaded on ZSM-5 by IMP, LS, and SS for catalytic performance testing in phenol hydroxylation.

2.4 References

- Abelló, S., Bonilla, A., and Pérez-Ramírez, J. (2009). Mesoporous ZSM-5 zeolite catalysts prepared by desilication with organic hydroxides and comparison with NaOH leaching. **Appl. Catal. A: Gen.** 364: 191-198.
- Adam, F., Andas, J., and Rahman, I. A. (2010). A study on the oxidation of phenol by heterogeneous iron silica catalyst. **Chem. Eng. J.** 165: 658-667.
- Caicedo-Realpe, R. and Pérez-Ramírez, J. (2010). Mesoporous ZSM-5 zeolites prepared by a two-step route comprising sodium aluminate and acid treatments. **Micropor. Mesopor. Mat.** 128: 91-100.
- Chareonpanich, M., Namto, T., Kongkachuichay, P., and Limtrakul, J. (2004). Synthesis of ZSM-5 zeolite from lignite fly ash and rice husk ash. **Fuel. Process. Technol.** 85: 1623-1634.
- Chen, X., Huang, S., Cao, D., and Wang, W. (2007). Optimal feed ratio of benzene-propylene binary mixtures for alkylation in ZSM-5 by molecular simulation. **Flu. Phase. Eq.** 260:146-152.
- Choi, J-S., Yoon, S-S., Jang, S-H., and Ahn, W-S. (2006). Phenol hydroxylation using Fe-MCM-41 catalysts. **Catal. Today.** 111: 280-287.
- Chumee, J., Grisdanurak, N., Neramittagapong, A., and Wittayakun, J. (2009). Characterization of platinum-iron catalysts supported on MCM-41 synthesized with rice husk silica and their performance for phenol hydroxylation. **Sci. Technol. Adv. Mat.** 10: 015006.

- Groen, J. C., Peffer, L. A. A., Moulijn, J. A., and Pérez-Ramírez, J. (2004). Mesoporosity development in ZSM-5 zeolite upon optimized desilication conditions in alkaline medium. **Colloid. Surface A.** 69: 29-34.
- Guzmán-Vargas, A., Delahay, G., Coq, B., Lima, E., Bosch, P., and Jumas, J-C. (2005). Influence of the preparation method on the properties of Fe-ZSM-5 for the selective catalytic reduction of NO by *n*-decane. **Catal. Today.** 107-108: 94-99.
- Kim, W. J., Lee, M. C., and Hayhurst, D. T. (1998). Synthesis of ZSM-5 at low temperature and atmospheric pressure in a pilot-scale batch reactor. **Micropor. Mesopor. Mat.** 26: 133-141.
- Kordatos, K., Gavela, S., Ntziouni, A., Pistiolas, K. N., Kyritsi, A., and Kasselouri-Rigopoulou, V. (2008). Synthesis of highly siliceous ZSM-5 zeolite using silica from rice husk ash. **Micropor. Mesopor. Mat.** 115: 189-196.
- Kulawong, S., Prayoonpokarach, S., Neramittagapong, A., and Wittayakun, J. (2011). Mordenite modification and utilization as supports for iron catalyst in phenol hydroxylation. **J. Ind. Eng. Chem.** 17: 346-351.
- Kulkarni, S. J., Srinivasu, P., Narender, N., and Raghavan, K. V. (2002). Fast and efficient synthesis of ZSM-5 under high pressure. **Catal. Commun.** 3:113-117.
- Li, Y., Liu, S., Xie, S., and Xu, L. (2009). Promoted metal utilization capacity of alkali-treated zeolite: Preparation of Zn/ZSM-5 and its application in 1-hexene aromatization. **Appl. Catal. A: Gen.** 360: 8-16.

- Li, G., Pidko, E. A., van Santen, R. A., Feng, Z., Li, C., and Hensen, E. J. M. (2011). Stability and reactivity of active sites for direct benzene oxidation to phenol in Fe/ZSM-5: A comprehensive periodic DFT study. **J. Catal.** 284: 194-206.
- Liu, C., Ye, X., Zhan, R., and Wu, Y. (1996). Phenol hydroxylation iron(II) phenanthroline: The reaction mechanism. **J. Mol. Catal. A: Chem.** 112: 15-22.
- Liu, H., Lu, G., Guo, Y., Guo, Y., and Wang, J. (2006). Synthesis of framework-substituted Fe-HMS and its catalytic performance for phenol hydroxylation. **Nanotechnol.** 17: 997-1003.
- Long, R. Q. and Yang, R. T. (2001). Fe-ZSM-5 for selective catalytic reduction of NO with NH₃: a comparative study of different preparation techniques. **Catal. Lett.** 74: 201-205.
- Ogura, M., Shinomiya, S-y., Tateno, J., Nara, Y., Nomura, M., Kikuchi, E., and Matsukata, M. (2001). Alkali-treatment technique-new method for modification of structure and acid-catalytic properties of ZSM-5 zeolite. **Appl. Catal. A: Gen.** 219: 33-43.
- Panpa, W. and Jinawath, S. (2009). Synthesis of ZSM-5 zeolite and silicalite from rice husk ash. **Appl. Catal. B: Environ.** 90: 389-394.
- Preethi, M. E. L., Revathi, S., Sivakumar, T., Manikandan, D., Divakar, D., Rupa, A. V., and Palanichami, M. (2008). Phenol hydroxylation using Fe/Al-MCM-41 catalysts. **Catal. Lett.** 120: 56-64.
- Villa, A. L., Caro, C. A., and de Correa, C. M. (2005). Cu- and Fe-ZSM-5 as catalysts for phenol hydroxylation. **J. Mol. Catal. A: Chem.** 228: 233-240.

Yu, R., Xiao, F-S., Wang, D., Sun, J., Liu, Y., Pang, G., Feng, S., Qiu, S., Xu, R., and Fang, C. (1999). Catalytic performance in phenol hydroxylation by hydrogen peroxide over a catalyst of V-Zr-O complex. **Catal. Today.** 51: 39-46.

CHAPTER III

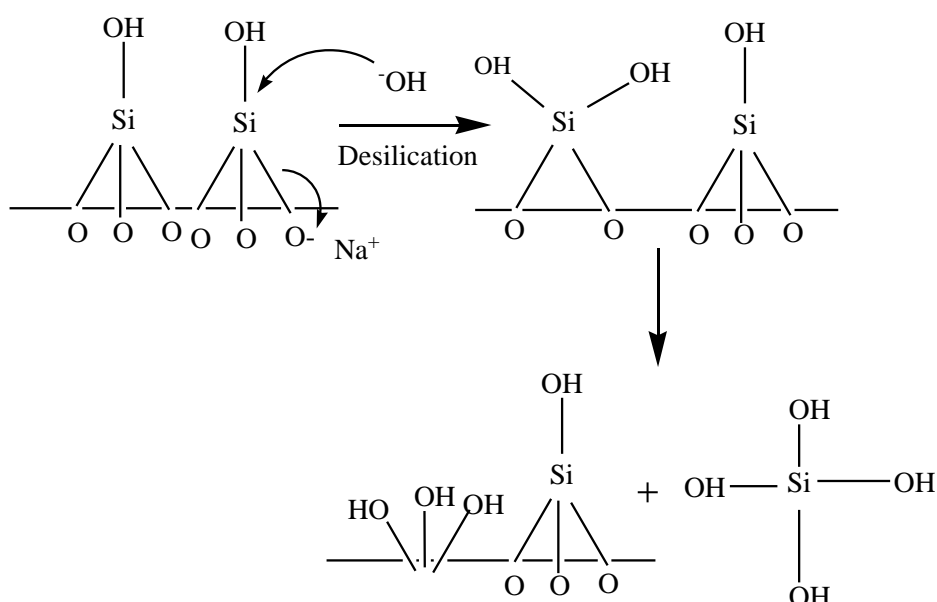
PHYSICOCHEMICAL PROPERTIES AND CATALYTIC PERFORMANCE OF IRON ON TYPICAL AND HIERARCHICAL NaZSM-5 ON PHENOL HYDROXYLATION

3.1 Abstract

NaZSM-5 was synthesized by a hydrothermal method using rice husk silica and modified by desilication with NaOH solution to generate mesopores. The removal of silicon atoms were confirmed by the decrease of Si/Al ratio from ICP-MS analysis. Both the parent and desilicated NaZSM-5 were used as support materials for Fe for phenol hydroxylation. All the supports and catalysts were characterized by XRD, TEM, and N₂ adsorption-desorption to confirm the zeolite structure, observe morphology and determine surface area and pore size distribution, respectively. Desilication did not destroy the zeolite structure but generated non-uniform mesopores and increased surface area. The oxidation state of Fe, analyzed by XANES was +3. Catalytic performance of Fe on NaZSM-5 and Fe on NaZSM-5(D) for phenol hydroxylation in a batch reactor using H₂O₂ as an oxidant, gave phenol conversion of ca. 67% at 70°C [phenol: H₂O₂ = 1:3]. The Fe/NaZSM-5(D) showed a faster phenol conversion to reach equilibrium. Products from both catalysts were catechol and hydroquinone with mole ratio about 2:1.

3.2 Introduction

This chapter focuses on synthesis of NaZSM-5 by using rice husk silica (RHS), modification by desilication using NaOH to produce NaZSM-5(D) and utilization of both NaZSM-5 and NaZSM-5(D) as supports for Fe catalyst. A possible mechanism of desilication from the zeolite framework modified from Groen et al. (2007) as shown in Scheme 3.1.



Scheme 3.1 Proposed mechanism of desilication from zeolite framework by alkaline treatment (0.2 M NaOH solution). Modified from Groen et al. (2007).

This mechanism modified from Groen et al. (2007) which appeared to exist for the sample treated with NaOH. Hydroxide anions attack to silicon extraction and sodium cations (Na^+) stabilized silicate anions in zeolite framework. The Na ions are strongly solvated in aqueous solution, due to their large effective cationic diameter ($\text{Na}^+ = 0.19 \text{ nm}$) and high hydration enthalpy of 406 kJ/mol, causing the attraction of

high water molecules. High efficiency of NaOH can be assumed to improve mesoporosity for each other (Abelló et al., 2009).

Framework aluminium prevents framework silicon from extraction and makes desilication selective towards mesopore formation (Groen et al., 2005). After desilication micropores were still remained and mesopores were generated. Then, surface area increased and diffusion of reactants was improved. Improvement in catalytic performance in the liquid-phase alkylation of benzene with ethylene mesoporous zeolite (97%) was higher than parent zeolite (90%) (Abelló et al., 2009).

Details of this chapter include synthesis of NaZSM-5 by hydrothermal method, modification by desilication with NaOH solution, preparation of Fe catalyst and characterization by X-ray diffraction (XRD) to confirm ZSM-5 structure. Oxidation state of the Fe was determined by X-ray absorption near edge structure (XANES). The morphology was studied by transmission electron microscopy (TEM). Adsorption-desorption isotherm and surface area were obtained from the N₂ adsorption analysis. All of the samples were tested in phenol hydroxylation.

3.3 Experimental

3.3.1 Extraction of rice husk silica (RHS) and characterization

RHS was prepared by a procedure from literature (Khemthong et al., 2007). Rice husk was washed with water to remove the soil and dust and dried at 100°C overnight in a hot-air oven. The dried rice husk was refluxed with 3 M HCl solution (prepared from 37%, Carlo Erba) at 85°C for 6 h, the ratio of RH:HCl solution was 85.0 g:700.0 ml. Then the sample was filtered and washed several times with water until pH was neutral. Then the sample was dried at 100°C overnight in a hot-air oven.

The refluxed rice husk was pyrolyzed in a muffle furnace at 550°C for 6 h. The obtained white powder was RHS.

Composition of the RHS was determined by X-ray fluorescence (XRF) (Oxford, ED2000) and the crystalline phase was studied by XRD (Bruker axs, D5005 diffractometer). RHS was used as a silica source for the synthesis of NaZSM-5.

For XRF technique, the sample was dried at 100°C overnight and cooled down in a desiccator. Then the sample was ground until homogeneous, pressed in an aluminium crucible by using hydraulic press and covered with plastic film. The sample was put in the sample holder and measured by using standard procedure. The measurement time was about 5 min per sample. For XRD technique, the sample was dried at 100°C overnight and cooled down in a desiccator. Then the sample was ground until homogeneous, pressed in a sample holder and put in XRD instrument. The Cu K α X-ray was generated with a current of 40 mA and a potential of 40 kV. The sample was scanned from 5 to 50 degree (2θ) with an increment 0.02 and scan speed 0.5 s/step.

3.3.2 Synthesis and desilication of NaZSM-5

NaZSM-5 was synthesized by a method modified from literature (Panpa and Jinawath, 2009). The RHS was sieved to a mesh size of 150-250 micron. The 6.0 g RHS was dissolved in 90.0 ml of 0.27 M NaOH solution (prepared from 97%, Carlo Erba). The mixture was stirred overnight until the RHS completely dissolved. This solution was referred to as solution 1. In a polypropylene bottle, 0.23 g NaAlO₂ (prepared from Al₂O₃ ~ 50-56% of NaAlO₂, Riedel-de Haën) was dissolved in 30.0 ml of NaOH solution and then mixed with a 0.18 M TPABr solution (prepared from 98 wt.%, ACROS). The resulting solution, referred to as solution 2 was added to solution

1 and the resulting mixture was stirred overnight at room temperature. The mixture pH was adjusted to 11 by 1 M HNO₃, transferred into a Teflon-lined autoclave for hydrothermal treatment at 150°C for 48 h in a muffle furnace. After that the product was centrifuged and washed with DI water until pH is neutral, dried at 80°C for 12 h and calcined at 550°C for 5 h in a muffle furnace to remove the organic template. The crystalline phase of the obtained NaZSM-5 was characterized by XRD.

The NaZSM-5 was modified by desilication with a method of Groen et al. (2004). In this method, silicon atoms were partially removed from the zeolite framework and mesopores were generated. One gram zeolite NaZSM-5 was added into 30.0 ml of 0.2 M NaOH solution in a polypropylene flask under a reflux set up and stirred at 65°C for 30 mins. After that, the zeolite suspension was cooled down in an ice-water bath, filtered and washed until pH of filtrate was neutral and finally dried at 100°C overnight. The final product was named NaZSM-5(D) where D stands for desilication. Crystalline phase of the product was analyzed by XRD, mesopores and particle size was determined by TEM; JEOL JEM, 2010. For TEM technique, about 2.0 mg of sample was dispersed in 10.0 ml of ethanol (99 wt.%, Merck) in a vial, sonicated for 30 mins and kept overnight at room temperature. Then the suspension with a volume of 10.0 µl was dropped on a carbon film on 200-square-mesh copper grid and dried at room temperature with UV light. The grid was put into TEM sample holder and inserted into the vacuum chamber. The voltage for electron acceleration was 200 mV.

The molar ratios of Si/Al of the parent NaZSM-5 and NaZSM-5(D) were determined by inductively coupled plasma-mass spectrometry (ICP-MS) on an Agilent 7500CE series instrument. For ICP-MS technique, the zeolite sample was digested

with acids by using microwave digestion until the zeolite was completely dissolved. The microwave digestion condition of maximum power, percent power, and time was 300 w, 45, and 60 mins, respectively. The ratio of Si/Al was calculated by external standard method of each component. Details of preparation method were given in Appendix A.

3.3.3 Preparation of supported Fe catalysts

The supported Fe catalysts were prepared by incipient wetness impregnation. One gram of both NaZSM-5 and NaZSM-5(D) were dried at 100°C overnight and cooled down in a desiccator before impregnation. $\text{Fe}(\text{NO}_3)_3 \cdot 9\text{H}_2\text{O}$ (98.5 wt.%, QRëC) was dissolved in 0.8 ml of deionized water and then the solution was impregnated to the zeolites. The samples were dried overnight at 105°C and calcined at 500°C for 3 h. After Fe load on zeolite support, the samples were referred to Fe/NaZSM-5 and Fe/NaZSM-5(D). The amount of loaded Fe was fixed at 5 wt.% for both samples. Fe/NaZSM-5 and Fe/NaZSM-5(D) were characterized by XRD to observe changes in zeolite structure. Intracrystalline mesopores and particle size were determined by TEM.

N_2 adsorption-desorption isotherms were obtained from a Micromeritics ASAP 2010. Before measurement, each sample was degassed and heated at 300°C for 3 h. N_2 adsorption-desorption was done at -196°C on relative pressure from 0.001 to 0.99. The surface area was calculated by Brunauer-Emmett-Teller (BET) method from the N_2 adsorption data in the relative pressure from 0.01 to 0.3. Pore size distribution could be calculated by using Barrett-Joyner-Halenda (BJH) method from the following equation:

$$\text{Pore size distribution} = \left(\frac{dV}{d \log (P_1/P_0)} \right)$$

Where dV is differential of cumulative volume (cm^3/g), and P_1/P_0 is ratio of pore width of final pore width to initial pore width (nm)

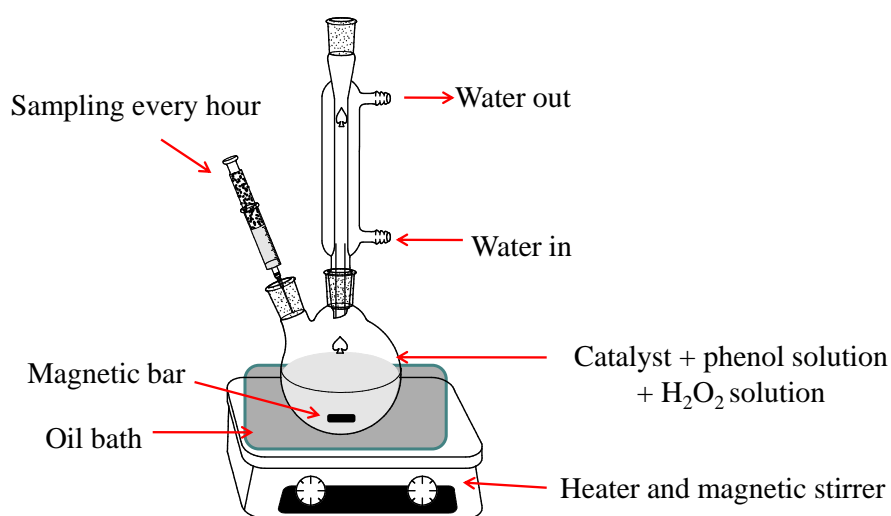
Oxidation state of Fe in the catalysts were determined by XANES at Beamline 8 of the Synchrotron Light Research Institute using Fe K-edge at 7112 eV compared with Fe standards (Fe foil, FeO, Fe₃O₄, and Fe₂O₃). The samples were dried at 100°C overnight in a hot-air oven, cooled down in a desiccator and then ground by mortar and pestle until homogeneous. The sample was prepared on Kapton tape, put into a holder and inserted into the radiation path. The x-ray beam was emitted from a storage ring running at 1.20 GeV with a current in range of 80-250 mA. The Fe K-edge were recorded at room temperature in the transmission mode and x-ray were detected by two ionization chambers; the first chamber for incident beam (I_0) gain = 9 was filled with N₂ and the second chamber for transmitted beam (I_1) gain = 9 was filled with Ar/N₂. The spectra were analyzed with Athena program.

Linear combination fit of XANES spectra was processed and analyzed with Athena program. The linear combination fit was performed on normalized spectra with energy range from -20.00 to 30.00 eV from the edge energy.

3.3.4 Catalytic testing for phenol hydroxylation

All the samples were tested for phenol hydroxylation by a procedure similar to that in literature (Chumee et al., 2009). The apparatus setup is shown in Scheme 3.2. A 100.0 ml two-neck round bottom flask containing the reaction mixture was connected to a reflux condenser and a thermometer. The reaction mixture consisted of 0.05 g catalyst powder and phenol 0.7836 g (99.5 wt.%, BDH) heated at room temperature to

70°C before an addition of 2.6 ml H₂O₂ solution (30 w/v%, UNIVAR). The mole ratio of phenol to H₂O₂ was 1:3 and the total volume of mixture solution was 27.6 ml. The mixture solution was magnetically stirred at 700 rpm and sampling about 0.5 ml was done every hour.



Scheme 3.2 Apparatus setup for catalytic testing.

After sampling, the solution was separated from the catalyst by filtration (NYLON, syringe filler, 13 mm, 0.2 μ m, Nanopak). 100.0 μ l of 1.0 M toluene as an internal standard was added to 380.0 μ l of sample and the solution was analyzed by a gas chromatograph (GC; SHIMADZU 14A series) equipped with an ID-BP1 coated capillary column and a flame ionization detector (FID). The GC injector temperature, initial column temperature, initial column time, column program rate, final column temperature, column hold, and detector temperature were 220°C, 40°C, 2 mins, 5°C/min., 190°C, 1 min., and 220°C, respectively. The quantities of the remaining phenol and products were determined from a calibration curve of each compound (see Appendix B).

Phenol conversion was calculated using equation 1; the selectivity to CAT, HQ and PBQ were calculated from equations 2, 3 and 4, respectively.

$$\% \text{ Phenol conversion} = \left(\frac{\text{Mole phenol}_{inlet} - \text{Mole phenol}_{outlet}}{\text{Mole phenol}_{inlet}} \right) \times 100 \quad (1)$$

$$\% \text{ Selectivity for CAT} = \left(\frac{\text{Mole CAT}}{\text{Mole CAT} + \text{Mole HQ} + \text{Mole PBQ}} \right) \times 100 \quad (2)$$

$$\% \text{ Selectivity for HQ} = \left(\frac{\text{Mole HQ}}{\text{Mole CAT} + \text{Mole HQ} + \text{Mole PBQ}} \right) \times 100 \quad (3)$$

$$\% \text{ Selectivity for PBQ} = \left(\frac{\text{Mole PBQ}}{\text{Mole CAT} + \text{Mole HQ} + \text{Mole PBQ}} \right) \times 100 \quad (4)$$

3.4 Results and discussion

3.4.1 Characterization of rice husk silica (RHS)

The compositions of RHS determined by XRF analysis were listed in Table 3.1. The major component was silica (SiO_2) around 98.0 wt.% along with small amount of Al_2O_3 , CaO , and S . The RHS has high purity suitable for using as SiO_2 source for synthesis of ZSM-5 zeolite. The impurity in RHS such as oxide of alkali metal could be removed by leaching with acid before calcination. The method of silicon extraction modified from literature (Khemthong et al., 2007). They calcined RHS at 550°C for 3 h, obtained the major component was SiO_2 around 98.0 wt.% and minor component such as Al_2O_3 , K_2O , CaO , and Fe_2O_3 . However, the method for extraction has effect to purities of RHS. Panpa and Jinawath (2009) reported that the SiO_2 purity of 99.6 wt.% was obtained by burning the acid leached rice husk at 700°C for 3 h. However, their RHS from pyrolysis of rice husk at high temperature contained

silica in crystalline form which took a long time to dissolve in NaOH and not suitable as SiO_2 source for zeolite synthesis.

The XRD pattern of RHS is shown in Figure 3.1. Only a broad peak at around 22 degree was observed indicating that RHS was in amorphous phase (Khemthong et al., 2007).

Table 3.1 Composition of rice husk silica measured by XRF analysis.

Compositions	Amount (wt.%)
SiO_2	97.884
Al_2O_3	0.554
CaO	0.429
S	0.945

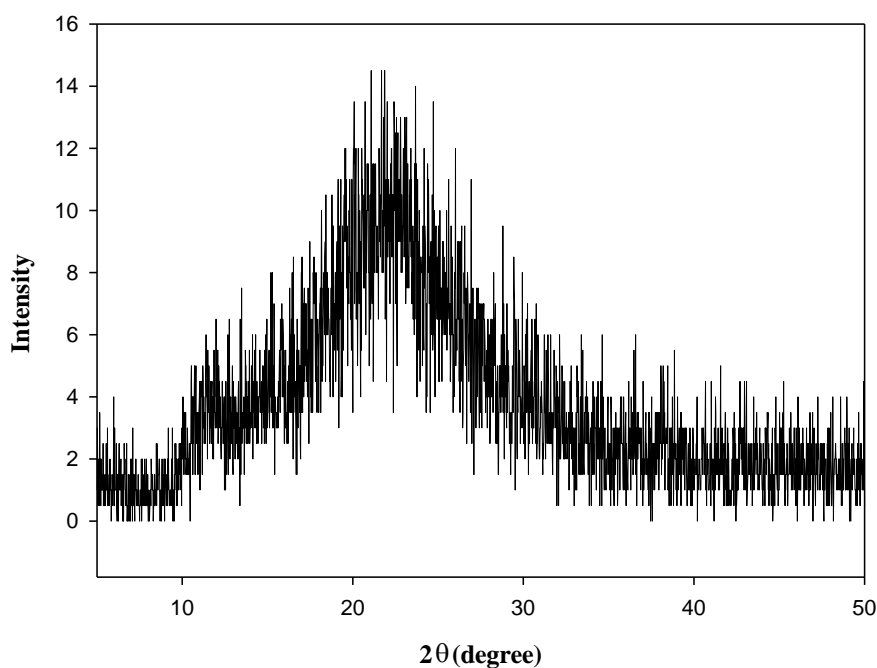


Figure 3.1 XRD spectrum of rice husk silica.

3.4.2 Determination of the Si/Al of NaZSM-5 and NaZSM-5(D)

The Si/Al ratio of the parent NaZSM-5 obtained from ICP-MS was 15. After desilication, the Si/Al ratio changed to 13 confirming that some of the Si atoms were removed. The degree of desilication depended on Si/Al ratio. Groen et al. (2004) reported that when Si/Al ratio of ZSM-5 was ≤ 15 , formation of mesopores were limited because of Al prevented the Si extraction. Saceda et al. (2012) tried to desilicate NH₄Y by NaOH solution but did not produce mesopores.

3.4.3 Catalysts characterization by XRD, ICP-MS and XANES

The XRD patterns of NaZSM-5, Fe/NaZSM-5, NaZSM-5(D), and Fe/NaZSM-5(D) are shown in Figure 3.2. All the samples showed typical reflections of the MFI structure as the only crystalline phase (Caicedo-Realpe and Pérez-Ramírez, 2010). The XRD patterns did not change after desilication suggesting that desilication removed some silicon atoms from the framework but did not cause the zeolite structure to collapse. However, the zeolite peak intensities were lower in supported Fe catalysts because of the Fe species could scatter and absorb the X-rays. After impregnation, peaks corresponding to common Fe compounds such as iron oxide at 33.2° and 33.5°, the strongest lines of hematite (α -Fe₂O₃, JCPDS PDF 33-0664) were not observed indicating that these species were well dispersed on the zeolite. From ICP-MS analysis, the Fe contents in Fe/NaZSM-5 and Fe/NaZSM-5(D) were 4.2 and 4.4 wt.%, respectively. Qi and Yang (2005) reported that when the loading of Fe on ZSM-5 was less than 5% the peaks of iron oxide were not observed.

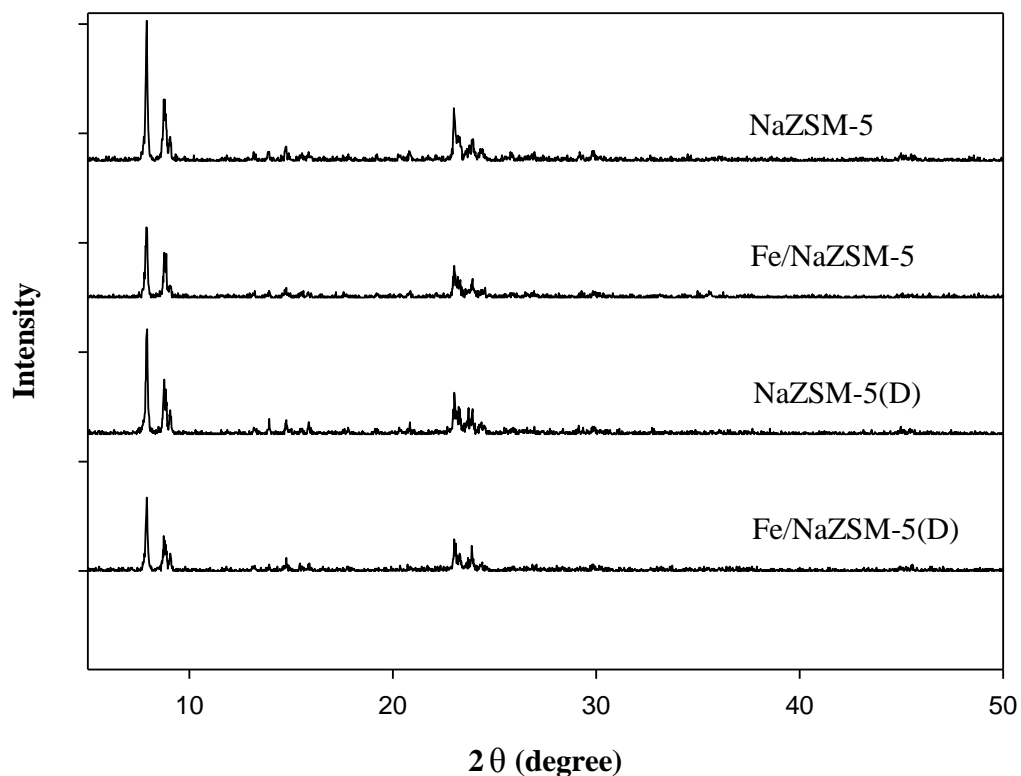


Figure 3.2 XRD patterns of NaZSM-5, Fe/NaZSM-5, NaZSM-5(D), and Fe/NaZSM-5(D).

The XANES spectra of Fe standards and calcined Fe catalysts are shown in Figure 3.3. The XANES spectra of Fe/NaZSM-5 and Fe/NaZSM-5(D) were similar, indicating that Fe species were in the same form. The spectrum of both Fe catalysts matched that of the Fe₂O₃ standard suggesting that the oxidation numbers of the Fe in both catalysts were mainly +3. The linear combination fitting also confirmed that Fe₂O₃ was the only component (see Table 3.2).

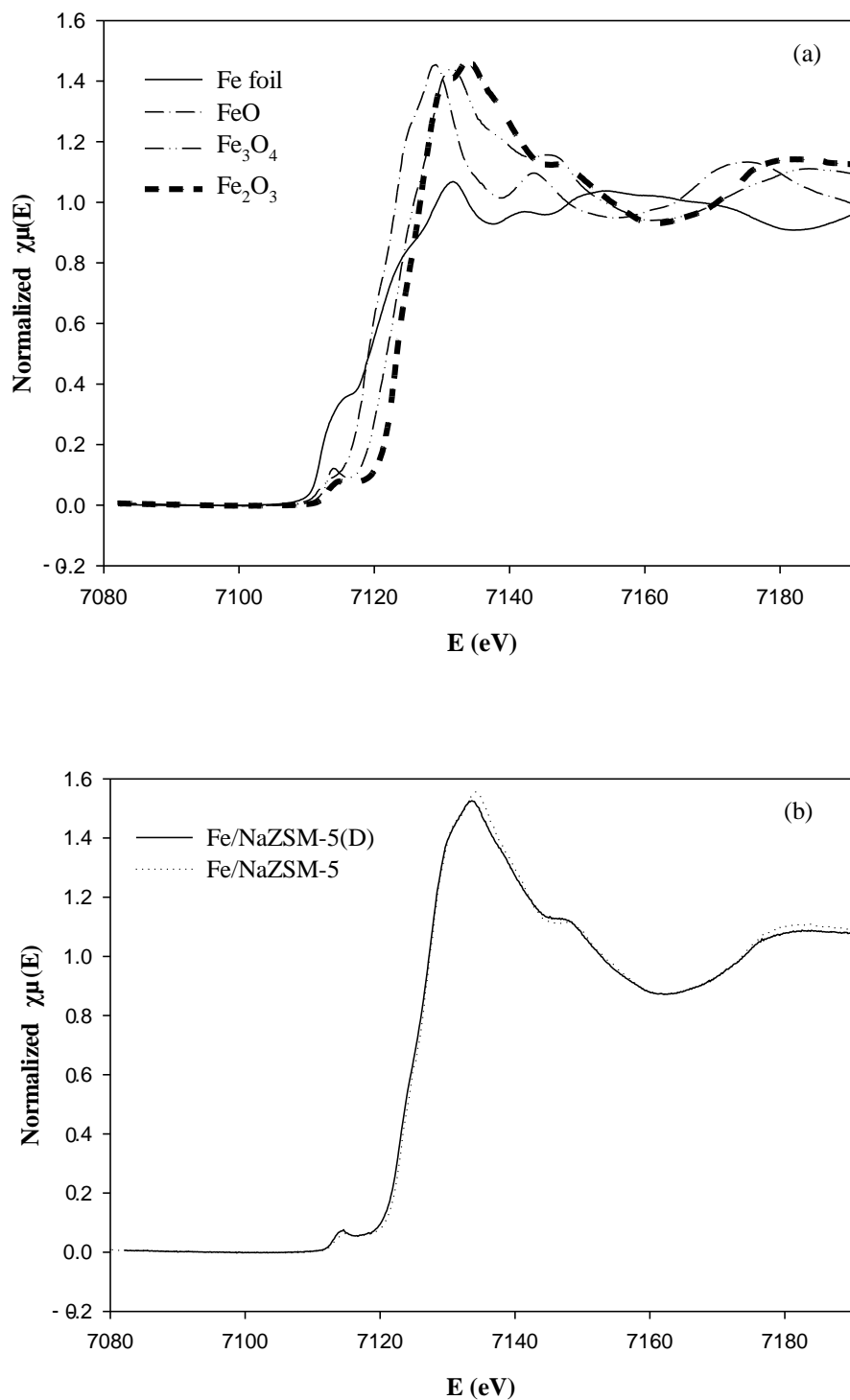


Figure 3.3 XANES spectra of (a) Fe standards: Fe foil, FeO, Fe₃O₄, Fe₂O₃, and (b) Fe catalysts: Fe/NaZSM-5, Fe/NaZSM-5(D) showing form of Fe as Fe₂O₃.

Table 3.2 Percent of Fe species in calcined Fe/NaZSM-5 and Fe/NaZSM-5(D) analyzed by linear combination fit in Athena program.

Samples	Weight (%)	R-factor	Chi-square	Reduced Chi-square
Fe/NaZSM-5		0.0046	1.0731	0.0044
Fe ₂ O ₃	1.000			
Fe ₃ O ₄	0.000			
FeO	0.000			
Fe foil	0.000			
Fe/NaZSM-5(D)		0.0024	0.5645	0.0023
Fe ₂ O ₃	1.000			
Fe ₃ O ₄	0.000			
FeO	0.000			
Fe foil	0.000			

3.4.4 Characterization by TEM

TEM images of NaZSM-5, Fe/NaZSM-5, NaZSM-5(D), and Fe/NaZSM-5(D) are shown in Figure 3.4. The image of NaZSM-5 (Figure 3.4(a)) shows smooth surface indicating that crystal sizes of the zeolite were very small. After loading with Fe the image of Fe/NaZSM-5 (Figure 3.4(b)) shows some dark spots which could be clusters of Fe oxides outside the zeolite pores. The TEM image of NaZSM-5(D) (Figure 3.4(c)) shows light spots with various sizes which were mesopores generated by partial dissolution of silicon atoms from the zeolite. Similar non-uniform mesopores were also observed in the image of Fe/NaZSM-5(D) along with clusters of oxides (Figure 3.4(d)). Li et al. (2009) reported that mesopores were produced in NaZSM-5

by treatment with NaOH solution. They observed intracrystalline mesopores in TEM images.

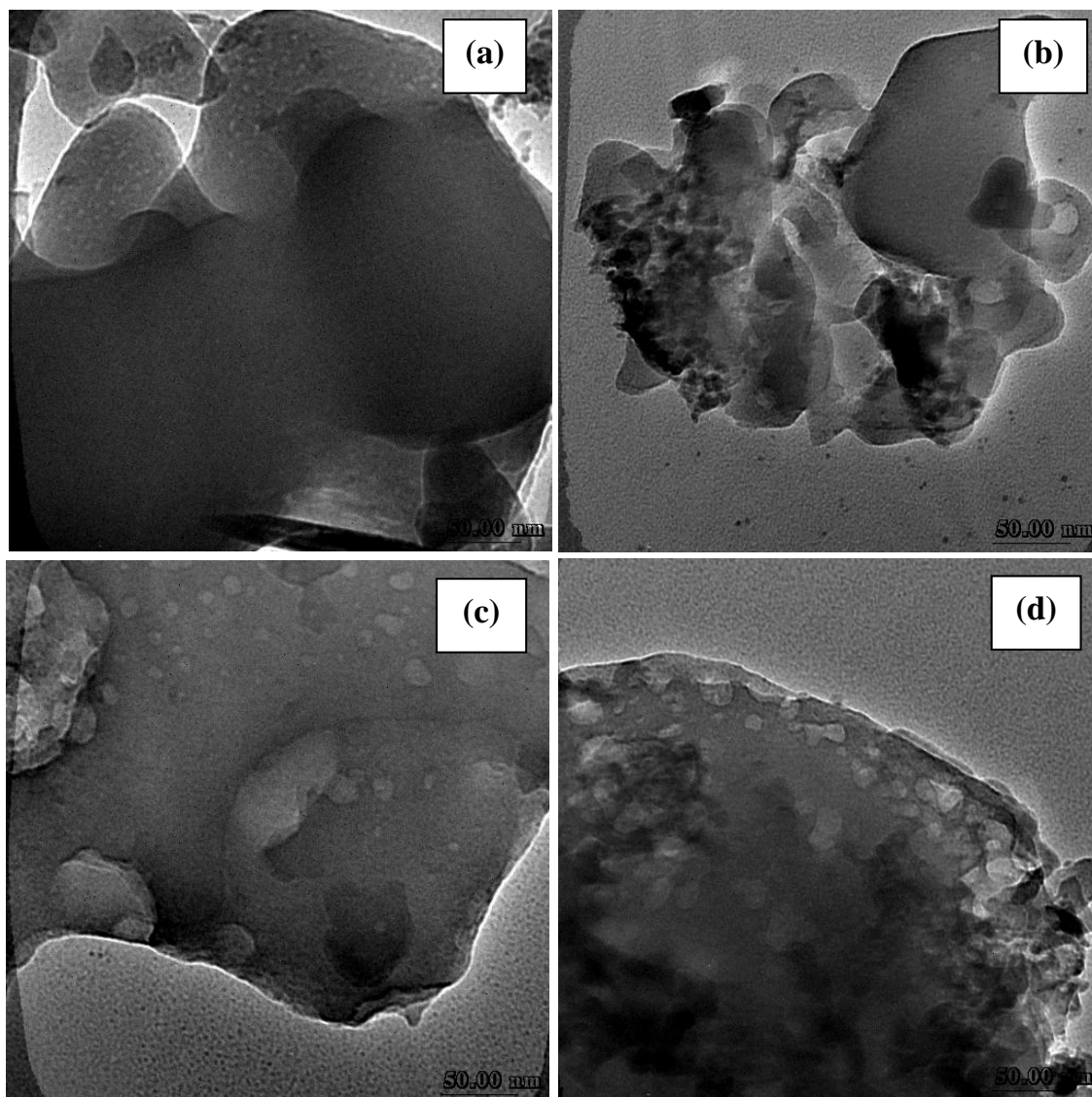


Figure 3.4 TEM micrographs of (a) NaZSM-5, (b) Fe/NaZSM-5, (c) NaZSM-5(D), and (d) Fe/NaZSM-5(D).

3.4.5 Characterization by N₂ adsorption-desorption

The N₂ adsorption-desorption isotherm of NaZSM-5, Fe/NaZSM-5, NaZSM-5(D), and Fe/NaZSM-5(D) are shown in Figure 3.5. The BET surface area, micropore

volume and external surface area of these samples calculated from the N₂ adsorption-desorption data are summarized in Table 3.3.

The isotherm of NaZSM-5 and Fe/NaZSM-5 (Figure 3.5) were nearly type I which is a characteristic of microporous materials. However, there were two areas that deviated slightly from type I. The first one was in the region of P/P_0 less than 0.2, where the adsorbed volume increased instead of becoming a plateau. This deviation indicated some multilayer adsorption which could be from defects in the zeolite structure. The second one was in the range 0.4 – 0.7 in which a narrow hysteresis was observed suggesting that the NaZSM-5 synthesized in one step contained some mesopores. A similar isotherm from similar synthesis was reported by Panpa and Jinawath (2009). Hysteresis loop was also observed in untreated MFI zeolite in ammonium form (Groen et al., 2004). After the NaZSM-5 was loaded with Fe, the shape of the isotherm did not change much from that of the NaZSM-5 except that the volume adsorbed on Fe/NaZSM-5 decreased in all regions and the hysteresis loop was nearly disappear. The result indicated that Fe species were dispersed mainly on the external surface area and mesopores. Slight decrease of adsorbed volume at the beginning suggested that some Fe species resided in micropores. Loading of Fe did not change surface area of NaZSM-5 significantly (Table 3.3).

The isotherm of NaZSM-5(D) was type IV (Figure 3.5). The adsorbed volume at low pressure was similar to the parent NaZSM-5 with higher adsorbed amount. A wide hysteresis loop was observed in the P/P_0 region of 0.45 – 0.95 caused by filling and emptying the mesopores. The loop can be classified to the H3-type which is a characteristic of slit-shaped pores (Rouquerol et al., 1999). After the NaZSM-5(D) was loaded with Fe, the adsorbed volume in the all-region decreased. The adsorption line

of the Fe/NaZSM-5 was nearly parallel to that of the bare NaZSM-5(D) and the hysteresis loop was slightly narrower. The results suggested that Fe species were well dispersed on all areas of NaZSM-5(D). Again, loading of Fe on NaZSM-5(D) did not cause significant changes in surface area (Table 3.3).

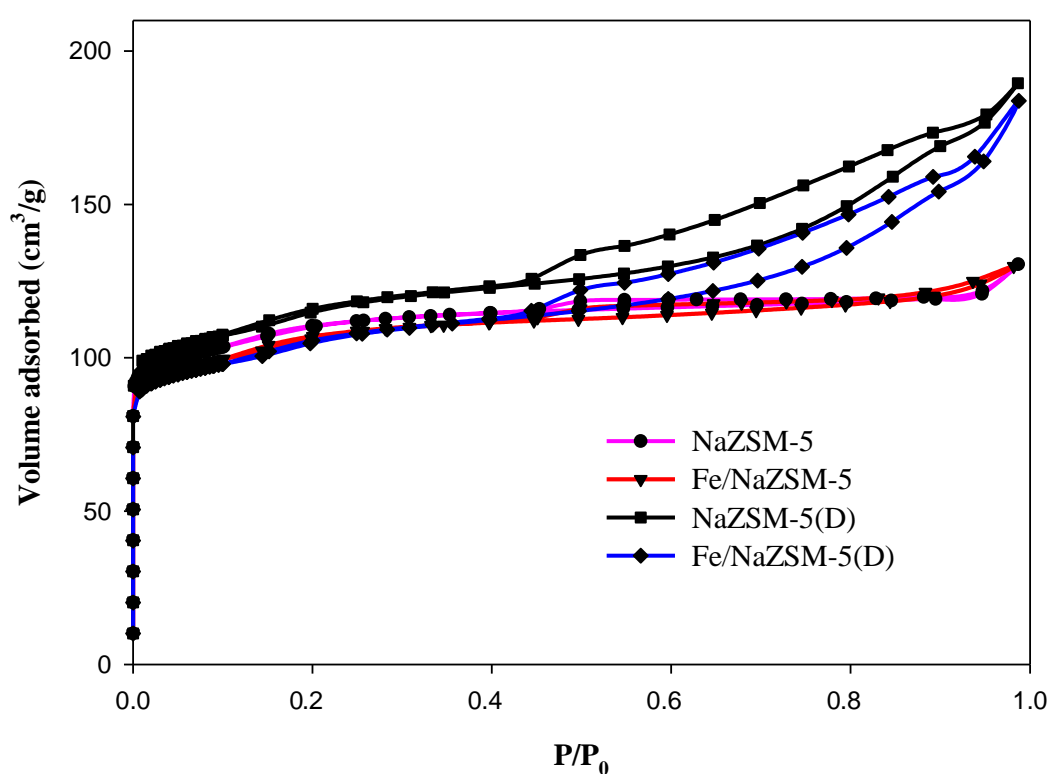


Figure 3.5 N₂ adsorption-desorption isotherm of NaZSM-5, Fe/NaZSM-5, NaZSM-5(D), and Fe/NaZSM-5(D).

The pore size distributions of NaZSM-5, Fe/NaZSM-5, NaZSM-5(D), and Fe/NaZSM-5(D) calculated by the BJH method are shown in Figure 3.6. The pore size distribution of NaZSM-5 confirms the presence of microporosity centered around 2 nm. When loaded with Fe, the distribution remained the same. The pore size distribution of NaZSM-5(D) and Fe/NaZSM-5(D) were similar. A broad range of

mesopores were observed in these samples (Figure 3.6). This result was similar to the results reported by Groen et al. (2004) and Abelló et al. (2009) that the formation of non-uniformed pores of 10 nm was obtained on NH₄ZSM-5 after desilication with 0.2 M of NaOH. Ogura et al. (2001) reported that HZSM-5 desilicated NaOH generated ink-bottle type mesopores which increased with the treatment time. Groen et al. (2004) stated that the counter-cation in the starting zeolite (H⁺, Na⁺, NH₄⁺) had a minor influence on the mesoporous surface area after desilication with NaOH solution.

Table 3.3 Results from N₂ adsorption-desorption analysis.

Samples	Surface area (m ² /g)	Micropore volume (cm ³ /g)	External surface area (m ² /g)
NaZSM-5	362 ± 4.9	0.11	133
Fe/NaZSM-5	351 ± 4.6	0.10	137
NaZSM-5(D)	380 ± 4.8	0.11	158
Fe/NaZSM-5(D)	348 ± 4.3	0.10	145

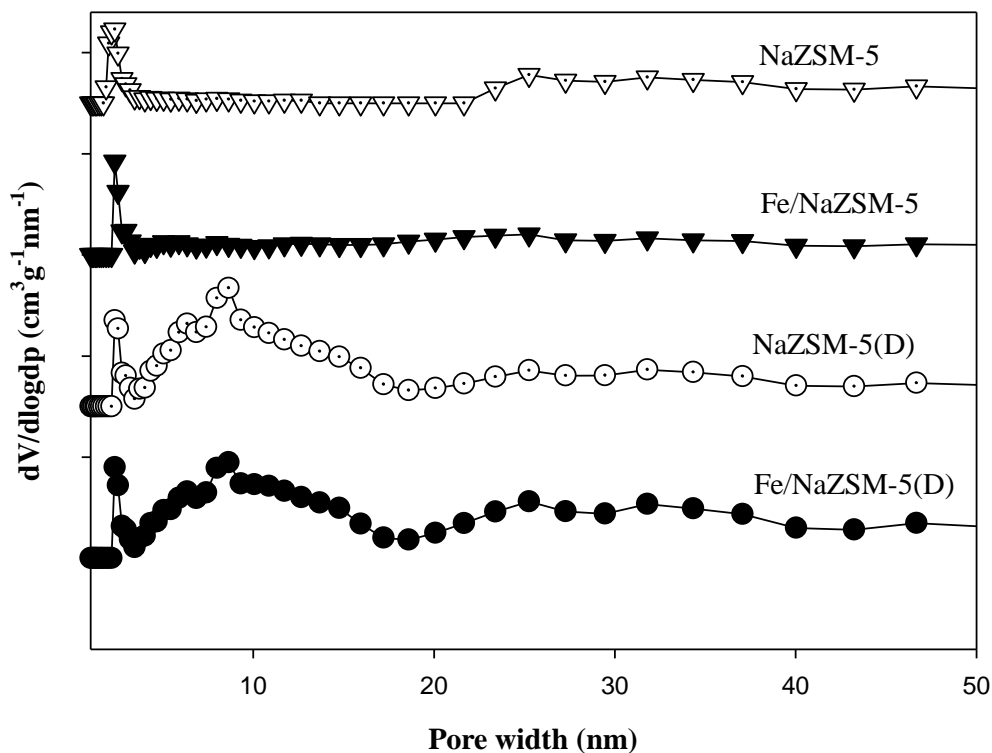


Figure 3.6 BJH pore size distribution of NaZSM-5, Fe/NaZSM-5, NaZSM-5(D), and Fe/NaZSM-5(D).

3.4.6 Catalytic testing for phenol hydroxylation

The supports (NaZSM-5 and NaZSM-5(D)) and Fe catalysts (Fe/NaZSM-5 and Fe/NaZSM-5(D)) were tested for phenol hydroxylation. Results in phenol conversion are shown in Figure 3.7. The phenol conversion on NaZSM-5 and NaZSM-5(D) were about 15%. However, the products were not detected by GC suggesting that the conversion was from phenol adsorption. Phenol adsorbed on NaZSM-5 was higher than NaZSM-5(D).

The phenol conversion on Fe/NaZSM-5(D) more increased and reached the maximum at 66.8% in 3 h, than that on Fe/NaZSM-5 which reached the maximum

69.2% in 4 h. The presence of mesopores in NaZSM-5(D) generated by desilication could facilitate the diffusion of the starting reagents to active sites of the Fe catalysts. Besides, NaZSM-5(D) had a lower Si/Al ratio suggesting that the Lewis acid sites, which are Al atoms, were more accessible for adsorption of reactants prior to the reactions. Thus, the reaction depended on the structure and properties of supports. The Fe catalyst on ZSM-5 without mesopores and with low Si/Al atomic ratio (Villa et al., 2005) showed faster reaction rate than that supported on silica (Liu et al., 2006). It was previously reported that the Fe catalyst supported on MOR modified by leaching with acid and base. Kulawong et al. (2011) gave a faster reaction and higher phenol conversion than Fe supported on MOR (Preethi et al., 2008). The rates of the reaction depend on various factors such as phenol: H₂O₂ mole ratio, metal loading, temperature, time, and types of support.

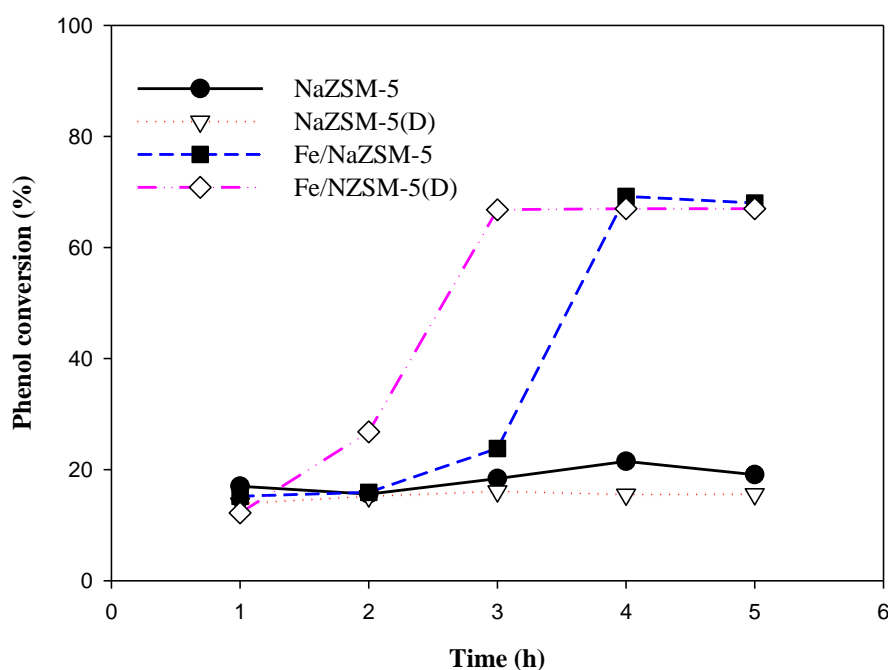


Figure 3.7 Phenol conversions of NaZSM-5, Fe/NaZSM-5, NaZSM-5(D), and Fe/NaZSM-5 (D).

Table 3.4 shows the product selectivity in phenol hydroxylation on Fe/NaZSM-5 and Fe/NaZSM-5(D) catalysts. The PBQ was first observed in both catalysts and disappeared in the next hour. Thus, PBQ was a kinetic product generated from the excess concentration of H₂O₂. After reaching equilibrium, the ratio of CAT:HQ was about 2:1 in both catalysts. This was not surprising because there are two ortho-positions (producing CAT) and one para- position (producing HQ) on phenol. These selectivities could be the result of the locations of Fe oxide which are on the external surface. Phenol hydroxylation, the role of Fe was to generate hydroxyl radical which could react with adsorbed phenol (Choi et al., 2006). In general, the selectivity of the product depended on the reaction conditions and the type of supports.

Table 3.4 Product selectivity of Fe/NaZSM-5 and Fe/NaZSM-5 (D).

Catalysts	Time (h)	% Selectivity		
		CAT	HQ	PBQ
Fe/NaZSM-5	1	0.0	0.0	0.0
	2	0.0	0.0	0.0
	3	0.0	0.0	100.0
	4	67.5	32.5	0.0
	5	67.9	32.1	0.0
Fe/NaZSM-5(D)	1	0.0	0.0	0.0
	2	0.0	0.0	100.0
	3	66.6	33.4	0.0
	4	67.2	32.8	0.0
	5	66.9	33.1	0.0

3.5 Conclusions

NaZSM-5 was synthesized by using RHS as a silica source and modified by desilication to remove silicon from the framework. After desilication, Si/Al molar ratio was decreased. The mesopores were generated and surface areas were increased. Fe was loaded on sample NaZSM-5 and NaZSM-5(D). When tested in phenol hydroxylation, both NaZSM-5 and NaZSM-5(D) only served as adsorption sites but did not convert phenol to any products. When both were used as supports for Fe, the Fe/NaZSM-5(D) shows the faster reaction to reach maximum conversion. Mesopores in ZSM-5 could improve the diffusion of the reactants. However, the selectivity was not much improved and the main products obtained are catechol and hydroquinone.

3.6 References

- Abelló, S., Bonilla, A., and Pérez-Ramírez, J. (2009). Mesoporous ZSM-5 zeolite catalysts prepared by desilication with organic hydroxides and comparison with NaOH leaching. **Appl. Catal. A: Gen.** 364: 191-198.
- Caicedo-Realpe, R. and Pérez-Ramírez, J. (2010). Mesoporous ZSM-5 zeolites prepared by a two-step route comprising sodium aluminate and acid treatments. **Micropor. Mesopor. Mat.** 128: 91-100.
- Choi, J-S., Yoon, S-S., Jang, S-H., and Ahn, W-S. (2006). Phenol hydroxylation using Fe-MCM-41 catalysts. **Catal. Today.** 111: 280-287.
- Chumee, J., Grisdanurak, N., Neramittagapong, A., and Wittayakun, J. (2009). Characterization of platinum-iron catalysts supported on MCM-41 synthesized with rice husk silica and their performance for phenol hydroxylation. **Sci. Technol. Adv. Mat.** 10: 015006.

- Groen, J. C., Peffer, L. A. A., Moulijn, J. A., and Pérez-Ramírez, J. (2004). On the introduction of intracrystalline mesoporosity in zeolites upon desilication in alkaline medium. **Micropor. Mesopor. Mat.** 69: 29-34.
- Groen, J. C., Peffer, L. A. A., Moulijn, J. A., and Pérez-Ramírez, J. (2005). Mechanism of hierarchical porosity development in MFI zeolites by desilication: the role of aluminium as a pore-directing agent. **Chem. Eur. J.** 11: 4983-4994.
- Groen, J. C., Peffer, L. A. A., Moulijn, J. A., and Pérez-Ramírez, J. (2007). Alkaline posttreatment of MFI zeolite from accelerated screening to scale-up. **Ind. Eng. Chem. Res.** 46: 4193-4201.
- Khemthong, P., Prayoonpokarach, S., and Wittayakun, J. (2007). Synthesis and characterization of zeolite LSX from rice husk silica. **Suranaree J. Sci. Technol.** 14: 367-379.
- Kulawong, S., Prayoonpokarach, S., Neramittagapong, A., and Wittayakun, J. (2011). Mordenite modification and utilization as supports for iron catalyst in phenol hydroxylation. **J. Ind. Eng. Chem.** 17: 346-351.
- Li, Y., Liu, S., Xie, S., and Xu, L. (2009). Promoted metal utilization capacity of alkali-treated zeolite: Preparation of Zn/ZSM-5 and its application in 1-hexene aromatization. **Appl. Catal. A: Gen.** 360: 8-16.
- Liu, H., Lu, G., Guo, Y., Guo, Y., and Wang, J. (2006). Synthesis of framework-substituted Fe-HMS and its catalytic performance for phenol hydroxylation. **Nanotechnol.** 17: 997-1003.
- Ogura, M., Shinomiya, S-y., Tateno, J., Nara, Y., Nomura, M., Kikuchi, E., and Matsukata, M. (2001). Alkali-treatment technique-new method for

- modification of structure and acid-catalytic properties of ZSM-5 zeolite. **Appl. Catal. A: Gen.** 219: 33-43.
- Panpa, W. and Jinawath, S. (2009). Synthesis of ZSM-5 zeolite and silicalite from rice husk ash. **Appl. Catal. B: Environ.** 90: 389-394.
- Preethi, M. E. L., Revathi, S., Sivakumar, T., Manikandan, D., Divakar, D., Rupa, A. V., and Palanichami, M. (2008). Phenol hydroxylation using Fe/Al-MCM-41 catalysts. **Catal. Lett.** 120: 56-64.
- Qi, G. and Yang, R. T. (2005). Ultra-active Fe/ZSM-5 catalyst for selective catalytic radiation of nitric oxide with ammonia. **Appl. Catal. B: Environ.** 60: 13-22.
- Rouquerol, F., Rouquerol, J., and Sing, K. (1999). **Adsorption by Powders and Porous Solids (vol. 1)**. (p. 204). Academic Press.
- Saceda, J-J. F., Rintramee, K., Khabuanchalad, S., Prayoonpokarach, S., de Leon, R. L., and Wittayakun, J. (2012). Properties of zeolite Y in various forms and utilization as catalysts or supports for cerium oxide in ethanol oxidation. **J. Ind. Eng. Chem.** 18: 420-424.
- Villa, A. L., Caro, C. A., and de Correa, C. M. (2005). Cu- and Fe-ZSM-5 as catalysts for phenol hydroxylation. **J. Mol. Catal. A: Chem.** 228: 233-240.

CHAPTER IV

CHARACTERIZATION AND PERFORMANCE IN PHENOL HYDROXYLATION OF IRON CATALYSTS SUPPORTED ON HZSM-5 AND HZSM-5(D)

4.1 Abstract

ZSM-5 zeolite in sodium form (NaZSM-5) was modified by desilication with NaOH referred to as NaZSM-5(D) to generate mesopores. Both NaZSM-5 and NaZSM-5(D) were converted to proton form referred to as HZSM-5 and HZSM-5(D), respectively. The removal of silicon atoms were confirmed by the decrease of Si/Al ratio from 15 to 10. The presence of mesopores was confirmed by N₂ adsorption-desorption analysis. Both HZSM-5 and HZSM-5(D) were used as supports for iron (Fe) catalyst and the Fe content were 4.1 and 3.9 wt.%, respectively. The oxidation state of Fe in Fe/HZSM-5 and Fe/HZSM-5(D) determined by XANES was +3. The Fe clusters dispersed on surface area and mesopores site of the catalysts, studied by TEM. Both catalysts were active for phenol hydroxylation using H₂O₂ as an oxidant in the batch reactor at 70°C [phenol: H₂O₂ = 1:3]. The presence of mesopores in Fe/HZSM-5(D) improved diffusion of reactants and increased phenol conversion to 75% at the first hour. However, the presence of mesopores did not improve the selectivity and the main products from both catalysts were catechol and hydroquinone with mole ratio about 2:1.

4.2 Introduction

In Chapter III, NaZSM-5 and NaZSM-5(D) were characterized and used as supports for Fe. In catalytic testing, the presence of mesopore was probably responsible for the faster reaction. Beside the presence of mesopores, form of zeolite could affect the zeolite properties and catalytic performance.

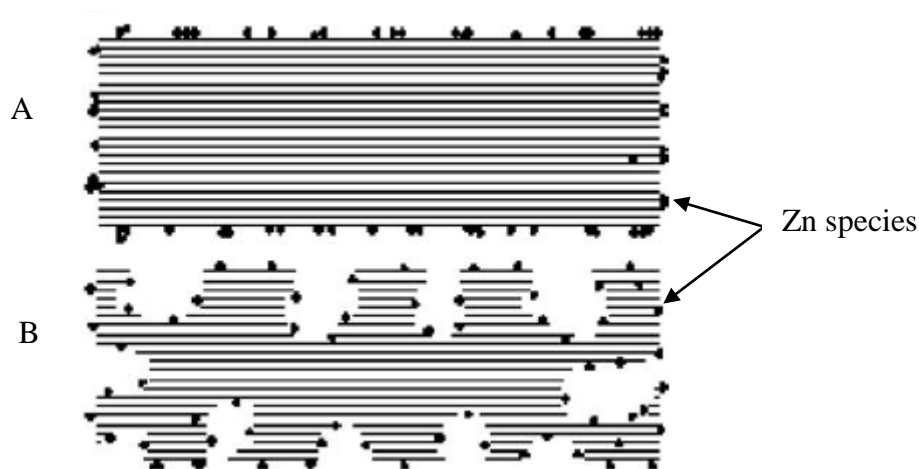
This Chapter compares zeolite properties and performance of catalysts supported on zeolite in proton form. The HZSM-5 and HZSM-5(D) were used as the supports for Fe catalysts and tested in phenol hydroxylation. The support with high surface area was expected to provide high metal dispersion and consequently enhance the catalytic performance. All the samples of HZSM-5, HZSM-5(D), Fe/HZSM-5, and Fe/HZSM-5(D) were characterized by XRD, ICP-MS, XANES, TEM, and N₂ adsorption-desorption.

Atoguchi et al. (2004) prepared different types of zeolite without metal loading and tested for phenol hydroxylation. They found that HMOR which has large pore with 12-membered oxygen ring aperture gave higher reaction yield than HUSY, HBEA and HZSM-5 which have 10-membered oxygen ring aperture. However, HZSM-5 has high acid strength but small pore lead to fast coking. The coke would block the pore and catalytic active sites in phenol hydroxylation. From these problems, the catalytic performance of HZSM-5 could be improved by desilication with NaOH to enhance diffusion of reactants and products. The desilicated HZSM-5, referred to as HZSM-5(D) was further loaded with Fe.

In desilication, silicon atoms could be removed from the framework of zeolite by base. The desilication mechanism was described in the Chapter III. Desilication could shorten the pore length so the diffusions were increased (Abelló et al., 2009).

The desilication method by using NaOH was suitable for MFI because mesopores could be randomly created in the zeolite framework. (Vernimmen et al., 2011).

Li et al. (2009) compared the Zn loading by incipient wetness impregnation on untreated HZSM-5 and alkaline treated HZSM-5 as shown in Scheme 4.1. The open micro-mesopore hierarchical structure allowed better Zn dispersion from impregnation process. In addition, the open zeolite structure facilitated the access to Al atoms and resulted in high Lewis acid sites, agreeing with the results reported in literature (Woolery et al., 1997). These results were evidenced by the STEM/EDS and pyridine-FTIR.



Scheme 4.1 Metal dispersed over the untreated (A) and alkali-treated (B) in HZSM-5 zeolite (Li et al., 2009).

In this chapter, Fe was dispersed on HZSM-5 and HZSM-5 (D) by incipient wetness impregnation. The resulting catalysts were tested in phenol hydroxylation to produce CAT and HQ.

4.3 Experimental

4.3.1 Alkali treatment and conversion of NaZSM-5 to HZSM-5 by ion exchange

The NaZSM-5 was modified by desilication with a method by Groen et al. (2004) in which silicon atoms were partially removed from the zeolite framework and mesopores were generated. One gram of NaZSM-5 was added into 30.0 ml of 0.2 M NaOH solution in a polypropylene flask under a reflux set up and stirred at 65°C for 30 mins. After that, the zeolite suspension was then cooled down in an ice-water bath, filtered and washed until pH of filtrate was neutral and dried at 100°C overnight. The final product was named NaZSM-5(D).

NaZSM-5 and NaZSM-5(D) were converted into proton form referred to as HZSM-5 and HZSM-5(D) respectively by three consecutive ion exchanges with NH_4NO_3 solution (Groen et al., 2004, Ogura et al., 2001). One gram of NaZSM-5(D) was added into 0.1 M NH_4NO_3 solution (prepared from 99.5 wt.%, QRëC) and stirred at 80°C for 2 h to replace Na^+ . The solid was separated by centrifugation at 3500 rpm for 15 mins and washed with DI water until pH of the solution was 5. The sample was then dried at 100°C overnight and calcined at 550°C for 5 h to convert $\text{NH}_4\text{ZSM-5}$ and $\text{NH}_4\text{ZSM-5(D)}$ to HZSM-5 and HZSM-5(D), respectively.

Both HZSM-5 and HZSM-5(D) were analyzed by XRD, TEM, and ICP-MS. The samples preparation and analysis procedures in XRD, TEM, and ICP-MS were mentioned in Chapter III.

4.3.2 Preparation of supported Fe catalysts

The supported Fe catalysts were prepared by incipient wetness impregnation method using $\text{Fe}(\text{NO}_3)_3 \cdot 9\text{H}_2\text{O}$ as an iron source. The samples preparation and analysis

procedures by XRD, TEM, ICP-MS, XANES, and N₂ adsorption-desorption were mentioned in Chapter III.

4.3.3 Catalytic testing for phenol hydroxylation

All of samples HZSM-5, HZSM-5(D), Fe/HZSM-5 and Fe/HZSM-5(D) were tested for phenol hydroxylation by a procedure similar that in literature (Chumee et al., 2009). The samples preparation, apparatus setup, and testing procedures were described in Chapter III.

4.4 Results and discussion

4.4.1 Analysis by ICP-MS

The Si/Al ratio of the sample HZSM-5 obtained from ICP-MS was 15. After desilication, the Si/Al ratio decreased and changed to 10 confirming that some of the Si atoms were removed. The degree of desilication depended on Si/Al ratio. When Si/Al ratio was ≤ 15 , formation of mesopores were limited because of Al prevented the Si extraction (Groen et al., 2004). The amount of Fe loading by incipient wetness impregnation of samples Fe/HZSM-5 and Fe/HZSM-5(D) analysis by ICP-MS were 4.1 and 3.9 wt.%, respectively.

4.4.2 Analysis by XRD and XANES

The XRD patterns of HZSM-5, Fe/HZSM-5, HZSM-5(D), and Fe/HZSM-5(D) are shown in Figure 4.1. All the samples showed typical reflections of the MFI structure as the only crystalline phase (Caicedo-Realpe and Pérez-Ramírez, 2010). The desilicated HZSM-5; HZSM-5(D) exhibited a diffraction pattern very similar to that of

untreated HZSM-5. The zeolite crystal structure was not significantly changed by desilication.

The peak intensities were low in supported Fe catalysts because the Fe loaded could also scatter and absorb the X-ray. The Fe supported on the support was well dispersed because peak corresponding to iron oxide at 33.2° and 33.5° were not observed. This behavior was also observed in Fe loaded on NaZSM-5 and NaZSM-5(D) in Chapter III. Qi and Yang. (2005) reported that when the loading of Fe was less than 5% the peaks of iron oxide was not observed but when the Fe loading was over 5% the peaks at 33.2° and 33.5° were observed corresponding to the strongest peak of hematite (α -Fe₂O₃, PDF 33-0664).

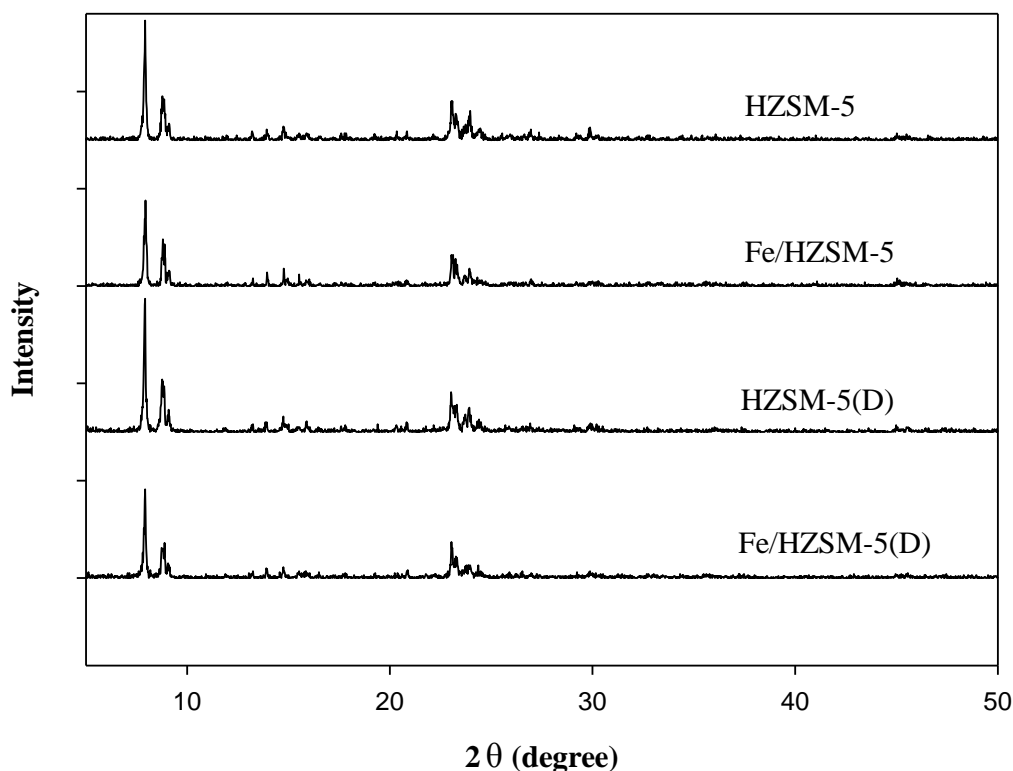


Figure 4.1 XRD patterns of HZSM-5, Fe/HZSM-5, HZSM-5(D), and Fe/HZSM-5(D).

Figure 4.2(a) and (b) showed the XANES spectra of Fe standards and Fe catalysts, respectively. The XANES spectrum at Fe K-edge of both Fe/HZSM-5 and Fe/HZSM-5(D) was compared with Fe standards and form of Fe in both catalysts were Fe_2O_3 . Thus the oxidation number of the Fe supported on ZSM-5 was +3. Again, the linear combination fitting of Fe in both of Fe/HZSM-5 and Fe/HZSM-5(D) confirmed that Fe_2O_3 was the only component (see Table 4.1).

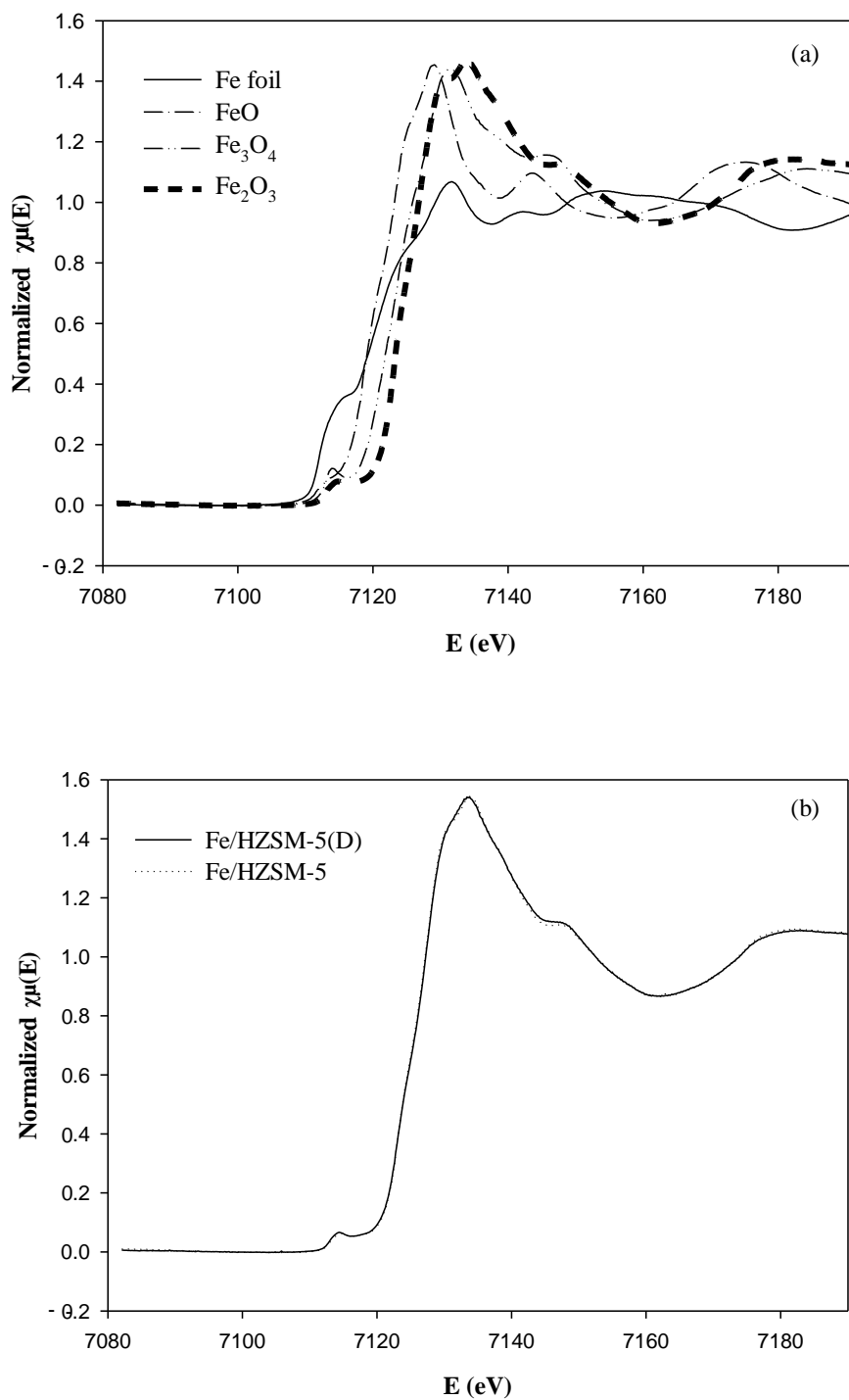


Figure 4.2 XANES spectra of (a) Fe standards: Fe foil, FeO, Fe_3O_4 , Fe_2O_3 , and (b) Fe catalysts: Fe/HZSM-5 and Fe/HZSM-5(D) showing form of Fe as Fe_2O_3 .

Table 4.1 Percent of Fe species in calcined Fe/HZSM-5 and Fe/HZSM-5(D) analyzed by linear combination fit in Athena program.

Samples	Weight (%)	R-factor	Chi-square	Reduced Chi-square
Fe/HZSM-5		0.0032	0.7248	0.0029
Fe ₂ O ₃	1.000			
Fe ₃ O ₄	0.000			
FeO	0.000			
Fe foil	0.000			
Fe/HZSM-5(D)		0.0037	0.9288	0.0037
Fe ₂ O ₃	1.000			
Fe ₃ O ₄	0.000			
FeO	0.000			
Fe foil	0.000			

4.4.3 Analysis by TEM

TEM images of HZSM-5, Fe/HZSM-5, HZSM-5(D), and Fe/HZSM-5(D) are shown in Figure 4.3. The TEM image of HZSM-5 in Figure 4.3(a) shows dark area which smooth surface. The TEM image of HZSM-5(D) in Figure 4.3(c) shows white spots which referred to intracrystalline mesopores. The pore sizes were not uniformed as large and small pores were observed. Both the samples in Figure 4.3(b) and (d) the catalysts show dark spots, which could be clusters of Fe species, dispersed on the external surface and inside the zeolite crystals. In Figure 4.4 the microporous lattice was observed in the framework of HZSM-5 but this morphology was not retained after

alkaline treatment. The mesopores through the particle were clearly seen on sample, and the edge was similarly traversed inside the particle (Groen et al., 2004).

The TEM morphology of sample Fe/HZSM-5(D) was a good example which showed clearly mesopores and Fe dispersion. Impregnation of Fe species on HZSM-5 has higher dispersion and phenol conversion than NaZSM-5, compared with the results in Chapter III because the Fe species favored to replace Brønsted acid proton in HZSM-5 zeolite (Lobree et al., 1999). Figure 4.5 showed the TEM morphology of Fe/HZSM-5(D) after desilication and loaded with Fe species. Mesopores or bright parts were observed in the framework of zeolite and appeared to be uniform; the size and position of mesopores did not control and Fe can be dispersed inside of micropores, mesopores and on the outer surface. From the TEM image indicates that there are lots of mesopores located inside and on the edge in single crystal. The Fe species dispersed on mesopores. The results agreeing with the result from literature Li et al. (2009) reported that a large part of Zn species located in the mesopores, leading to the better metal distribution and more Lewis acid sites. Chen et al. (2009) prepared Fe catalyst by Fe loaded on HZSM-5 with incipient wetness impregnation with Fe content of 1.5 wt.% which analyzed by HRTEM. The result shows small particle of Fe species orienting inside the zeolite structure including the channels. Figure 4.6, the TEM morphology of sample Fe/HZSM-5(D) showed distribution of mesopores as bright parts and Fe dispersion as dark parts.

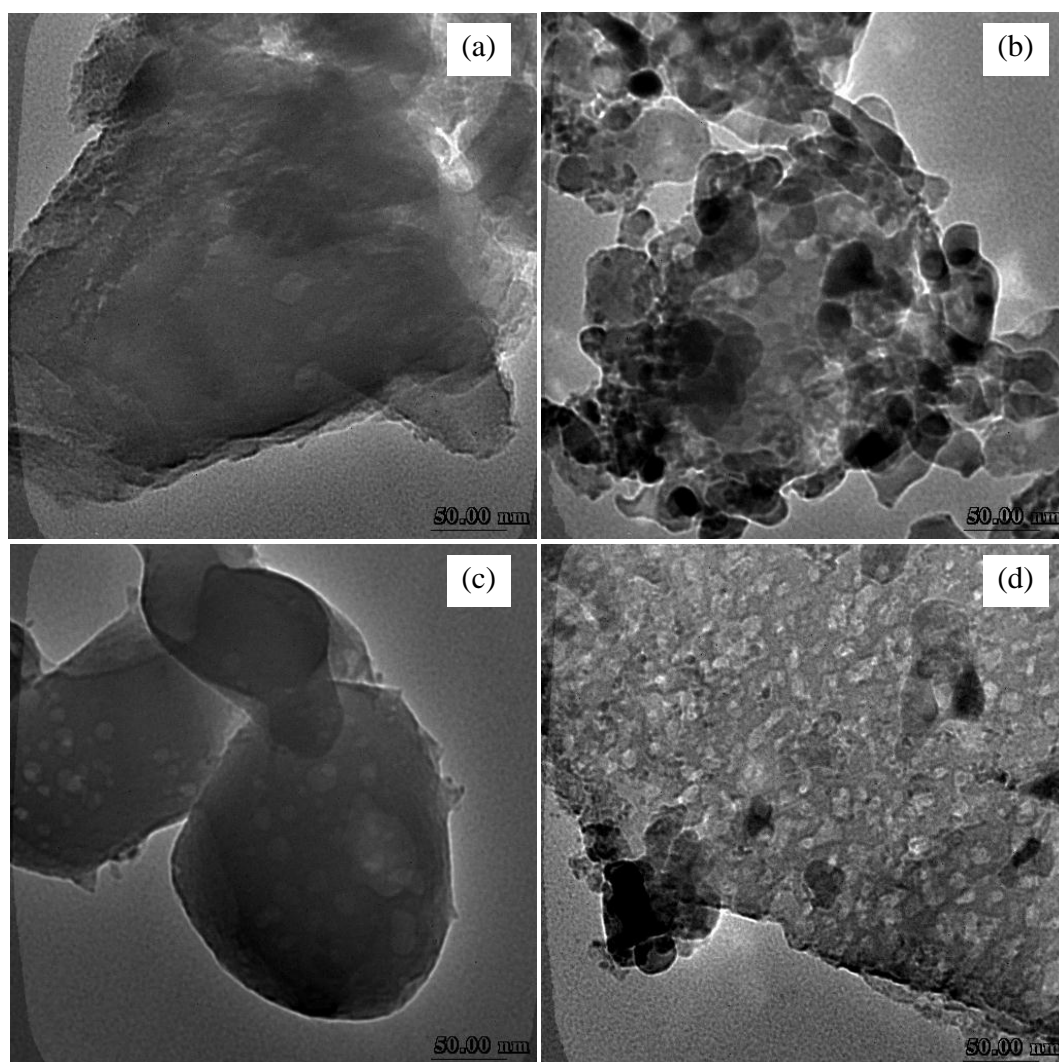


Figure 4.3 TEM micrographs of (a) HZSM-5, (b) Fe/HZSM-5, (c) HZSM-5(D), and (d) Fe/HZSM-5(D).

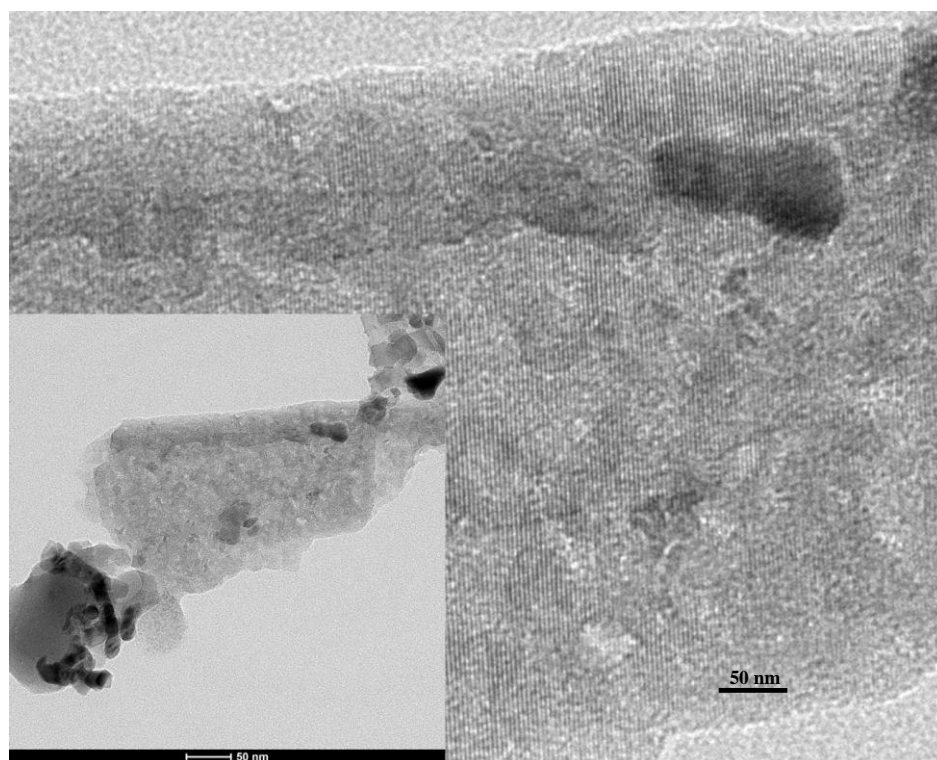


Figure 4.4 TEM micrographs of Fe/HZSM-5(D) at 50 nm.

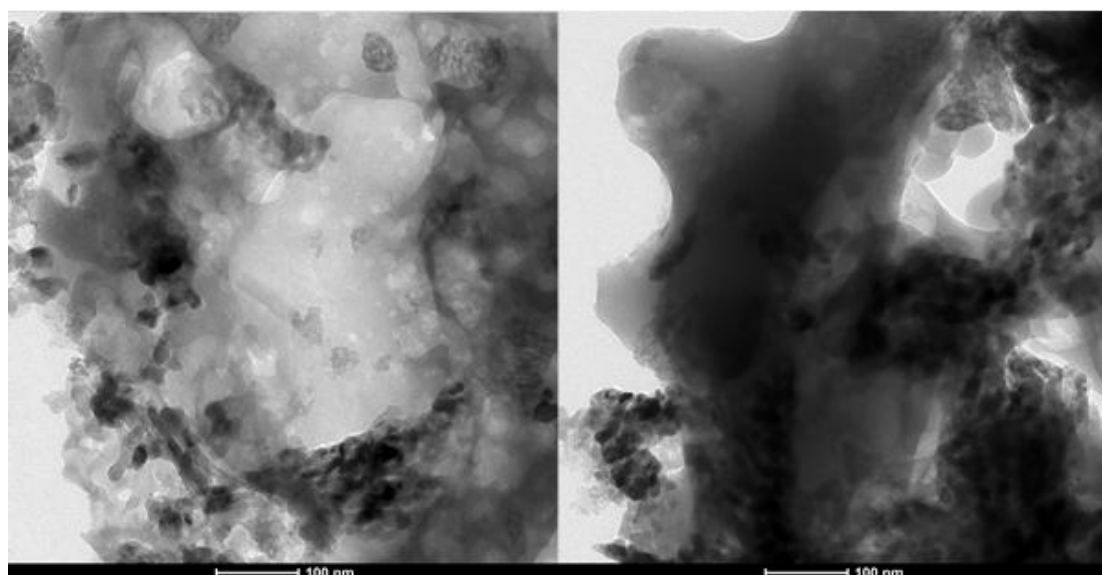


Figure 4.5 TEM micrographs of sample Fe/HZSM-5(D) at 100 nm.

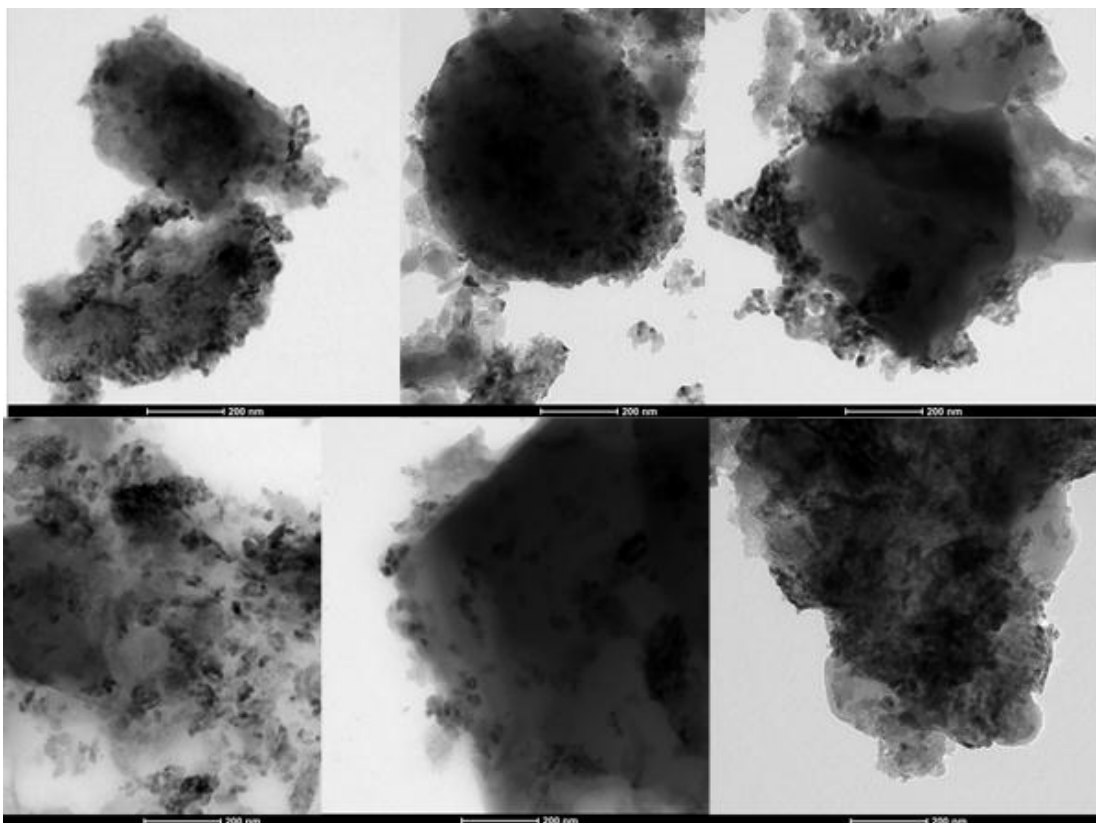


Figure 4.6 TEM micrographs of Fe/HZSM-5(D) at 200 nm.

4.4.4 Analysis by N₂ adsorption-desorption

The N₂ adsorption-desorption of zeolites and catalysts are shown in Figure. 4.7. The adsorption isotherms of HZSM-5 and Fe/HZSM-5 were nearly type I which is a characteristic of microporous materials. A hysteresis loop was observed at P/P_0 from 0.45 to 0.95. After loading with Fe, the volume adsorbed decreased in all regions indicating that Fe resided on external surface area, micropores and mesopores.

Table 4.2 shows a decrease in surface area after loading with Fe. The adsorption-desorption isotherms of HZSM-5(D) and Fe/HZSM-5(D) were type IV. Desilication of HZSM-5 resulted in an increase of surface area. The formation of mesopores was confirmed by H3-type hysteresis loop which is a characteristic of

slit-shaped pores (Rouquerol et al., 1999). Loading of Fe on the HZSM-5 resulted in the decrease of adsorbed volume in all regions and slightly narrower hysteresis loop. These results suggested the location of Fe on external surface area, in micro- and mesopores. Groen et al. (2004) reported that non-treated $\text{NH}_4\text{ZSM-5}$ zeolite exhibit a type I isotherm with a plateau at higher relative pressure as the result of the microporous nature of the material with limited meso-porosity. After desilication with NaOH solution the structure of zeolite shows an enhanced N_2 uptake at higher relative pressures accompanied by a hysteresis loop, an indication of extra mesoporosity.

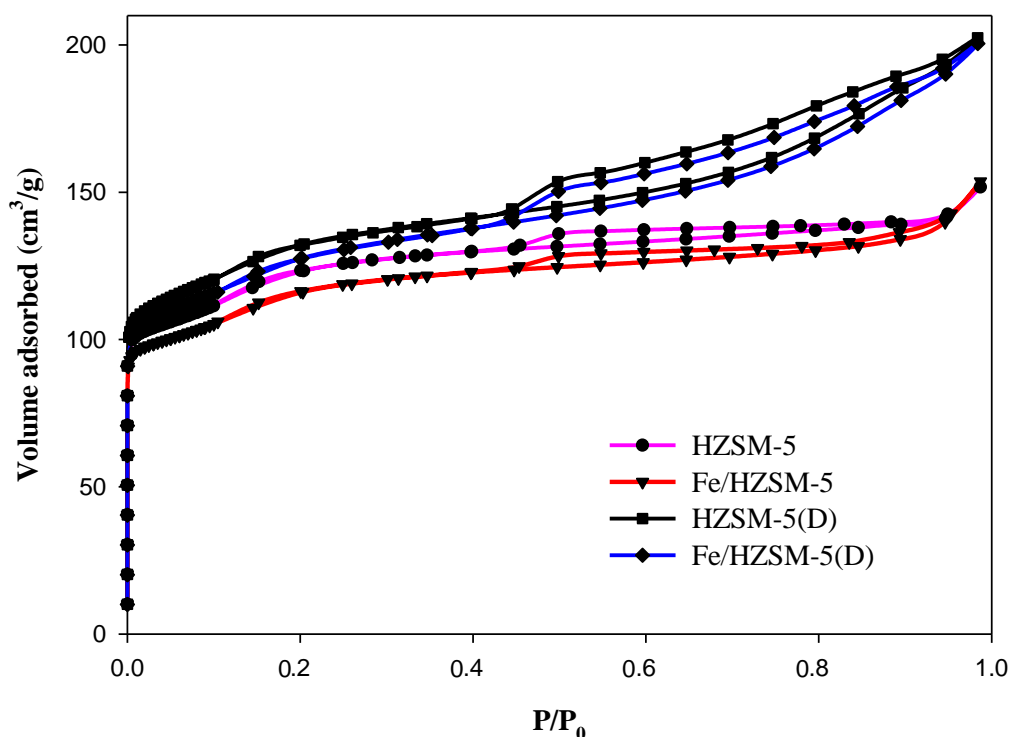


Figure 4.7 N_2 adsorption-desorption isotherms of HZSM-5, Fe/HZSM-5, HZSM-5(D), and Fe/HZSM-5(D).

Table 4.2 Results from N₂ adsorption-desorption analysis.

Samples	Surface area (m ² /g)	Micropore volume (cm ³ /g)	External surface area (m ² /g)
HZSM-5	403 ± 4.6	0.09	224
Fe/HZSM-5	381 ± 4.2	0.09	209
HZSM-5(D)	435 ± 4.7	0.10	230
Fe/HZSM-5(D)	421 ± 4.2	0.09	233

The pore size distributions of zeolites and catalysts calculated by BJH method is shown in Figure 4.8. The pore size distribution of HZSM-5 confirms the presence of microporosity in a pore-size distribution centered around 2 nm. When loading with Fe, the sample Fe/HZSM-5 shows a slightly narrower pore-size distribution. The BJH method of samples HZSM-5(D) and Fe/HZSM-5(D) confirmed the presence of mesoporosity after desilication with NaOH solution, showing a development of a broad pore-size distribution centered around 8 nm. This result is agreement with Groen et al. (2004) and Abello et al. (2009), who claimed the formation of uniform pores of 10 nm at the similar condition of desilication.

The modified ZSM-5 zeolites show the properties of hierarchical zeolite, the formation of uniform pore sizes. Abello et al. (2009) reported that the hierarachical zeolites combining micro- and mesoporosity in the framework. The counter-cation in the starting zeolite (H⁺, Na⁺, NH₄⁺) had a minor influence on the mesoporous surface area by silicon extraction with NaOH solution. At high Si/Al ratios desilication is still favorable because of the extremely low Al content and could be easily created. A

molar ratio in the range 25-50 has leads to an optimal mesoporosity centered about 10 nm (Groen et al., 2005).

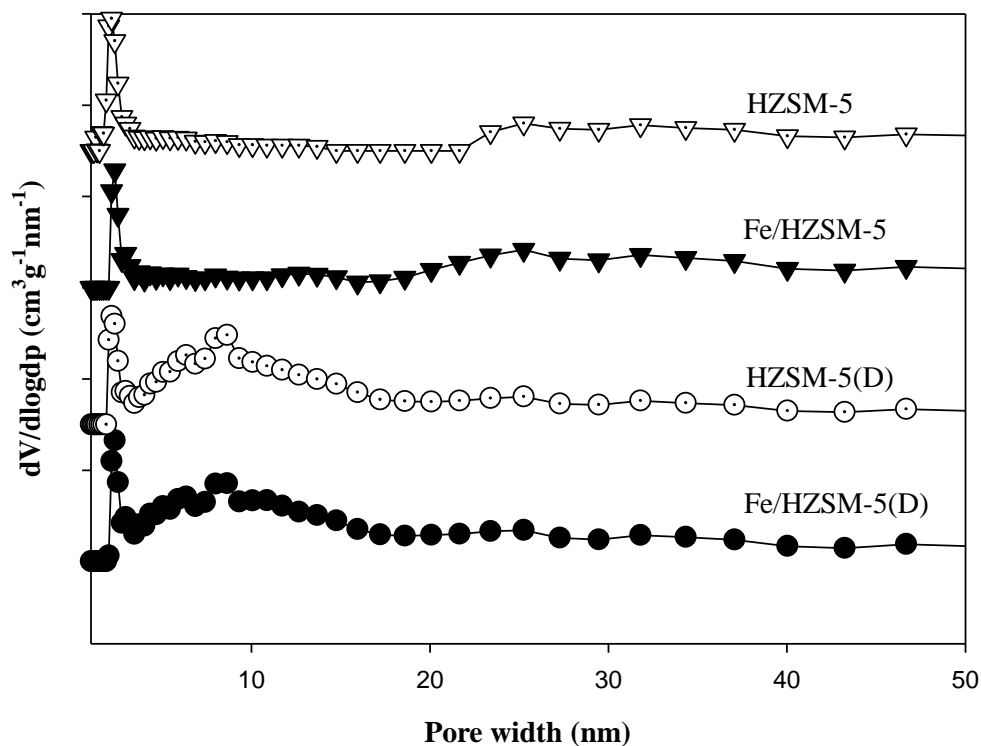


Figure 4.8 BJH pore size distribution of HZSM-5, Fe/HZSM-5, HZSM-5(D), and Fe/HZSM-5(D).

4.4.5 Catalytic performance for phenol hydroxylation

The phenol conversion of HZSM-5, HZSM-5(D), Fe/HZSM-5, and Fe/HZSM-5(D) is shown in Figure 4.9. The bare HZSM-5 and HZSM-5(D) gave phenol conversion about 10 and 20%, respectively but products were not detected by GC suggesting that phenol adsorbed on the zeolites. The higher adsorption on HZSM-5(D) indicated the higher number of adsorption sites. Desilication resulted in higher number of Brønsted acid sites which could for hydrogen bond with phenol. On Fe/HZSM-5,

the phenol conversion was similar to the bare support in the first three hours and products were not detected. The conversion and selectivity (Table 4.3) then increased in the fourth and fifth hour. The sample Fe/HZSM-5(D) showed the fastest phenol conversion at the first hour giving phenol conversion of about 75%. The presence of mesopores could facilitate the diffusion of starting reagents to active sites of Fe catalysts. The catalytic performance of Fe catalysts depended on the support type. Villa et al. (2005) showed that Fe supported on microporous NaZSM-5 with low Si/Fe ratio gave a faster rate than that supported on silica. The reaction rate could be improved when Fe was supported on zeolites with mesopores. Kulawong et al. (2011) showed that Fe supported on MOR with mesopores gave a faster rate than Fe on untreated MOR (Preethi et al., 2008).

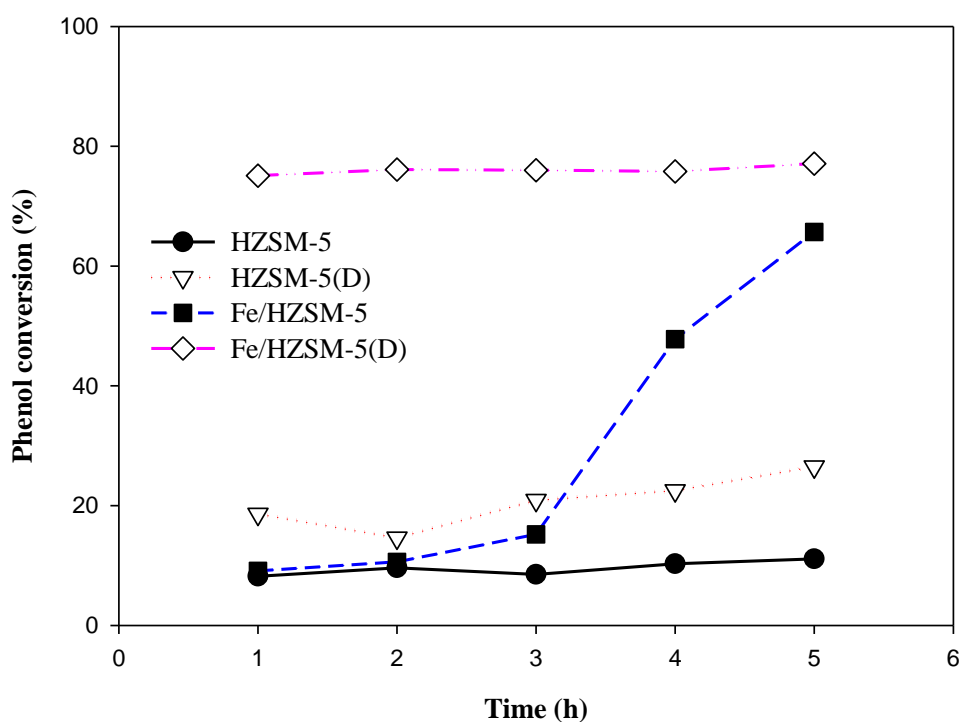


Figure 4.9 Phenol conversions of HZSM-5, HZSM-5(D), Fe/HZSM-5, and Fe/HZSM-5 (D).

The Table 4.3 shows the product selectivity from phenol hydroxylation on Fe/HZSM-5 and Fe/HZSM-5 (D). The PBQ was observed from Fe/HZSM-5 in the fourth hour and then disappeared. On Fe/HZSM-5(D) only CAT and HQ were observed. The selectivity of catechol was higher than hydroquinone because the active site at ortho-position of catechol to para-position of hydroquinone ratio of 2:1 and products can be produced on external and internal surface. When high amount of Fe, the phenol conversion increased also CAT was decreased (Villa et al., 2005). The selectivity depends on reaction condition and type of support.

Comparison the catalytic performance with different form of ZSM-5 in sodium and proton form were used as support for Fe loading in catalytic testing for phenol hydroxylation. The Fe/HZSM-5(D) has higher phenol conversion than Fe/NaZSM-5(D) because HZSM-5(D) has high Brønsted acid site in the framework of zeolite. The desilication, conversion to proton form by exchanged with ammonium nitrate and calcination which were generated Lewis acid site in tetrahedral framework (Woolery et al., 1997). Thus, the Fe/HZSM-5(D) has higher adsorption site for reactants than Fe/NaZSM-5(D). The reactants over Fe/HZSM-5(D) catalysts require a joint participation of Brønsted acid sites and metal Lewis acid sites (Li et al., 2009).

Table 4.3 Product selectivity of Fe/HZSM-5 and Fe/HZSM-5 (D).

Catalysts	Time (h)	% Selectivity		
		CAT	HQ	PBQ
Fe/HZSM-5	1	0.0	0.0	0.0
	2	0.0	0.0	0.0
	3	0.0	0.0	100.0
	4	70.3	0.0	29.7
	5	68.8	31.2	0.0
Fe/HZSM-5(D)	1	62.7	37.3	0.0
	2	61.6	38.4	0.0
	3	60.5	39.5	0.0
	4	61.0	39.0	0.0
	5	61.4	38.6	0.0

4.5 Conclusions

Both HZSM-5 and HZSM-5(D) were tested in phenol hydroxylation; their only served as adsorption site but did not convert phenol to any products. This results were similar the result in sodium form of ZSM-5. The desilication and exchange to proton form of ZSM-5 increased phenol adsorption rate. When loading with Fe species, the Fe/HZSM-5(D) gave the highest phenol conversion and selectivity to CAT and HQ at the first hour.

4.6 References

Abelló, S., Bonilla, A., and Pérez-Ramírez, J. (2009). Mesoporous ZSM-5 zeolite catalysts prepared by desilication with organic hydroxides and comparison with NaOH leaching. *Appl. Catal. A: Gen.* 364: 191-198.

- Atoguchi, T., Kanougi, T., Yamamoto, T., and Yao, S. (2004). Phenol hydroxylation into catechol and hydroquinone over H-MFI, H-MOR, H-USY and H-BEA in the presence of ketone. **J. Mol. Catal. A: Chem.** 220: 183-187.
- Caicedo-Realpe, R. and Pérez-Ramírez, J. (2010). Mesoporous ZSM-5 zeolites prepared by a two-step route comprising sodium aluminate and acid treatments. **Micropor. Mesopor. Mat.** 128: 91-100.
- Chen, H., Chen, J., and Wang, R. (2009). A structural study of the Fe/ZSM-5 catalyst by through-focus exit-wavefunction reconstruction in HRTEM. **Micropor. Mesopor. Mat.** 120: 472-476.
- Chumee, J., Grisdanurak, N., Neramittagapong, A., and Wittayakun, J. (2009). Characterization of platinum–iron catalysts supported on MCM-41 synthesized with rice husk silica and their performance for phenol hydroxylation. **Sci. Technol. Adv. Mater.** 10: 1-6.
- Groen, J. C., Peffer, L. A. A., Moulijn, J. A., and Pérez-Ramírez, J. (2004). On the introduction of intracrystalline mesoporosity in zeolites upon desilication in alkaline medium. **Micropor. Mesopor. Mat.** 69: 29-34.
- Groen, J. C., Peffer, L. A. A., Moulijn, J. A., and Pérez-Ramírez, J. (2005). Mechanism of hierarchical porosity development in MFI zeolites by desilication: the role of aluminium as a pore-directing agent. **Chem. Eur. J.** 11: 4983-4994.
- Kulawong, S., Prayoonpokarach, S., Neramittagapong, A., and Wittayakun, J. (2011). Mordenite modification and utilization as supports for iron catalyst in phenol hydroxylation. **J. Ind. Eng. Chem.** 17: 346-351.

- Li, Y., Liu, S., Xie, S., and Xu, L. (2009). Promoted metal utilization capacity of alkali-treated zeolite: Preparation of Zn/ZSM-5 and its application in 1-hexene aromatization. **Appl. Catal. A: Gen.** 360: 8-16.
- Lobree, L. J., Hwang, I-C., Reimer, J. A., and Bell, A. T. (1999). Investigations of the state of Fe in H-ZSM-5. **J. Catal.** 186: 242-253.
- Ogura, M., Shinomiya, S-y., Tateno, J., Nara, Y., Nomura, M., Kikuchi, E., and Matsukata, M. (2001). Alkali-treatment technique-new method for modification of structure and acid-catalytic properties of ZSM-5 zeolite. **Appl. Catal. A: Gen.** 219: 33-43.
- Preethi, M. E. L., Revathi, S., Sivakumar, T., Manikandan, D., Divakar, D., Rupa, A. V., and Palanichami, M. (2008). Phenol hydroxylation using Fe/Al-MCM-41 catalysts. **Catal. Lett.** 120: 56-64.
- Qi, G. and Yang, R. T. (2005). Ultra-active Fe/ZSM-5 catalyst for selective catalytic radiation of nitric oxide with ammonia. **Appl. Catal. B: Environ.** 60: 13-22.
- Rouquerol, F., Rouquerol, J., and Sing, K. (1999). **Adsorption by Powders and Porous Solids (vol. 1)**. (p. 204). Academic Press.
- Vernimmen, J., Meynen, V., and Cool, P. (2011). Synthesis and catalytic applications of combined zeolitic/mesoporous materials. **Beilstein J. Nanotechnol.** 2: 785-801.
- Villa, A. L., Caro, C. A., and de Correa, C. M. (2005). Cu- and Fe-ZSM-5 as catalysts for phenol hydroxylation. **J. Mol. Catal. A: Chem.** 228: 233-240.
- Woolery, G. L., Kuehl, G. H., Timken, H. C., Chester, A. W., and Vartuli, J. C. (1997). On the nature of framework Brønsted and Lewis acid sites in ZSM-5. **Zeolites.** 19: 288-296.

CHAPTER V

PREPARATION OF IRON CATALYSTS BY ION EXCHANGE FOR PHENOL HYDROXYLATION

5.1 Abstract

HZSM-5 and HZSM-5(D) were used as the supports in the preparation of Fe catalysts by liquid-state ion exchange (LS) and solid-state ion exchange (SS). All the samples were characterized by XRD, TEM, and N₂ adsorption-desorption to confirm the zeolite structure, observe morphology and determine surface area, respectively. The amount of Fe content was determined by the ICP-MS analysis. The different methods for Fe loading have influence on the location of Fe and consequently, catalytic performance for phenol hydroxylation. All catalysts except Fe_{SS}/HZSM-5 were active for phenol hydroxylation. The Fe_{SS}/HZSM-5(D) gave the phenol conversion of 35% and selectivity to CAT only. The Fe_{LS}/HZSM-5(D) provided the highest phenol conversion of 65% in the first hour; the conversion was the highest probably because Fe was dispersed on the support with the highest surface area.

5.2 Introduction

Various techniques are available for introducing metals into zeolites. The most widely used methods are impregnation and ion exchange. Impregnation leads to a rather weak metal support interaction, and thus, large metal particles are usually obtained while ion exchange results in a high initial dispersion (Kinger et al., 2000).

In Chapter III, NaZSM-5 and NaZSM-5(D) were used as supports for Fe loading by incipient wetness impregnation (IMP). In catalytic testing, the presence of mesopores was responsible for the faster reaction. In Chapter IV, HZSM-5 and HZSM-5(D) were used as supports for Fe with the same loading method. In catalytic testing, changing to proton form increased Brønsted acid sites which were probably responsible to increase in phenol adsorption sites but the product selectivity was not improved. Fe loading by IMP located Fe on various position including external surface and zeolite cavities which could be the reason for poor selectivity. To solve this problem Fe was loaded to exchange position of zeolite by ion exchange.

LS can be limited by steric constraints due to the formation of bulky hydration shells of exchangeable cations. Intermediate calcination is required to facilitate cation migration. Furthermore, the degree of exchange is limited by thermodynamic equilibrium, which makes it necessary to repeat the exchange procedure several times to reach a high exchange level (Ertl et al., 1997). In SS, zeolite and metal precursor were mixed directly. The major advantage over the LS is that the significantly higher degree of exchange can be reached in one step. (Ertl et al., 1997).

Ion exchange method is widely used for Fe loading in several reactions especially in the selective catalytic reduction (SCR) of NO_x. Guzmán-Vargas et al. (2005) studied the influence of the preparation method of Fe/ZSM-5 for the SCR of

NO_x by *n*-decane. They prepared Fe catalysts by IMP, LS and SS. The maximum conversion of NO_x was obtained on Fe/ZSM-5(SS). Long and Yang (2001) prepared Fe/ZSM-5 by LS and SS. Both the catalysts showed high activities for SCR of NO_x by ammonia. However, Fe/ZSM-5(LS) was active more than on Fe/ZSM-5(SS).

This Chapter focuses on the Fe catalysts prepared by two ion exchange method including liquid-state ion exchange (LS) and solid-state ion exchange (SS). The results were compared to catalysts prepared by IMP from Chapter IV. Although Fe catalysts prepared by LS and SS were active for the reduction of NO but there were no reports on the testing them for phenol hydroxylation. Thus, they were tested in this work.

5.3 Experimental

5.3.1 Preparation of ZSM-5 and Fe catalysts

NaZSM-5 was synthesized by rice husk silica and modified by desilication as described in Chapter III. The NaZSM-5 and NaZSM-5(D) were converted to ammonium (NH_4^+) form for LS and proton (H^+) form for SS. The method was also described in Chapter IV.

Fe was loaded on $\text{NH}_4\text{ZSM-5}$ and $\text{NH}_4\text{ZSM-5(D)}$ by LS with the method modified from literature (Centi and Vazzana., 1999). Two grams of sample were added to 100 ml of an aqueous solution of 0.5 M $\text{Fe}(\text{NO}_3)_3 \cdot 9\text{H}_2\text{O}$ (prepared from 98.5 wt.%, QR $\ddot{\text{C}}$). The slurry was refluxed at 80°C for 12 h under stirring at 500 rpm. After that the sample was filtered and washed several times with deionized water. The solid was dried at 150°C overnight and calcined at 550°C for 6 h with heating rate at 1.5°C/min. The samples, called $\text{Fe}_{\text{LS}}/\text{HZSM-5}$ and $\text{Fe}_{\text{LS}}/\text{HZSM-5(D)}$ were

characterized by XRD, TEM, ICP-MS, and N₂ adsorption-desorption. The characterization procedures were described in Chapter III.

Fe was loaded on HZSM-5 and HZSM-5(D) by SS modified from literature (Long and Yang, 2001). Two grams of HZSM-5 and HZSM-5(D) were dried at 100°C overnight. The sample was mixed with 0.12 g FeCl₃ (98%, Unilab) by grinding with pestle and mortar until homogeneous. The mixture was pressed hydraulically and sieved to 1.0 mm-425 micron, transferred to a quartz tube and heated at 550°C for 6 h in He (100 ml/min). The obtained sample was washed with deionized water to remove chlorine, filtered and dried at 120°C overnight, then calcined at 500°C for 6 h in muffle furnace. The samples were characterized by XRD, TEM, ICP-MS, and N₂ adsorption-desorption; the procedures were similar to those in Chapter III. The samples were called Fe_{SS}/HZSM-5 and Fe_{SS}/HZSM-5(D).

Catalysts including Fe_{LS}/HZSM-5, Fe_{LS}/HZSM-5(D), Fe_{SS}/HZSM-5, and Fe_{SS}/HZSM-5(D) were tested for phenol hydroxylation by a procedure described in Chapter III and IV.

5.4 Results and discussion

5.4.1 Analysis by XRD and ICP-MS

XRD patterns of the calcined Fe_{LS}/HZSM-5, Fe_{LS}/HZSM-5(D), Fe_{SS}/HZSM-5, and Fe_{SS}/HZSM-5(D) were displayed in Figure 5.1(a) and (b), respectively. All the catalysts showed characteristic of ZSM-5 with a strong peak at $2\theta = 7-9^\circ$ and $22.5-24.5$ (Kim et al., 1998). The XRD patterns of zeolites were similar in Chapter III. No other phase was observed when loading Fe species indicating that Fe species were well dispersion in the catalysts. However, the intensity of the main peak decreased after

metal addition because the Fe loaded could also scatter and absorb the X-ray. From the results were corresponding with amount of Fe of $\text{Fe}_{\text{LS}}/\text{HZSM-5(D)}$, $\text{Fe}_{\text{SS}}/\text{HZSM-5(D)}$, $\text{Fe}_{\text{LS}}/\text{HZSM-5}$, and $\text{Fe}_{\text{SS}}/\text{HZSM-5}$ were 4.9, 2.6, 2.0, and 2.3 respectively.

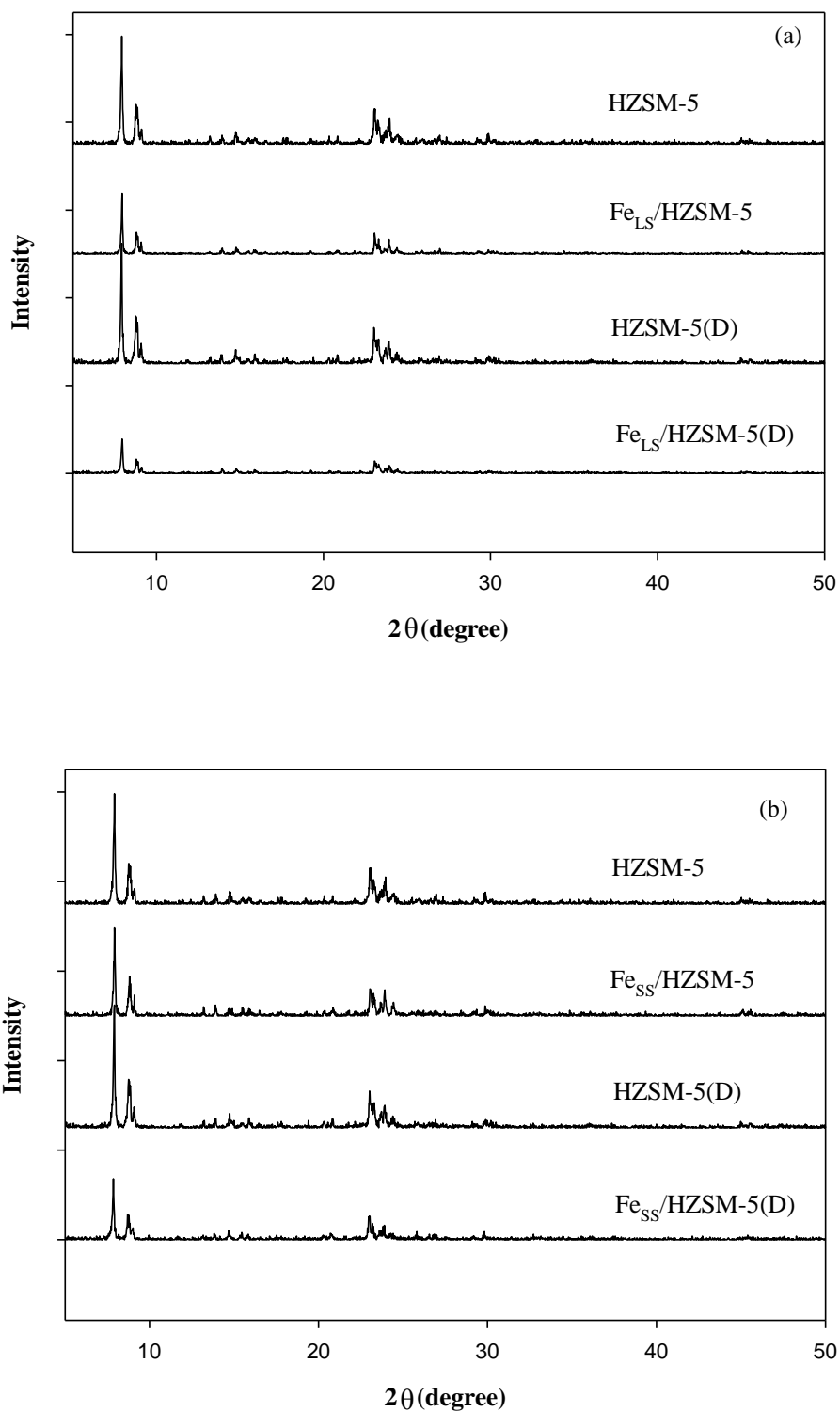


Figure 5.1 XRD patterns of (a) supports and Fe catalysts by liquid-state ion exchange (LS), (b) supports and Fe catalysts by solid-state ion exchange (SS).

5.4.2 Analysis by TEM

The TEM micrograph of Fe_{LS}/HZSM-5 is shown in Figure 5.2. The dark spots were assigned to particles of iron oxides. Similar assignment of spots to Fe₂O₃ clusters was reported by Ribera et al. (2000). Centi et al. (1999) and Long et al. (2001) prepared Fe/ZSM-5 by LS and SS using iron nitrate and iron chloride precursors. After ion exchange almost all iron was present as Fe³⁺. The TEM micrograph of Fe_{LS}/HZSM-5(D) is shown in Figure 5.3. The sample showed dark spots and white spots on the crystal particles corresponding to Fe₂O₃ clusters and mesopores. The Fe clusters were well dispersed in Fe_{LS}/HZSM-5 and Fe_{LS}/HZSM-5(D). On the other hand, the samples of Fe_{SS}/HZSM-5 and Fe_{SS}/HZSM-5(D) (Figure 5.4(a), (b) and (c), (d), respectively) had poor dispersion with agglomeration of Fe clusters. After SS, the shape of the crystals was unchanged; however, the edges become rounded and the crystals partly sintered together (Figure 5.4(d)).

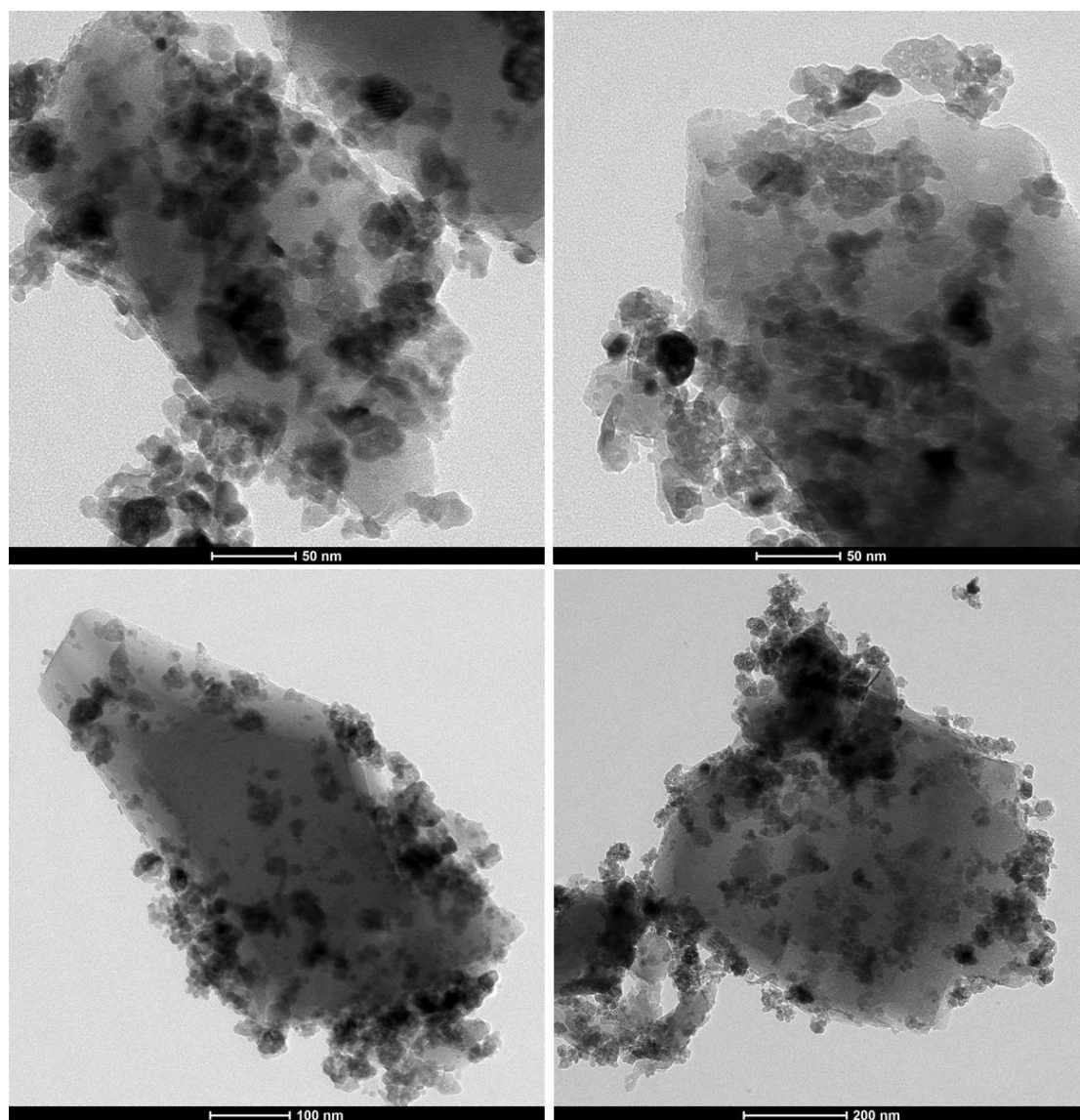


Figure 5.2 TEM micrographs of Fe_L/HZSM-5.

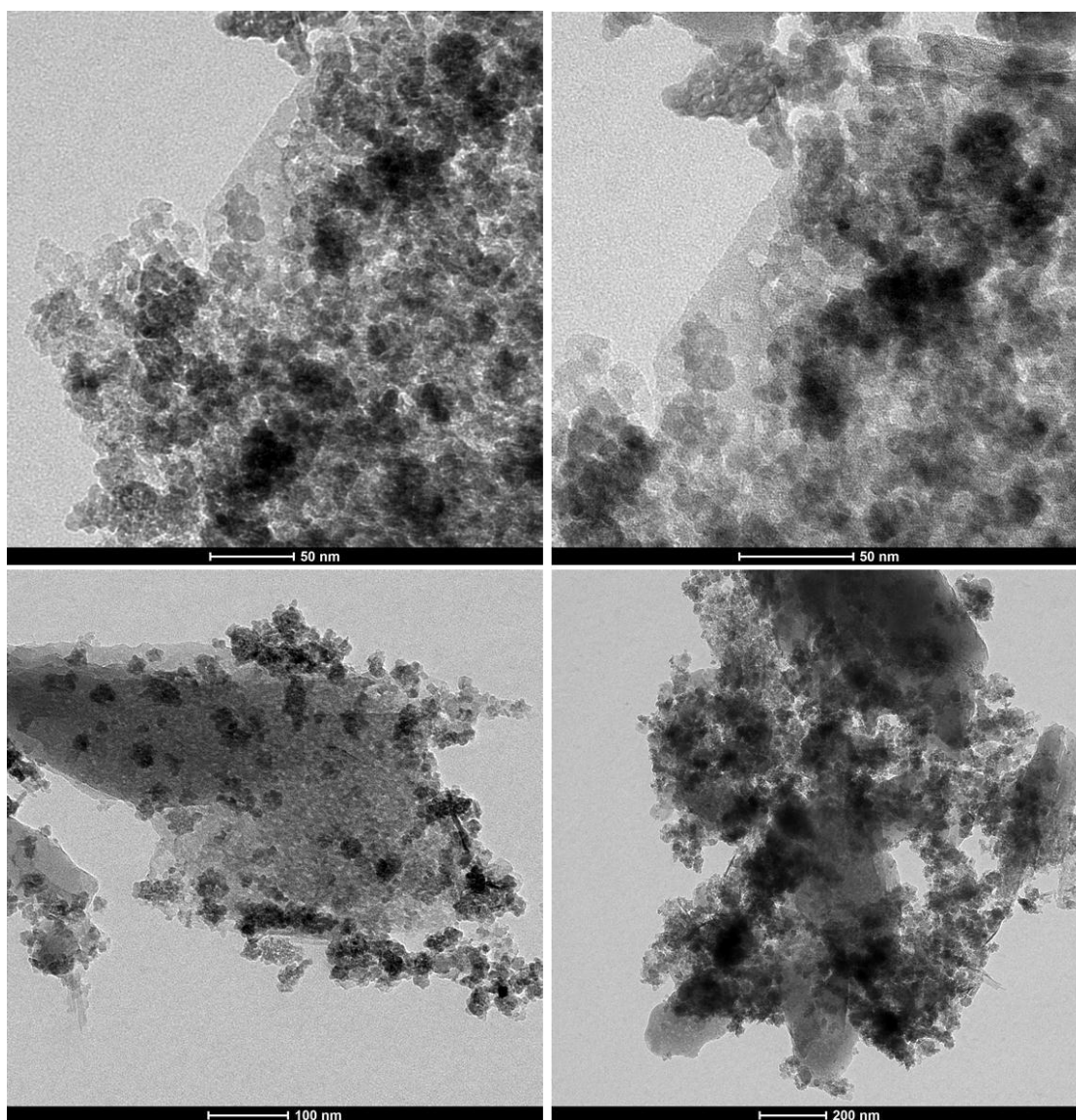


Figure 5.3 TEM micrographs of Fe_L/HZSM-5(D).

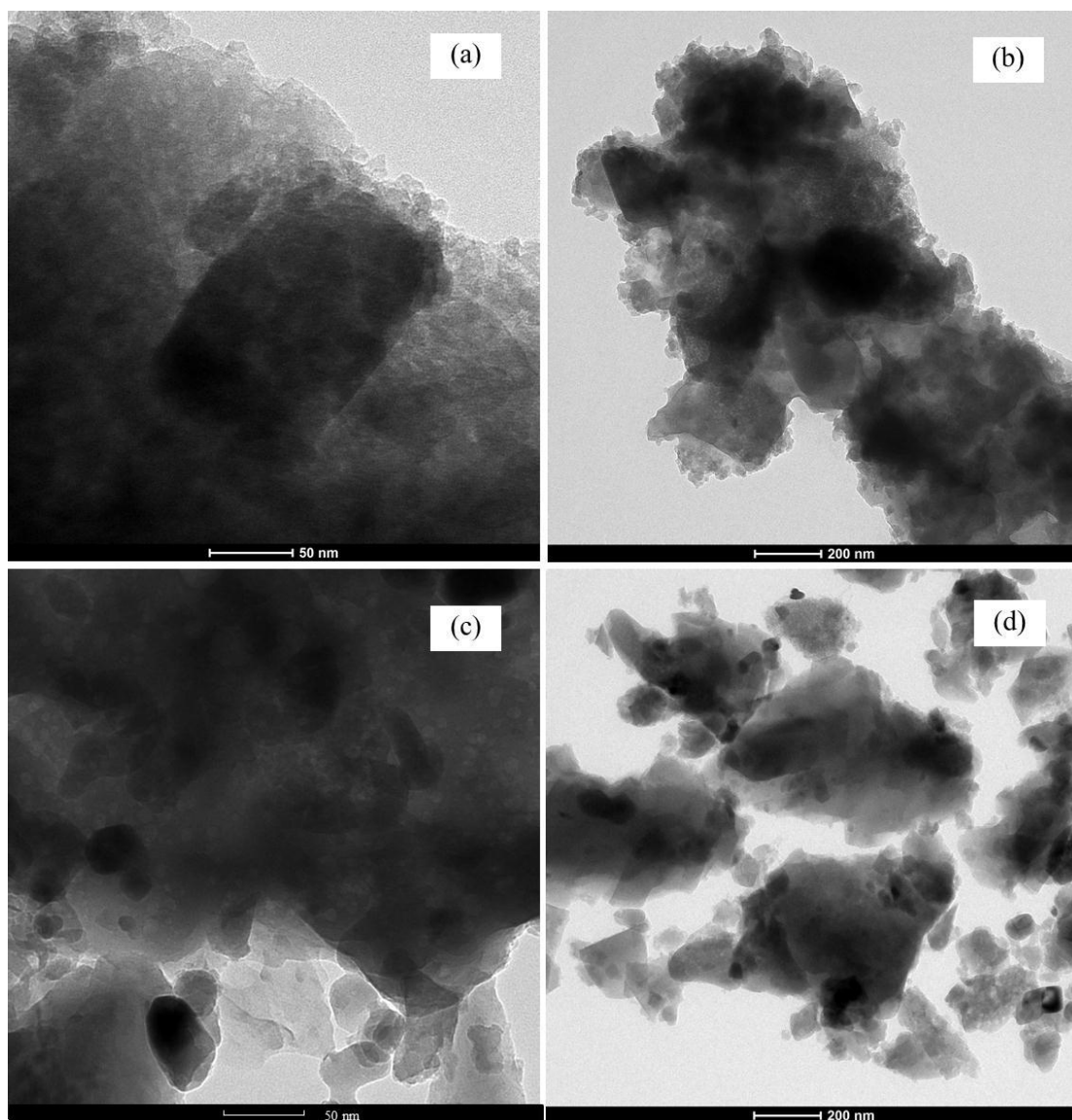


Figure 5.4 TEM micrographs (a) and (b) of $\text{Fe}_{\text{SS}}/\text{HZSM-5}$; (c) and (d) of $\text{Fe}_{\text{SS}}/\text{HZSM-5(D)}$.

5.4.3 Analysis by N_2 adsorption-desorption

The N_2 adsorption isotherms of $\text{Fe}_{\text{LS}}/\text{HZSM-5}$, $\text{Fe}_{\text{LS}}/\text{HZSM-5(D)}$, $\text{Fe}_{\text{SS}}/\text{HZSM-5}$ and $\text{Fe}_{\text{SS}}/\text{HZSM-5(D)}$ (Figure 5.5) were type IV which is typical for mesoporous materials. At the beginning, the adsorbed amount increased quickly in the microporous and concaved to the P/P_0 axis due to adsorption on external surface to form monolayer.

The N_2 adsorption increased again in the relative pressure range of 0.45-0.99. This range corresponded to N_2 adsorbed in mesoporous of HZSM-5(D) (Li et al., 2009). The adsorbed amount of $Fe_{SS}/HZSM-5(D)$ was lower than that of $Fe_{LS}/HZSM-5(D)$ indicating that their surface area decreased which the effect of sintering (result from TEM).

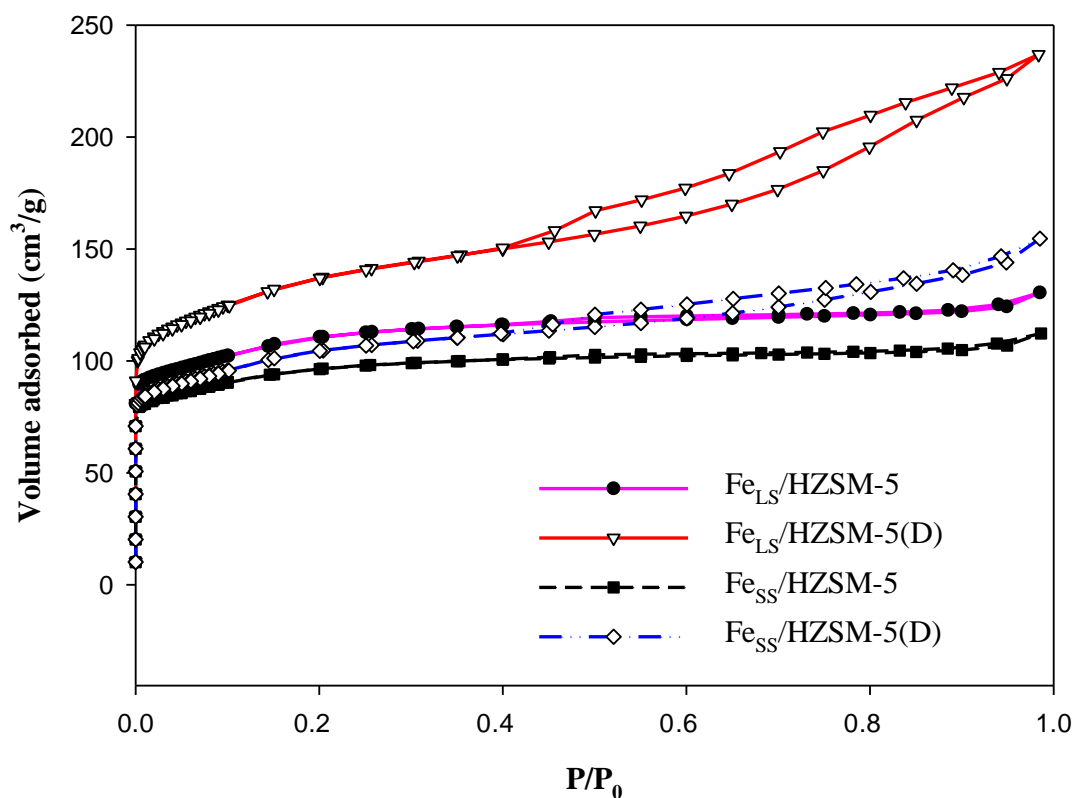


Figure 5.5 N_2 adsorption-desorption isotherms of $Fe_{LS}/HZSM-5$, $Fe_{LS}/HZSM-5(D)$, $Fe_{SS}/HZSM-5$, and $Fe_{SS}/HZSM-5(D)$.

When Fe was loaded on ZSM-5 by different methods including IMP, LS, and SS, the physical properties of all catalysts listed in Table 5.1. Surface areas were in the range of 300-450 m^2/g . The total pore volume and mesopores volume of desilicated

catalysts were increased but micropores volume did not change significantly. Comparison the results from three different methods for Fe loading, indicating that IMP and LS were better than SS because the amount of Fe species and physical properties were increased.

Table 5.1 Results from N₂ adsorption-desorption analysis.

Samples	S _{BET} ² (m ² /g)	V _{pore} ³ (cm ³ /g)	V _{micro} ³ (cm ³ /g)	V _{meso} ³ (cm ³ /g)	S _{external} ² (m ² /g)	Fe (wt.%)
Fe/HZSM-5	381±4.2	0.24	0.09	0.15	209	4.1
Fe/HZSM-5(D)	421±4.2	0.31	0.09	0.22	233	3.9
Fe _{LS} /HZSM-5	348±6.3	0.20	0.09	0.11	167	2.0
Fe _{LS} /HZSM-5(D)	441±6.8	0.37	0.10	0.27	253	4.9
Fe _{SS} /HZSM-5	303±5.6	0.17	0.09	0.08	123	2.3
Fe _{SS} /HZSM-5(D)	332±5.6	0.24	0.08	0.16	178	2.6

5.4.4 Catalytic testing for phenol hydroxylation

Figure 5.6 shows the phenol conversion on the Fe_{LS}/HZSM-5, Fe_{LS}/HZSM-5(D), Fe_{SS}/HZSM-5, and Fe_{SS}/HZSM-5(D) catalysts. Conversions on Fe_{SS}/HZSM-5 and Fe_{SS}/HZSM-5(D) were about 20 and 35%, respectively. However, the product from Fe_{SS}/HZSM-5 was not detected by GC suggesting that phenol only adsorbed on catalyst indicating that the effect of sintering which reducing the surface area and blocking access to active sites (Rothenberg., 2008). On the other hand, higher phenol adsorption on Fe_{SS}/HZSM-5(D) indicated higher number of adsorption sites to produce CAT only.

In Figure 5.6 the catalytic performance of the $\text{Fe}_{\text{LS}}/\text{HZSM-5(D)}$ was compared with that of the $\text{Fe}_{\text{LS}}/\text{HZSM-5}$, $\text{Fe}_{\text{SS}}/\text{HZSM-5}$, and $\text{Fe}_{\text{SS}}/\text{HZSM-5(D)}$ at 70°C with phenol: H_2O_2 ratio of 1:3. In the first hour, conversion of phenol increased and reached equilibrium. In addition, the phenol conversion of $\text{Fe}_{\text{LS}}/\text{HZSM-5}$ were gradually increased and reached equilibrium thus para-benzoquinone was observed. The conversion of phenol of $\text{Fe}_{\text{LS}}/\text{HZSM-5(D)}$ was highest at 65%.

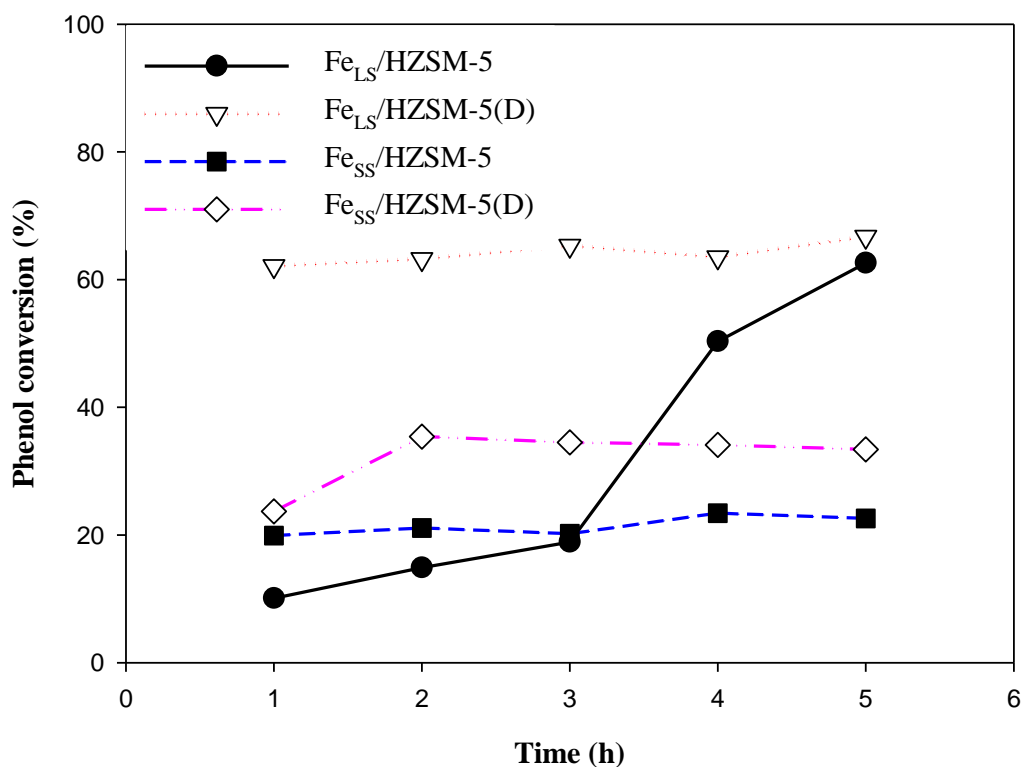


Figure 5.6 Phenol conversions of $\text{Fe}_{\text{LS}}/\text{HZSM-5}$, $\text{Fe}_{\text{LS}}/\text{HZSM-5(D)}$, $\text{Fe}_{\text{SS}}/\text{HZSM-5}$, and $\text{Fe}_{\text{SS}}/\text{HSZM-5(D)}$.

Table 5.2 shows product selectivity from phenol hydroxylation on all catalysts. The para-benzoquinone was firstly observed in the reaction except $\text{Fe}/\text{HZSM-5(D)}$. The CAT was produced more than hydroquinone and the ratio was 2:1. Products can

be produced on external and internal surface. The Fe_{SS}/HZSM-5(D) produced only catechol at the third hour onwards. The catechol was also preferably obtained over low Fe loaded ZSM-5 (Villa et al., 2005).

Table 5.2 Product selectivity of all Fe catalysts.

Catalysts	Time (h)	% Selectivity		
		CAT	HQ	PBQ
Fe _{LS} /HZSM-5	1	0.0	0.0	0.0
	2	0.0	0.0	0.0
	3	0.0	0.0	0.0
	4	4.5	1.3	94.2
	5	62.9	37.1	0.0
Fe _{LS} /HZSM-5(D)	1	60.4	39.6	0.0
	2	60.3	39.7	0.0
	3	60.4	39.6	0.0
	4	60.4	39.6	0.0
	5	60.3	39.7	0.0
Fe _{SS} /HZSM-5	1	0.0	0.0	0.0
	2	0.0	0.0	0.0
	3	0.0	0.0	0.0
	4	0.0	0.0	0.0
	5	0.0	0.0	0.0
Fe _{SS} /HZSM-5(D)	1	0.0	0.0	100.0
	2	4.4	0.0	95.6
	3	100.0	0.0	0.0
	4	100.0	0.0	0.0
	5	100.0	0.0	0.0

Comparison of the catalytic performance for phenol hydroxylation by Fe loaded on HZSM-5 by IMP, LS, and SS method, the IMP and LS produced CAT and HQ at ratio 2:1. The catalysts from both techniques had better dispersion of Fe species, leading to higher number of phenol adsorption site. On the other hand, catalysts from SS method showed poor catalytic performance. Products were not observed from $\text{Fe}_{\text{SS}}/\text{HZSM-5}$ whereas low conversion was obtained from $\text{Fe}_{\text{SS}}/\text{HZSM-5(D)}$ with selectivity to CAT only.

5.5 Conclusions

Liquid-state ion exchange was a suitable method to prepare Fe on HZSM-5 because the resulting catalysts were active high active for phenol hydroxylation. The $\text{Fe}_{\text{LS}}/\text{HZSM-5(D)}$ showed the highest conversion at 65%.

In contrast, products were not observed on $\text{Fe}_{\text{SS}}/\text{HZSM-5}$ probably because high temperature was used in the catalyst preparation and lead to inactive form. On the other hand, catalysts from SS method showed poor catalytic performance. Products were not observed from $\text{Fe}_{\text{SS}}/\text{HZSM-5}$ whereas low conversion was obtained from $\text{Fe}_{\text{SS}}/\text{HZSM-5(D)}$ with selectivity to CAT only.

5.6 References

- Centi, G. and Vazzana, F. (1999). Selectivity catalytic reduction of N_2O in industrial emissions containing O_2 , H_2O and SO_2 : behavior of Fe/ZSM-5 catalysts. **Catal. Today**. 53: 683-693.
- Ertl, G., Knözinger, H., and Weitkamp, J. (1997). **Handbook of Heterogeneous Catalysis (vol.1)**. (pp. 191-194). Germany: VCH Verlagsgesellschaft mbH.

- Guzmán-Vargas, A., Delahay, G., Coq, B., Lima, E., Bosch, P., and Jumas, J-C. (2005). Influence of the preparation method on the properties of Fe-ZSM-5 for the selective catalytic reduction of NO by *n*-decane. **Catal. Today.** 107-108: 94-99.
- Kim, w. J., Lee, M. C., and Hayhurst, D. T. (1998). Synthesis of ZSM-5 at low temperature and atmospheric pressure in a pilot-scale batch reactor. **Micropor. Mesopor. Mat.** 26: 133-141.
- Kinger, G., Lugstein, A., Swagera, R., Ebel, M., Jentys, A., and Vinek, H. (2000). Comparison of impregnation, liquid- and solid-state ion exchange procedures for the incorporation of nikel in HMFI, HMOR and HBEA. **Micropor. Mesopore. Mat.** 39: 307-317.
- Li, Y., Liu, S., Xie, S., and Xu, L. (2009). Promoted metal utilization capacity of alkali-treated zeolite: Preparation of Zn/ZSM-5 and its application in 1-hexene aromatization. **Appl. Catal. A: Gen.** 360: 8-16.
- Long, R. Q. and Yang, R. T. (2001). Fe-ZSM-5 for selective catalytic of NO with NH₃: a comparative study of different preparation techniques. **Catal. Lett.** 74: 201-205.
- Ribera, A., Arends, I. W. C. E., de Vries, S., Pérez-Ramírez, J., and Sheldon, R. A. (2000). Preparation, characterization, and performance of FeZSM-5 for the selective oxidation of benzene to phenol with N₂O. **J. Catal.** 195: 287-297.
- Rothenberg, G. (2008). **Catalysis Concepts and Green Applications.** (pp. 66-67). Germany: WILEY-VCH Verlag GmbH & Co. KGaA.
- Villa, A. L., Caro, C. A., and de Correa, C. M. (2005). Cu- and Fe-ZSM-5 as catalysts for phenol hydroxylation. **J. Mol. Catal. A: Chem.** 228: 233-240.

CHAPTER VI

CONCLUSIONS AND RECOMMENDATION

In this thesis, NaZSM-5 was synthesized by hydrothermal method with utilization of amorphous rice husk silica, and modified by desilication. After desilication, Si/Al molar ratio decreased, mesopores were generated and surface areas increased. In catalytic testing for phenol hydroxylation, both NaZSM-5 and NaZSM-5(D) only served as adsorption sites but did not convert phenol to any products. When both were used as supports for Fe, the Fe/NaZSM-5(D) shows the faster reaction to reach maximum conversion. Mesopores in ZSM-5 could improve the diffusion of the reactants. However, the selectivity was not much improved and the main products obtained were catechol (CAT) and hydroquinone (HQ).

Both NaZSM-5 and NaZSM-5(D) were converted to proton form to increase acidic strength, and the resulting HZSM-5 and HZSM-5(D) were tested for phenol hydroxylation. Similar to sodium form, they only served as adsorption site because no products were observed. The desilication and exchange to proton form of ZSM-5 increased phenol adsorption rate. When loading with Fe species, the Fe/HZSM-5(D) gave the highest phenol conversion and selectivity to CAT and HQ.

Liquid-state ion exchange was a suitable method to prepare Fe on HZSM-5 because the resulting catalysts were active high active for phenol hydroxylation. The Fe_{LS}/HZSM-5(D) showed the highest conversion at 65 %.

In contrast, products were not observed on Fe_{SS}/HZSM-5 probably because high temperature was used in the catalyst preparation and lead to inactive form. On the other hand, catalysts from SS method showed poor catalytic performance. Products were not observed from Fe_{SS}/HZSM-5 whereas low conversion was obtained from Fe_{SS}/HZSM-5(D) with selectivity to CAT only. From the results phenol conversion and product selectivity could be improved by generating mesopores, proton form and the method for Fe loading. The SS could produce only catechol with low phenol conversion.

Therefore, in future work for phenol hydroxylation reaction was suggesting that the selectivity will improve by the method for preparation catalyst because types of support did not effect for selectivity. The selectivity for CAT or HQ only might be useful application. Thus, ortho- and para-position of phenol should block before testing in phenol hydroxylation.

APPENDICES

APPENDIX A

Si/Al RATIOS AND THE AMOUNT OF Fe CATALYSTS

ANALYZED BY ICP-MS

Determination of quantitative of Si/Al ratio and the amount of Fe catalyst by external calibration curve

1. Preparation of standard:

(Range detection of ICP-MS instrument for Si, Al of 0-500 ppb and for Fe of 0-100 ppb)

1.1 Preparation of stock standard of Si, Al, Fe

- From concentration of standard of Si, Al, Fe was 1,000 ppm (1,000,000 ppb).
- Dilution of standards of 1,000x; the concentration of standard of 1,000 ppb.

1.1.1 Preparation of Fe; (1,000 ppb, 50.0 ml)

- Pipette 50.0 μ l of Fe standard into volumetric flask and adjusted volume with 2% HNO₃ solution until the final volume of 50.0 ml.

Calculation:

$$C_1 V_1 = C_2 V_2$$

$$V_1 = \left(\frac{C_2 V_2}{C_1} \right)$$

$$V_1 = \left(\frac{1,000 \text{ ppb} \times 50.0 \text{ ml}}{1,000,000 \text{ ppb}} \right)$$

$$V_1 = 0.05 \text{ ml}$$

$$V_1 = 50.0 \mu\text{l}$$

1.1.2 Preparation of Si; (1,000 ppb, 250.0 ml)

- Pipette 250.0 μl of Si standard into volumetric flask and adjusted volume with 2% HNO_3 solution until the final volume of 250.0 ml.

Calculation:

$$C_1 V_1 = C_2 V_2$$

$$V_1 = \left(\frac{C_2 V_2}{C_1} \right)$$

$$V_1 = \left(\frac{1,000 \text{ ppb} \times 250.0 \text{ ml}}{1,000,000 \text{ ppb}} \right)$$

$$V_1 = 0.25 \text{ ml}$$

$$V_1 = 250.0 \mu\text{l}$$

1.1.3 Preparation of Al; (1,000 ppb, 250.0 ml)

- Pipette 250.0 μl of Al standard into volumetric flask and adjusted volume with 2% HNO_3 solution until the final volume of 250.0 ml.

Calculation:

$$C_1 V_1 = C_2 V_2$$

$$V_1 = \left(\frac{C_2 V_2}{C_1} \right)$$

$$V_1 = \left(\frac{1,000 \text{ ppb} \times 250.0 \text{ ml}}{1,000,000 \text{ ppb}} \right)$$

$$V_1 = 0.25 \text{ ml}$$

$$V_1 = 250.0 \mu\text{l}$$

1.2 Preparation of mixed standard solution

- Mixed standard solution and adjusted the final volume with 2% HNO_3 solution follow the table.
- Calculation equation: $C_1 V_1 = C_2 V_2$

Flasks/Std.	1	2	3	4	5	Conc.
Si	0	160	320	400	480	ppb
Al	0	80	160	240	320	ppb
Fe	0	20	40	60	80	Ppb

1.3 Preparation of sample

1.3.1 Digestion of sample by microwave digestion

- All the samples were digested with acid solution as shown in the table.
- Then adjusted volume with 2% HNO₃ solution until the final volume of 50.0 ml.

Weight of sample (g)	37% HCl (Conc.)	70% HNO ₃ (Conc.)	48% HF (Conc.)	4% H ₃ BO ₃
0.05	800 µl	1.2 ml	400 µl	6.0 ml

External calibration curve of Fe

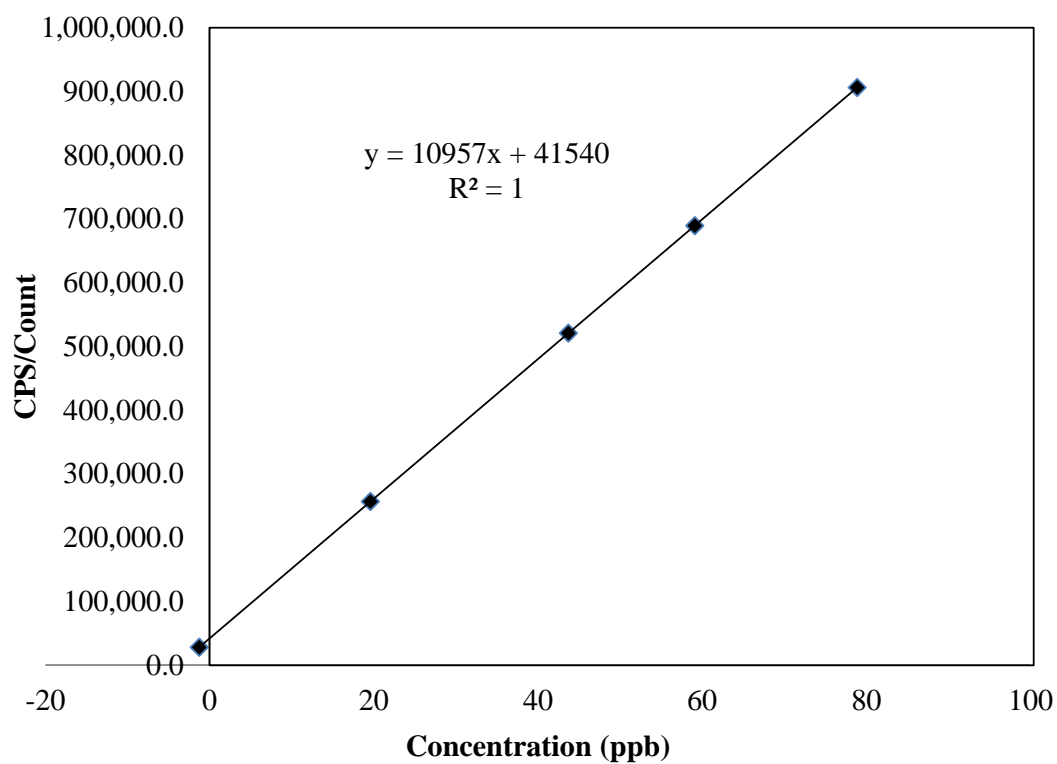


Figure A-1 External calibration curve of Fe standard measured by ICP-MS.

External calibration curve of Si

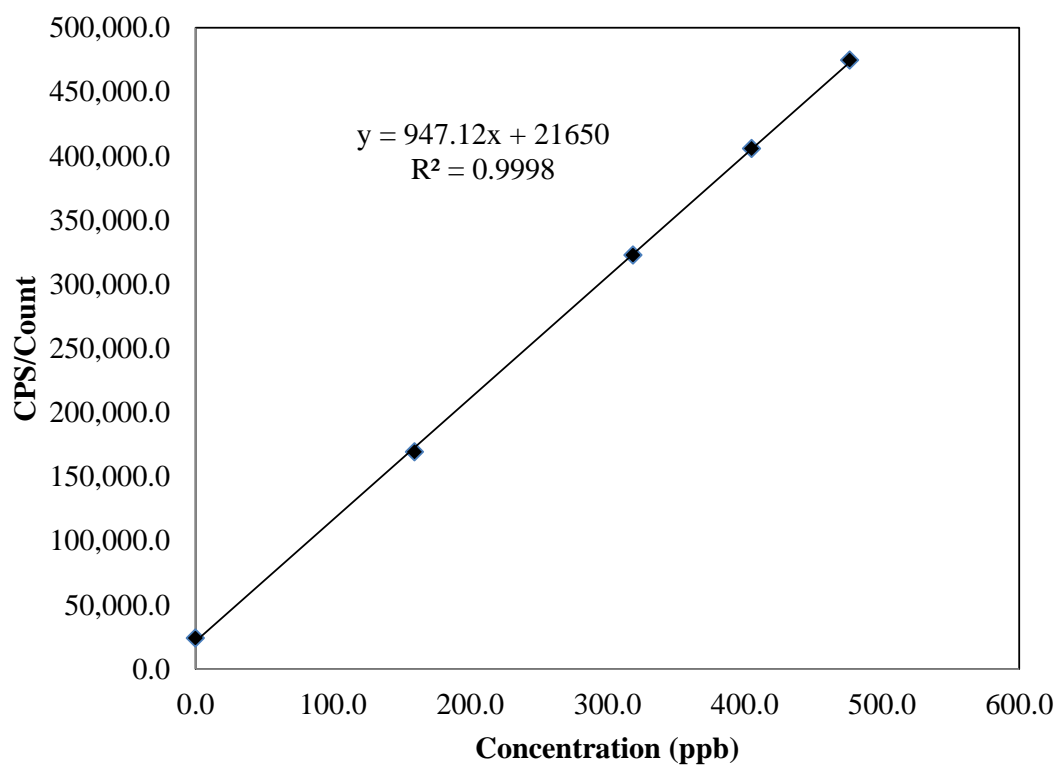


Figure A-2 External calibration curve of Si standard measured by ICP-MS.

External calibration curve of Al

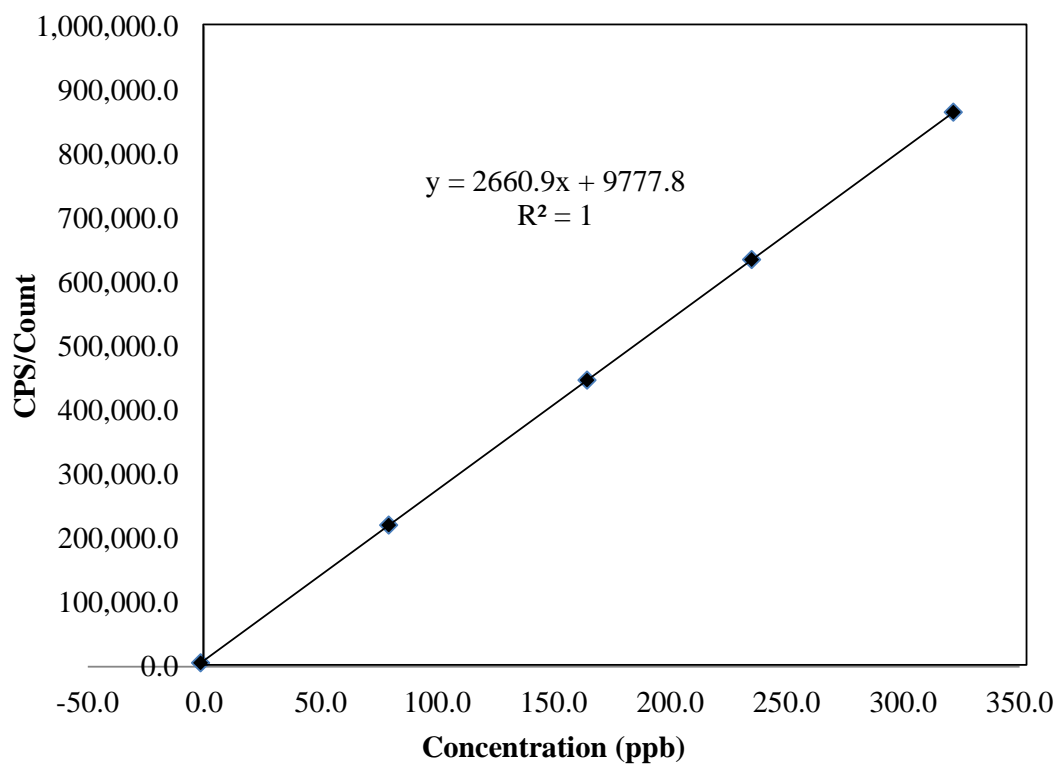


Figure A-3 External calibration curve of Al standard measured by ICP-MS.

Calculation for the amount of Fe

The mole of Fe was calculated as follows:

$$y = 10957x + 415440, R^2 = 1$$

where

y is signal intensity (CPS/Count)

x is mole of Fe

Calculation of mole of Si

The mole of Si was calculated as follows:

$$y = 947.12x + 21650, R^2 = 0.9998$$

where

y is signal intensity (CPS/Count)

x is mole of Si

Calculation of mole of Al

The mole of Al was calculated as follows:

$$y = 2660.9x + 9777.8, R^2 = 1$$

where

y is signal intensity (CPS/Count)

x is mole of Al

APPENDIX B

DETERMINATION OF PRODUCTS AND REACTANTS

FOR PHENOL HYDROXYLATION

**Determination of phenol (PhOH), catechol (CAT),
hydroquinone (HQ), and para-benzoquinone (PBQ) using for
internal standard method**

1. Preparation of standard

1.1 Preparation of internal standard (1 M Toluene, 50.0 ml):

- 5.3 ml of toluene was mixed with ethanol in volumetric flask until the final volume of 50.0 ml.

Calculation:

Toluene; MW= 92.142 g/mol, assay= 99.5%, D= 0.867 g/cm³

From

$$C = \left(\frac{10\%D}{MW} \right)$$

$$C = \left(\frac{10 \times 99.5 \times 0.867 \text{ g/cm}^3}{92.142 \text{ g/mol}} \right)$$

$$C = 9.3623 \text{ M}$$

From

$$C_1 V_1 = C_2 V_2$$

$$V_1 = \left(\frac{1 \text{ M} \times 50.0 \text{ ml}}{9.3626 \text{ M}} \right)$$

$$V_1 = 5.3406 \text{ ml}$$

1.2 Preparation of stock standard

1.2.1 Preparation of initial phenol (0.333 M)

- 0.7835 g of phenol was dissolved with deionized (DI) water under stirring until completely dissolve.
- The solution was transferred into a volumetric flask, the final volume of 25.0 ml and added 2.6 ml of DI water to solution.

Calculation:

Phenol; MW= 94.11 g/mol, assay= 99.5%, D= 1.07 g/cm³

From

$$\frac{g}{MW} = \frac{CV}{1000}$$

$$g = \left(\frac{CV}{1000} \times MW \right)$$

$$g = \left(\frac{0.333 \text{ M} \times 25.0 \text{ ml}}{1000} \times 94.11 \text{ g/mol} \right)$$

$$g = 0.7835 \text{ g}$$

1.2.2 Preparation of stock standard

Calculation:

Preparation the amount of CAT (0.5 M, 25.0 ml):

From MW= 110.11 g/mol

$$\frac{g}{MW} = \frac{CV}{1000}$$

$$g = \left(\frac{CV}{1000} \times MW \right)$$

$$g = \left(\frac{0.5 \text{ M} \times 25.0 \text{ ml}}{1000} \times 110.11 \text{ g/mol} \right)$$

$$g = 1.3764 \text{ g}$$

Another standard were calculated the same method with properties of:

0.5 M HQ, 25.0 ml, MW= 110.11 g/mol

0.5 M PhOH, 25.0 ml, MW= 94.11 g/mol

0.1 M PBQ, 25.0 ml, MW= 108.10 g/mol

The results after calculation are shown in the table.

The amount of standard weight follows in the table:

Standard	Weight (g) for 25.0 ml in ethanol solution
CAT	1.3764
HQ	1.3764
PhOH	1.1764
PBQ	0.2702

1.2.3 Dilution of stock standard: 0x, 10x, 50x, 150x, 200x

➤ Standard diluted of 0x

- Pipette of 100 μ l of toluene into volumetric flask and adjusted volume with ethanol solution until the final volume of 5.0 ml.

➤ Standard diluted of 10x

- Pipette of 500.0 μ l of stock standard solution and added 100 μ l of toluene into volumetric flask, adjusted volume with ethanol solution until the final volume of 5.0 ml.

- Standard diluted of 50x
 - Pipette of 100.0 μl of stock standard solution and added 100 μl of toluene into volumetric flask, adjusted volume with ethanol solution until the final volume of 5.0 ml.
- Standard diluted of 150x
 - Pipette of 30.0 μl of stock standard solution and added 100 μl of toluene into volumetric flask, adjusted volume with ethanol solution until the final volume of 5.0 ml.
- Standard diluted of 200x
 - Pipette of 25.0 μl of stock standard solution and added 100 μl of toluene into volumetric flask, adjusted volume with ethanol solution until the final volume of 5.0 ml.
- Dilution of all of standard by pipette 200.0 μl of standard into volumetric flask and added ethanol solution until the final volume of 1.0 ml. Then the standard was analyzed by GC with FID

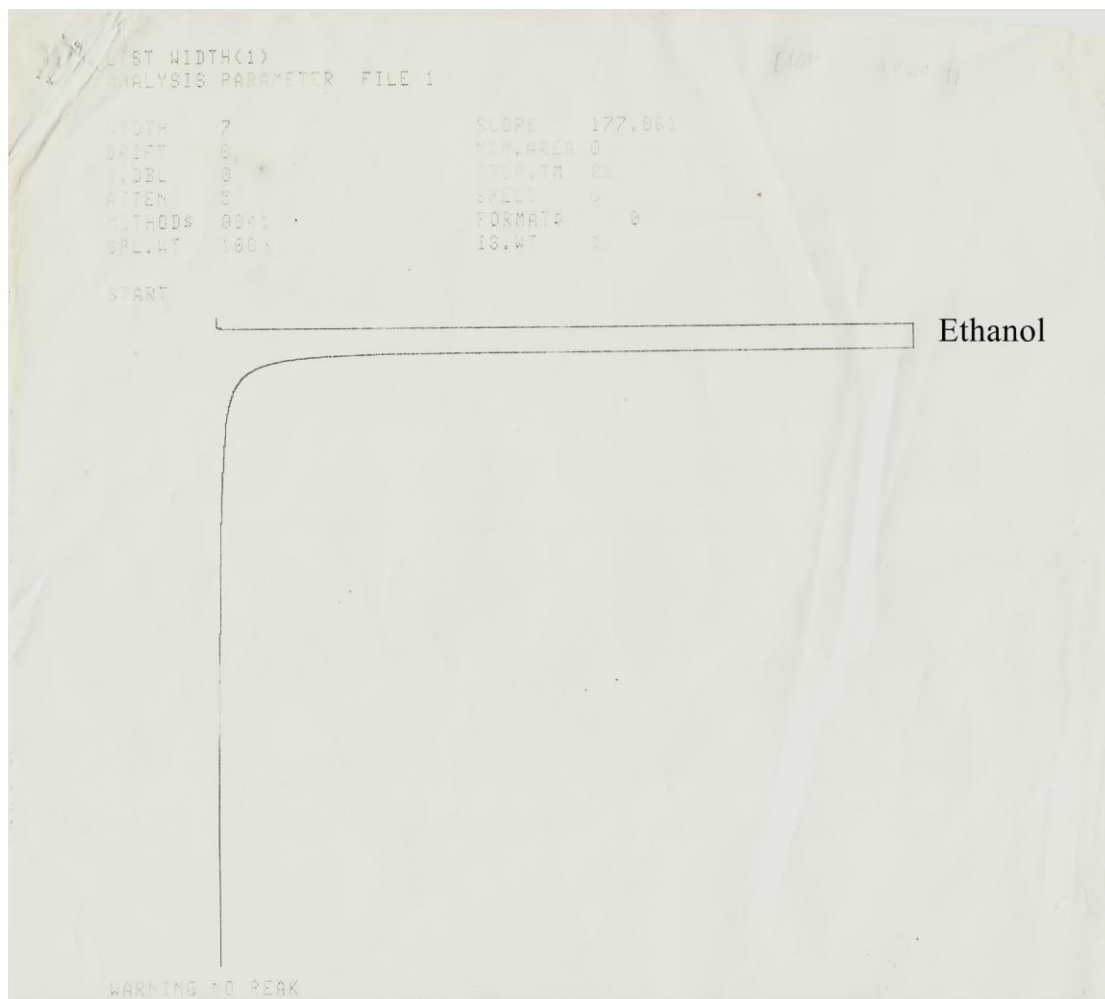
1.2.4 Preparation of sample

- Pipette of 380 μl of sample and added 100 μl of toluene into volumetric flask, adjusted volume with ethanol solution until the final volume of 5.0 ml.
- Dilution of sample by pipette 200.0 μl of sample into volumetric flask and added ethanol solution until the final volume of 1.0 ml.
- Then the sample was analyzed by GC with FID

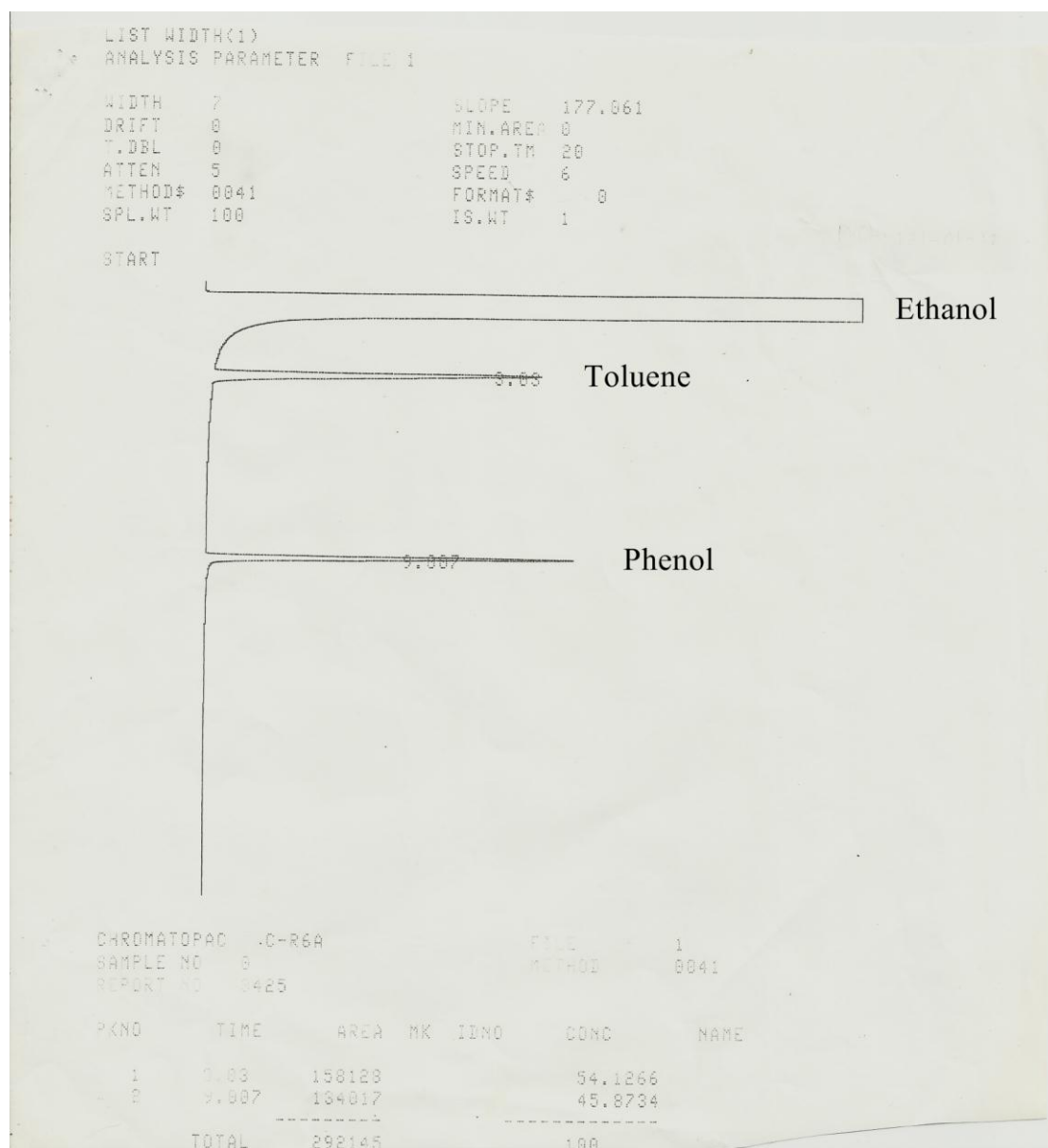
1.2.5 Preparation of initial phenol

- Pipette of 380 μ l of phenol and added 100 μ l of toluene into volumetric flask, adjusted volume with ethanol solution until the final volume of 5.0 ml.
- Dilution of phenol by pipette 200.0 μ l of phenol into volumetric flask and added ethanol solution until the final volume of 1.0 ml.
- Then the sample was analyzed by GC with FID

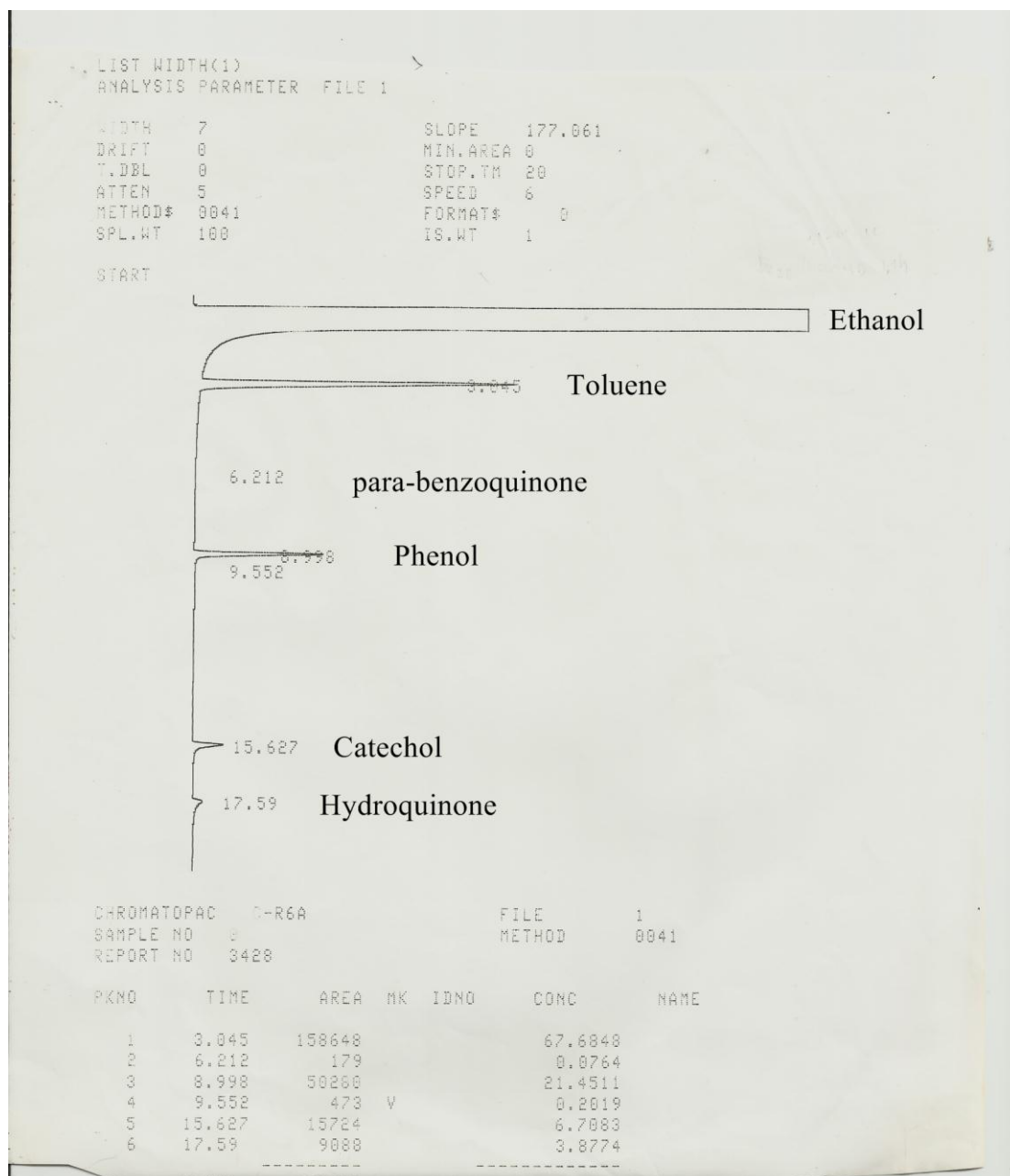
Chromatogram of ethanol



Chromatogram of initial phenol



Chromatogram of sample



Internal standard calibration curve of phenol

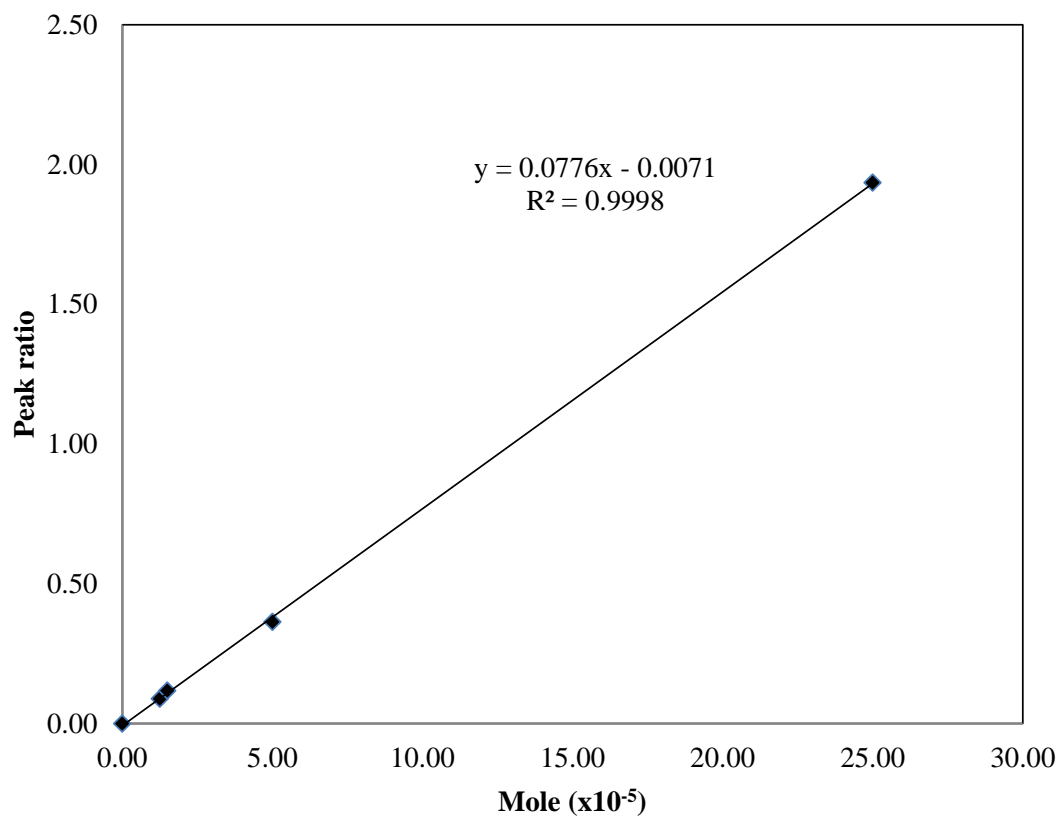


Figure B-1 Internal standard calibration curve of phenol for phenol hydroxylation.

Internal standard calibration curve of catechol

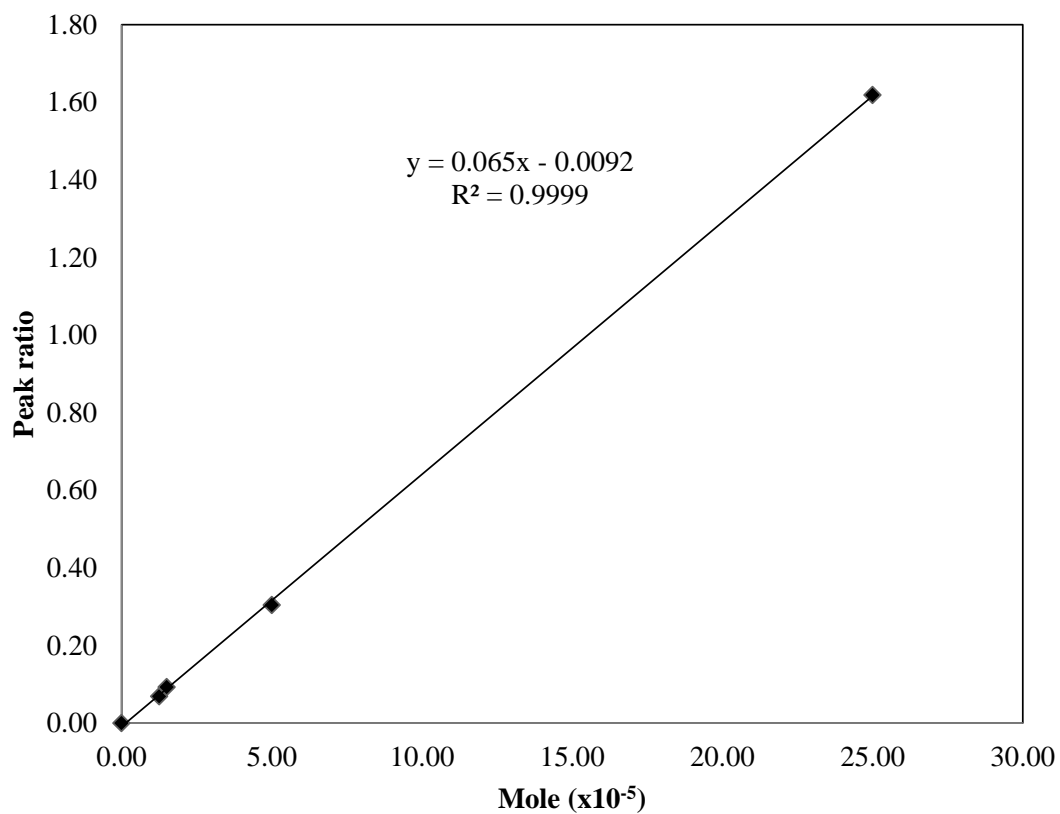


Figure B-2 Internal standard calibration curve of catechol for phenol hydroxylation.

Internal standard calibration curve of hydroquinone

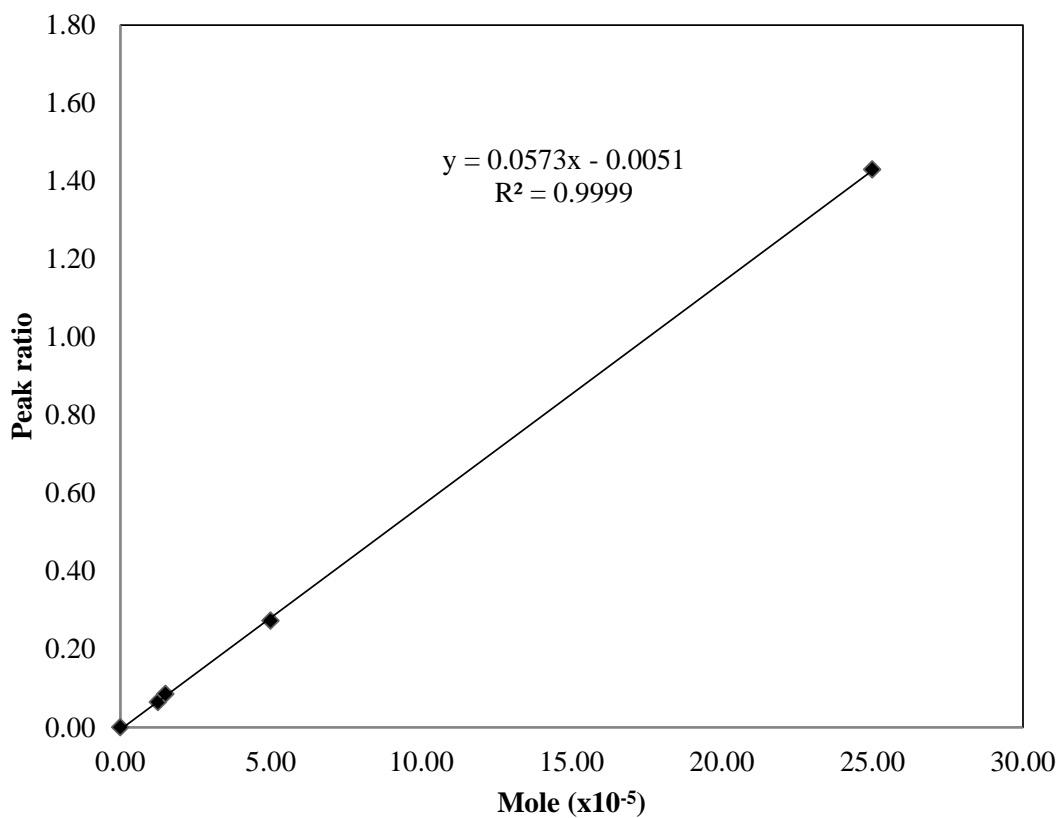


Figure B-3 Internal standard calibration curve of hydroquinone for phenol hydroxylation.

Internal standard calibration curve of para-benzoquinone

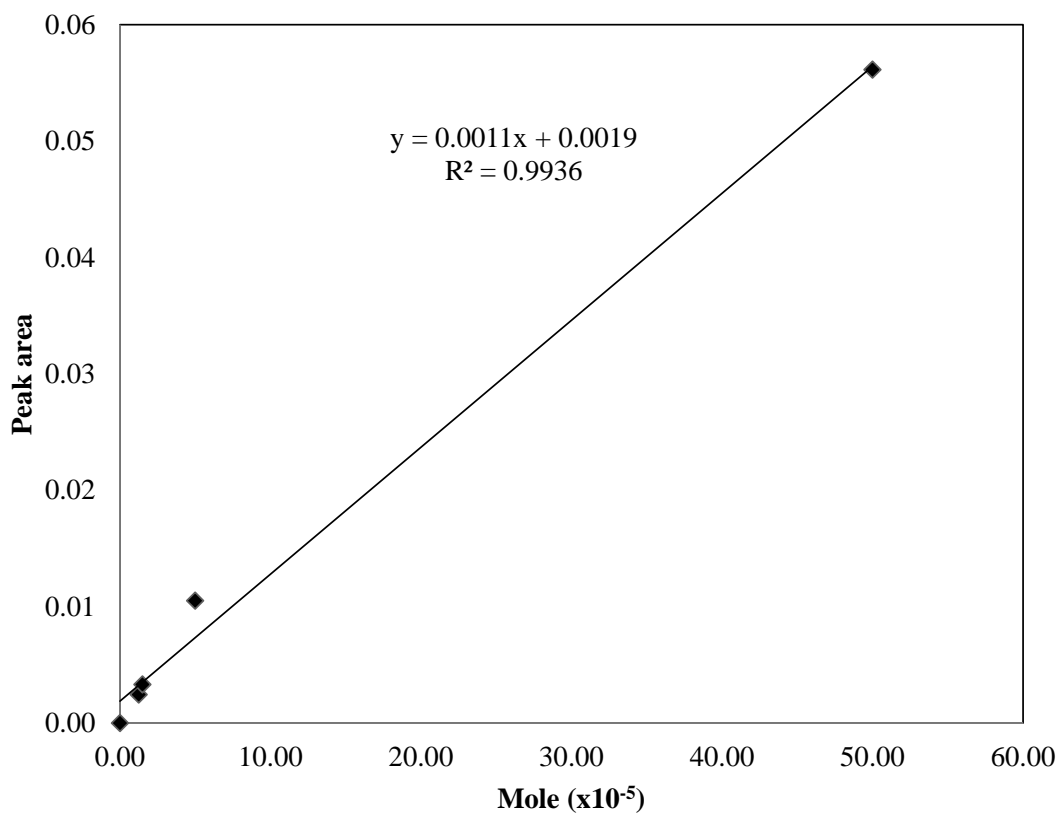


Figure B-4 Internal standard calibration curve of para-benzoquinone for phenol hydroxylation.

Calculation for phenol conversion

The conversion was calculated as follows:

$$X_{\text{Phenol}}(\%) = \left(\frac{[\text{PhOH}]_i - [\text{PhOH}]_f}{[\text{PhOH}]_i} \right) \times 100$$

where

X_{Phenol} is the conversion of phenol

$[\text{PhOH}]_i$ is the mole of phenol before reaction

$[\text{PhOH}]_f$ is the mole of phenol after sampling

PhOH_i was calculated as follows;

$$y = 0.0776x - 0.0071, R^2 = 0.9998$$

y = peak ratio of phenol to toluene before reaction

x = mole of phenol before reaction

PhOH_f was calculated as follows;

$$y = 0.0776x - 0.0071, R^2 = 0.9998$$

y = peak ratio of phenol to toluene after sampling

x = mole of phenol after sampling

Calculation of product selectivity

The selectivity was calculated as follows:

$$\% \text{ Selectivity for CAT} = \left(\frac{[\text{Mole CAT}]_f}{[\text{Mole CAT}]_f + [\text{Mole HQ}]_f + [\text{Mole PBQ}]_f} \right) \times 100$$

$$\% \text{ Selectivity for HQ} = \left(\frac{[\text{Mole HQ}]_f}{[\text{Mole CAT}]_f + [\text{Mole HQ}]_f + [\text{Mole PBQ}]_f} \right) \times 100$$

$$\% \text{ Selectivity for PBQ} = \left(\frac{[\text{Mole PBQ}]_f}{[\text{Mole CAT}]_f + [\text{Mole HQ}]_f + [\text{Mole PBQ}]_f} \right) \times 100$$

where

$[\text{Mole CAT}]_f$ is mole concentration of catechol after the reaction.

$[\text{Mole HQ}]_f$ is mole concentration of hydroquinone after the reaction.

$[\text{Mole PBQ}]_f$ is mole concentration of para-benzoquinone after the reaction.

APPENDIX C

DATA FROM N₂ ADSORPTION-DESORPTION

Table C-1 N₂ adsorption-desorption of NaZSM-5.

Relative pressure (P/P ₀)	Volume adsorbed (cm ³ /g STP)	Relative pressure (P/P ₀)	Volume adsorbed (cm ³ /g STP)
0.000017091	10.1198	0.7954	118.1359
0.000017360	20.2426	0.8455	118.6062
0.000014919	30.3647	0.8948	119.1761
0.000012013	40.4876	0.9464	120.8128
0.000009869	50.6086	0.9870	130.4808
0.000008902	60.7306	0.9472	121.8572
0.000010899	70.8530	0.8817	119.7956
0.000046333	80.9686	0.8284	119.3427
0.001581626	90.7414	0.7780	119.1543
0.002947725	92.1652	0.7280	119.0607
0.005266802	93.4728	0.6774	119.0187
0.007078987	94.5944	0.6284	118.9760
0.010600000	95.4433	0.5971	118.9352
0.015600000	96.2991	0.5480	118.8491
0.019300000	96.8233	0.4988	118.4508
0.024500000	97.4669	0.4531	115.8970
0.029700000	98.0039	0.3989	114.5616
0.034800000	98.4984	0.3319	113.6007
0.040100000	98.9718	0.2815	112.7020
0.045100000	99.4161	0.2493	111.9360
0.049800000	99.7860	0.1997	110.3836
0.054800000	100.1790	0.1518	107.8435
0.060600000	100.6233	0.1013	103.6585
0.065300000	100.9854	0.0895	102.7437
0.070300000	101.3539	0.0801	102.0536
0.075200000	101.7146	0.0699	101.3023
0.080200000	102.0721	0.0601	100.5796
0.084900000	102.4047	0.0496	99.7679
0.090600000	102.8014	0.0400	98.9784
0.095500000	103.1472	0.0303	98.0950
0.099800000	103.4428	0.0206	97.0481
0.149400000	106.9965	0.0103	95.5128
0.204000000	110.2541		
0.257200000	112.0883		
0.307900000	113.2446		
0.353000000	114.0003		
0.398300000	114.5969		
0.448300000	115.1240		
0.496300000	115.5726		
0.546700000	115.9951		
0.595800000	116.4096		
0.646200000	116.8196		
0.695600000	117.2277		
0.745900000	117.6479		

Table C-2 N₂ adsorption-desorption of Fe/NaZSM-5.

Relative pressure (P/P ₀)	Volume adsorbed (cm ³ /g STP)	Relative pressure (P/P ₀)	Volume adsorbed (cm ³ /g STP)
0.000015678	10.1062	0.8440	118.3822
0.000015032	20.2186	0.8929	120.1065
0.000012649	30.3342	0.9445	124.0607
0.000010451	40.4521	0.9819	129.8344
0.000009134	50.5716	0.9363	124.9524
0.000008788	60.6923	0.8835	121.3989
0.000012808	70.8141	0.8309	119.5656
0.000082079	80.9223	0.7792	118.7568
0.003871924	90.1441	0.7284	118.2590
0.005210701	90.8417	0.6784	117.8863
0.006897281	91.4778	0.6473	117.6656
0.008969970	92.0866	0.5968	117.3226
0.009825466	92.2789	0.5476	116.9120
0.014400000	93.1260	0.4990	115.9951
0.020200000	93.8995	0.4510	113.1452
0.024900000	94.4130	0.3978	111.6369
0.030100000	94.9015	0.3322	110.5853
0.035000000	95.3125	0.2815	109.5740
0.040200000	95.7127	0.2494	108.7402
0.045000000	96.0710	0.2006	107.0135
0.050200000	96.4316	0.1512	104.1162
0.055100000	96.7639	0.1010	99.6330
0.060100000	97.0937	0.0896	98.8544
0.065300000	97.4253	0.0805	98.2777
0.069500000	97.6872	0.0703	97.6303
0.075100000	98.0337	0.0596	96.9374
0.079900000	98.3249	0.0502	96.3123
0.085300000	98.6596	0.0403	95.6312
0.090400000	98.9660	0.0304	94.8401
0.095500000	99.2680	0.0206	93.8876
0.100200000	99.5410	0.0103	92.4284
0.143700000	102.2789		
0.198600000	106.2738		
0.256500000	108.6555		
0.308200000	109.9714		
0.346300000	110.6980		
0.397100000	111.4464		
0.446900000	112.0537		
0.496600000	112.6042		
0.545800000	113.1844		
0.595400000	113.8641		
0.645300000	114.6168		
0.694700000	115.4171		
0.744900000	116.2845		
0.794300000	117.2471		

Table C-3 N₂ adsorption-desorption of NaZSM-5(D).

Relative pressure (P/P ₀)	Volume adsorbed (cm ³ /g STP)	Relative pressure (P/P ₀)	Volume adsorbed (cm ³ /g STP)
0.000018056	10.1207	0.9000	168.9957
0.000021511	20.2434	0.9495	176.6571
0.000020367	30.3667	0.9865	189.5031
0.000017904	40.4897	0.9512	179.3497
0.000015572	50.6134	0.8919	173.3830
0.000014165	60.7381	0.8413	167.7266
0.000015895	70.8639	0.7982	162.3693
0.000042953	80.9870	0.7473	156.1839
0.000859689	90.8904	0.6987	150.4440
0.011000000	98.7302	0.6485	144.9238
0.015400000	99.6135	0.5982	140.2258
0.021100000	100.4927	0.5480	136.4764
0.024900000	101.0000	0.4989	133.5117
0.030000000	101.6416	0.4443	125.7344
0.035200000	102.1912	0.3974	123.3052
0.040000000	102.6623	0.3342	121.3861
0.045100000	103.1334	0.2837	119.7400
0.050100000	103.5655	0.2497	118.4183
0.055400000	104.0078	0.2003	115.9883
0.060100000	104.3871	0.1519	112.2595
0.065300000	104.7869	0.0996	107.5488
0.070200000	105.1522	0.0888	106.7853
0.075400000	105.5325	0.0806	106.1997
0.080300000	105.8856	0.0701	105.4449
0.085300000	106.2421	0.0603	104.6881
0.090300000	106.5901	0.0502	103.8803
0.095500000	106.9449	0.0405	103.0045
0.100300000	107.2789	0.0303	101.9728
0.143700000	110.1348	0.0205	100.7587
0.198100000	114.7033	0.0105	99.0436
0.256800000	118.0725		
0.309800000	120.1118		
0.346800000	121.2990		
0.397800000	122.7548		
0.447700000	124.1424		
0.497400000	125.6475		
0.547300000	127.4510		
0.596400000	129.7581		
0.646700000	132.6953		
0.695600000	136.5813		
0.745900000	142.0318		
0.795700000	149.4243		
0.847100000	159.0377		

Table C-4 N₂ adsorption-desorption of Fe/NaZSM-5(D).

Relative pressure (P/P ₀)	Volume adsorbed (cm ³ /g STP)	Relative pressure (P/P ₀)	Volume adsorbed (cm ³ /g STP)
0.000011535	10.0953	0.8983	154.2209
0.000013673	20.1908	0.9482	164.0148
0.000013153	30.3041	0.9875	183.7499
0.000010743	40.4157	0.9386	165.5620
0.000009846	50.5301	0.8920	159.0023
0.000010704	60.6467	0.8423	152.4552
0.000021901	70.7640	0.7976	146.7187
0.000324228	80.8016	0.7466	140.7572
0.007492824	89.0104	0.6974	135.5939
0.009275068	89.5581	0.6474	131.0317
0.010900000	89.9692	0.5968	127.2763
0.015100000	90.8169	0.5480	124.4668
0.020100000	91.5946	0.4988	122.0611
0.025000000	92.2245	0.4441	115.2849
0.030100000	92.7895	0.3969	112.7012
0.035100000	93.2906	0.3340	110.7648
0.040000000	93.7439	0.2833	109.1917
0.045100000	94.1696	0.2492	107.9343
0.050100000	94.5751	0.2001	105.6491
0.055300000	94.9735	0.1518	102.1122
0.060200000	95.3263	0.0994	97.9367
0.065300000	95.6863	0.0894	97.2937
0.070200000	96.0274	0.0805	96.7139
0.075300000	96.3650	0.0701	96.0201
0.080400000	96.6939	0.0601	95.3161
0.085400000	97.0352	0.0502	94.5784
0.090400000	97.3498	0.0397	93.7025
0.095400000	97.6593	0.0303	92.7966
0.100300000	97.9605	0.0209	91.6754
0.144100000	100.5788	0.0098	89.6969
0.197700000	104.6823		
0.255600000	107.8272		
0.308200000	109.7374		
0.355900000	111.1607		
0.397500000	112.3117		
0.447400000	113.7023		
0.497100000	115.2331		
0.546900000	117.0121		
0.596800000	119.1516		
0.646600000	121.7851		
0.696300000	125.1572		
0.745900000	129.6463		
0.795500000	135.8503		
0.846100000	144.2870		

Table C-5 N₂ adsorption-desorption of HZSM-5.

Relative pressure (P/P ₀)	Volume adsorbed (cm ³ /g STP)	Relative pressure (P/P ₀)	Volume adsorbed (cm ³ /g STP)
0.000015703	10.1201	0.8953	139.0809
0.000017157	20.2430	0.9470	141.1973
0.000015465	30.3659	0.9872	151.7830
0.000013117	40.4885	0.9493	142.5566
0.000011272	50.6109	0.8839	139.9147
0.000010171	60.7328	0.8296	139.1138
0.000011448	70.8551	0.7791	138.6210
0.000024193	80.9703	0.7471	138.3660
0.000187251	91.0438	0.6972	137.9989
0.005851255	99.8446	0.6473	137.6430
0.007196539	100.3463	0.5977	137.2515
0.009192853	100.9129	0.5480	136.7871
0.009790759	101.0731	0.4992	135.8526
0.014900000	102.0340	0.4546	131.9870
0.019800000	102.7381	0.3986	129.9188
0.024900000	103.3670	0.3331	128.3500
0.030000000	103.9341	0.2832	126.9912
0.035000000	104.4628	0.2499	125.7828
0.040100000	104.9954	0.2006	123.4566
0.045000000	105.4979	0.1523	119.6603
0.050000000	106.0093	0.0995	111.6474
0.055100000	106.5326	0.0889	110.1914
0.060000000	107.0374	0.0801	109.1573
0.065000000	107.5595	0.0705	108.1009
0.069900000	108.0979	0.0602	107.0160
0.075000000	108.6397	0.0503	105.9937
0.080000000	109.1602	0.0403	104.9818
0.085000000	109.7093	0.0299	103.9390
0.089900000	110.2628	0.0206	102.8830
0.094900000	110.8237	0.0104	101.3737
0.099900000	111.3924		
0.144700000	117.5375		
0.204000000	123.3024		
0.260700000	126.0774		
0.315000000	127.8250		
0.346700000	128.6437		
0.397500000	129.7453		
0.447400000	130.6838		
0.497200000	131.5472		
0.547000000	132.3896		
0.596800000	133.2355		
0.646500000	134.1281		
0.696400000	135.0764		
0.746200000	136.0507		
0.796000000	137.0278		
0.845800000	137.9946		

Table C-6 N₂ adsorption-desorption of Fe/HZSM-5.

Relative pressure (P/P ₀)	Volume adsorbed (cm ³ /g STP)	Relative pressure (P/P ₀)	Volume adsorbed (cm ³ /g STP)
0.000013885	10.1211	0.8944	134.0148
0.000016593	20.2446	0.9463	139.8393
0.000015994	30.3686	0.9871	153.6737
0.000015614	40.4602	0.9534	142.7694
0.000013645	50.5831	0.8932	136.4102
0.000013250	60.7069	0.8352	133.0165
0.000016876	70.8307	0.7805	131.7365
0.000051259	80.9389	0.7292	131.0495
0.001181854	90.7935	0.6792	130.5258
0.002885695	92.9625	0.6473	130.2137
0.005138113	94.3381	0.5975	129.7440
0.006789228	95.0093	0.5479	129.2283
0.008910661	95.6235	0.4989	128.2971
0.009727116	95.8163	0.4533	124.8527
0.015200000	96.7829	0.3982	122.9276
0.020000000	97.4280	0.3330	121.3468
0.024900000	97.9912	0.3010	120.4823
0.030200000	98.5290	0.2493	118.7304
0.035100000	99.0046	0.2007	116.4053
0.040100000	99.4742	0.1519	112.5378
0.045100000	99.9379	0.1048	106.0492
0.050100000	100.3931	0.0891	104.1379
0.055300000	100.8674	0.0803	103.2227
0.060200000	101.3272	0.0704	102.2589
0.065100000	101.7855	0.0602	101.2967
0.070100000	102.2521	0.0501	100.4008
0.075200000	102.7417	0.0404	99.5185
0.080100000	103.2139	0.0303	98.5728
0.085200000	103.7122	0.0205	97.5627
0.090100000	104.1996	0.0102	96.0900
0.095200000	104.7201		
0.100100000	105.2154		
0.145700000	110.6692		
0.203100000	116.1391		
0.259800000	118.9717		
0.313600000	120.7494		
0.346800000	121.6294		
0.397600000	122.7456		
0.447500000	123.6887		
0.497300000	124.5498		
0.547200000	125.3815		
0.597000000	126.2233		
0.646800000	127.1030		
0.696600000	128.0587		
0.746500000	129.0896		
0.796200000	130.2424		
0.845800000	131.6541		

Table C-7 N₂ adsorption-desorption of HZSM-5(D).

Relative pressure (P/P ₀)	Volume adsorbed (cm ³ /g STP)	Relative pressure (P/P ₀)	Volume adsorbed (cm ³ /g STP)
0.000014323	10.1170	0.8464	176.6803
0.000014707	20.2352	0.8973	185.4089
0.000012650	30.3459	0.9473	193.3784
0.000010857	40.4577	0.9837	202.4706
0.000009321	50.5719	0.9430	195.1247
0.000009012	60.6879	0.8894	189.3966
0.000010233	70.8056	0.8393	184.0567
0.000020793	80.9230	0.7973	179.3196
0.000110833	91.0226	0.7472	173.2581
0.001667785	100.7670	0.6949	167.7576
0.002922640	102.6758	0.6463	163.6765
0.004795959	104.4254	0.5988	160.0347
0.007263182	105.8684	0.5471	156.6051
0.009421123	106.8618	0.4979	153.5770
0.010900000	107.4077	0.4448	144.3424
0.015000000	108.6055	0.3986	141.0444
0.020000000	109.6993	0.3353	138.3229
0.025000000	110.6330	0.2841	136.2480
0.030100000	111.4865	0.2493	134.6746
0.035200000	112.2753	0.1998	131.9842
0.040100000	112.9856	0.1516	128.1796
0.045100000	113.6424	0.0994	120.1094
0.050000000	114.2875	0.0909	118.9591
0.054500000	114.9319	0.0804	117.7024
0.060000000	115.6985	0.0711	116.5831
0.065100000	116.3395	0.0610	115.3393
0.069800000	116.9292	0.0507	114.0635
0.075200000	117.5592	0.0401	112.6813
0.079500000	118.1277	0.0303	111.2826
0.085600000	118.7852	0.0205	109.5318
0.089800000	119.3321	0.0101	106.9779
0.094800000	119.8405		
0.100300000	120.4966		
0.145400000	126.4799		
0.204500000	132.4486		
0.260400000	135.6393		
0.313400000	137.9913		
0.346500000	139.3131		
0.397300000	141.2236		
0.446800000	143.1054		
0.497000000	145.1027		
0.546100000	147.2815		
0.596200000	149.8630		
0.646100000	152.9580		
0.695500000	156.7679		
0.745500000	161.7758		
0.795100000	168.3859		

Table C-8 N₂ adsorption-desorption of Fe/HZSM-5(D).

Relative pressure (P/P ₀)	Volume adsorbed (cm ³ /g STP)	Relative pressure (P/P ₀)	Volume adsorbed (cm ³ /g STP)
0.000013424	10.0735	0.8952	181.1347
0.000015620	20.1518	0.9468	190.1319
0.000010724	30.2708	0.9840	200.4610
0.000008266	40.3892	0.9435	191.9931
0.000007151	50.5096	0.8903	185.8047
0.000007217	60.6319	0.8411	179.4036
0.000010272	70.7552	0.7949	174.0140
0.000031264	80.8770	0.7483	168.5730
0.000273895	90.9425	0.6951	163.4359
0.004273573	100.0269	0.6474	159.6679
0.004862345	100.4594	0.5980	156.2667
0.006954311	101.7355	0.5479	153.2186
0.008931848	102.6281	0.4988	150.2830
0.009735515	102.9413	0.4438	141.3339
0.014500000	104.3906	0.3988	137.6280
0.020200000	105.6622	0.3528	135.3072
0.024400000	106.4357	0.3021	133.0535
0.030100000	107.3454	0.2506	130.4840
0.035000000	108.0626	0.2003	127.4029
0.040100000	108.7633	0.1513	123.1192
0.045200000	109.4278	0.1046	116.1008
0.049600000	109.9782	0.0910	114.2887
0.054500000	110.5809	0.0806	113.0341
0.059400000	111.1643	0.0712	111.8980
0.065100000	111.8287	0.0613	110.7110
0.070100000	112.4082	0.0515	109.5165
0.075200000	113.0019	0.0409	108.1747
0.079700000	113.5155	0.0314	106.8300
0.084700000	114.0859	0.0206	104.9737
0.089500000	114.6549	0.0104	102.1719
0.095200000	115.2734		
0.099900000	115.7965		
0.146300000	121.4428		
0.202100000	127.6071		
0.258400000	131.2514		
0.312300000	133.9756		
0.347100000	135.5475		
0.397200000	137.6957		
0.447000000	139.8464		
0.496300000	142.0619		
0.546700000	144.5313		
0.596000000	147.2381		
0.645800000	150.3825		
0.694900000	154.0805		
0.744700000	158.7405		
0.794700000	164.7630		
0.844900000	172.3357		

Table C-9 N₂ adsorption-desorption of Fe_{LS}/HZSM-5.

Relative pressure (P/P ₀)	Volume adsorbed (cm ³ /g STP)	Relative pressure (P/P ₀)	Volume adsorbed (cm ³ /g STP)
0.000022978	10.1138	0.800278643	120.5340
0.000020131	20.2378	0.850196594	121.1418
0.000016558	30.3621	0.899878242	122.0948
0.000013649	40.4870	0.948922553	124.2572
0.000011595	50.6115	0.985053785	130.5073
0.000011237	60.7355	0.939923885	125.1887
0.000018366	70.8579	0.885181084	122.6507
0.000125989	80.9402	0.832553335	121.7447
0.003990753	89.5818	0.781841857	121.2376
0.004996251	90.0511	0.731484606	120.8679
0.007057222	90.7860	0.700591714	120.6512
0.009148201	91.3692	0.650234402	120.3601
0.010002732	91.5765	0.600506822	120.0484
0.015102315	92.5468	0.550405702	119.6948
0.020019690	93.2900	0.500421595	119.2813
0.024893450	93.9394	0.452347157	117.6278
0.030223403	94.5926	0.398823736	116.1703
0.035122234	95.1693	0.350392503	115.1934
0.039976469	95.7266	0.301072595	114.1185
0.044834338	96.2785	0.250764454	112.6995
0.050291303	96.8862	0.200764372	110.6894
0.055221220	97.4410	0.151347416	107.4661
0.060140595	97.9841	0.101174968	102.1426
0.065002740	98.5356	0.090064293	100.8984
0.070255487	99.1137	0.080118703	99.7961
0.075293515	99.6671	0.070303760	98.6990
0.080250371	100.2114	0.060173613	97.5686
0.085268247	100.7516	0.050241142	96.4445
0.090358889	101.2942	0.040884991	95.3740
0.095318653	101.8133	0.029839332	94.0456
0.100212944	102.3254	0.020361700	92.7977
0.144571526	106.5026	0.009559029	90.9112
0.203847040	110.6827		
0.257272512	112.8919		
0.308455576	114.3156		
0.349604577	115.2049		
0.400131679	116.0661		
0.450155134	116.7830		
0.500239773	117.4148		
0.550273228	117.9836		
0.600285423	118.5144		
0.650268481	119.0200		
0.700281513	119.5162		
0.750289032	120.0086		

Table C-10 N₂ adsorption-desorption of Fe_{LS}/HZSM-5(D).

Relative pressure (P/P ₀)	Volume adsorbed (cm ³ /g STP)	Relative pressure (P/P ₀)	Volume adsorbed (cm ³ /g STP)
0.000020122	10.1261	0.8507	207.4549
0.000017198	20.2616	0.9021	217.7690
0.000013897	30.3977	0.9490	226.1490
0.000011232	40.5320	0.9836	236.9077
0.000009412	50.6669	0.9405	228.9314
0.000009028	60.8006	0.8891	221.9951
0.000013101	70.9343	0.8387	215.3858
0.000041280	81.0578	0.8005	209.7781
0.000301023	91.0521	0.7486	202.3045
0.002387337	100.1376	0.7021	193.4989
0.002941316	101.0830	0.6466	183.6521
0.005040652	103.6657	0.5988	177.1903
0.006922001	105.1805	0.5512	171.9679
0.008734789	106.3502	0.5010	167.1459
0.010022223	107.0505	0.4565	158.2391
0.014898720	109.0753	0.3998	150.4764
0.020070654	110.7026	0.3507	146.9718
0.024966886	111.9793	0.3037	144.0841
0.030069505	113.1524	0.2511	140.6894
0.035186542	114.2181	0.2008	136.9405
0.040139102	115.1854	0.1510	132.0966
0.045148423	116.1189	0.1022	124.7078
0.050198611	117.0176	0.0901	122.7753
0.054981367	117.8442	0.0802	121.2119
0.060165478	118.7190	0.0703	119.6075
0.065197948	119.5480	0.0602	117.9240
0.070200000	120.3643	0.0502	116.2012
0.075200000	121.1610	0.0402	114.3697
0.080200000	121.9434	0.0299	112.2450
0.085200000	122.6844	0.0205	109.8911
0.090200000	123.4989	0.0100	106.1237
0.095200000	124.2583		
0.100200000	125.0101		
0.143800000	130.9944		
0.203700000	137.3548		
0.257100000	141.3236		
0.308400000	144.5876		
0.354300000	147.3457		
0.399900000	150.0674		
0.449900000	153.1532		
0.499800000	156.4969		
0.549800000	160.2750		
0.599600000	164.6821		
0.649600000	170.0152		
0.699400000	176.6106		
0.749200000	185.0196		
0.799400000	195.6018		

Table C-11 N₂ adsorption-desorption of Fe_{SS}/HZSM-5.

Relative pressure (P/P ₀)	Volume adsorbed (cm ³ /g STP)	Relative pressure (P/P ₀)	Volume adsorbed (cm ³ /g STP)
0.000023727	10.1168	0.800413931	103.5265
0.000017906	20.2446	0.850342221	104.0362
0.000013009	30.3715	0.900189710	104.8641
0.000009255	40.4977	0.949242331	106.7953
0.000007583	50.6230	0.986285709	112.2745
0.000010287	60.7475	0.938200624	107.7347
0.000069942	70.8510	0.884698866	105.4758
0.003767087	79.4089	0.832551607	104.5796
0.004977787	79.9215	0.781856578	104.0933
0.007227126	80.6284	0.731532913	103.7858
0.009007677	81.0669	0.681470567	103.5238
0.010141637	81.3105	0.650490307	103.3640
0.014874850	82.1242	0.600367929	103.1612
0.019777750	82.8015	0.550612692	102.9253
0.024762482	83.3966	0.500515240	102.6429
0.029772931	83.9507	0.451498143	101.6657
0.034807015	84.4807	0.399796554	100.6307
0.040262744	85.0369	0.350073032	99.8743
0.045241639	85.5353	0.300862884	99.0306
0.050327522	86.0074	0.250650835	97.9222
0.055183536	86.4970	0.200608543	96.3645
0.060282502	86.9918	0.150861823	93.9989
0.065389323	87.4735	0.100235137	90.2194
0.070322446	87.9139	0.090321125	89.3305
0.075309932	88.3987	0.080232597	88.4382
0.080303277	88.8571	0.070340465	87.5141
0.085299642	89.3033	0.060227204	86.5467
0.090440845	89.7493	0.050192325	85.5701
0.095464796	90.1831	0.040271466	84.5712
0.100536096	90.6072	0.030759424	83.5569
0.146257297	93.8548	0.018183055	82.0386
0.203699582	96.5883	0.010232588	80.7670
0.255582708	98.1487		
0.305041260	99.2036		
0.352816119	99.9529		
0.400133984	100.5483		
0.450353431	101.0554		
0.500336151	101.4871		
0.550362065	101.8616		
0.600289449	102.2121		
0.650457326	102.5304		
0.700325317	102.8436		
0.750453089	103.1694		

Table C-12 N₂ adsorption-desorption of Fe_{SS}/HZSM-5(D).

Relative pressure (P/P ₀)	Volume adsorbed (cm ³ /g STP)	Relative pressure (P/P ₀)	Volume adsorbed (cm ³ /g STP)
0.000017330	10.1209	0.8508	134.4774
0.000012557	20.2514	0.9005	138.3508
0.000008428	30.3809	0.9485	143.9397
0.000005772	40.5092	0.9850	154.6015
0.000004915	50.6371	0.9429	146.7163
0.000010419	60.7634	0.8905	140.4475
0.000076333	70.8657	0.8365	136.8752
0.001987116	80.1618	0.7851	134.2219
0.002890025	81.1492	0.7517	132.5544
0.004934015	82.6123	0.7006	130.1488
0.006934242	83.5480	0.6509	127.7428
0.008889685	84.2496	0.6006	125.2710
0.010000000	84.6002	0.5505	122.8674
0.015100000	85.7958	0.5004	120.6696
0.020100000	86.6746	0.4542	116.2439
0.025000000	87.4074	0.3979	112.2027
0.030100000	88.0840	0.3505	110.3492
0.035200000	88.7042	0.3024	108.7282
0.040200000	89.2752	0.2512	106.7964
0.045200000	89.8374	0.2008	104.4621
0.050300000	90.3912	0.1510	101.1988
0.055200000	90.9174	0.1015	95.6940
0.060300000	91.4649	0.0901	94.2745
0.065200000	91.9962	0.0802	93.1354
0.070400000	92.5440	0.0703	92.0455
0.075200000	93.0588	0.0603	90.9470
0.080300000	93.6006	0.0503	89.8560
0.085300000	94.1511	0.0403	88.7406
0.090300000	94.6918	0.0302	87.5197
0.095300000	95.2337	0.0204	86.1156
0.100300000	95.7794	0.0105	84.1482
0.144600000	100.4163		
0.204400000	104.6852		
0.257100000	107.1169		
0.307200000	108.9598		
0.350000000	110.3699		
0.400400000	111.9210		
0.450300000	113.4752		
0.500300000	115.1266		
0.550400000	116.9230		
0.600300000	118.9641		
0.650400000	121.3244		
0.700400000	124.0722		
0.750500000	127.2780		
0.800800000	130.8139		

APPENDIX D

THESIS OUTPUT

1. Pimsuta, M., Neramittagapong, A., Prayoonpokarach, S., and Wittayakun, J.,
Desilication of NaZSM-5 and utilization as support of Fe for phenol hydroxylation,
International Journal of Chemical Engineering and Applications, 3 (2012) 86-91.

CURRICULUM VITAE

Name Miss Mustika Pimsuta
Birth date 31 March 1986
Address 183 Moo 1, Tambon Khaopun, Amphoe Kudkhaopun,
Ubonratchathani, 34270, Thailand
Email oob_mus@hotmail.com

Education

2005-2008 B. Sc. (Chemistry), Ubon Ratchathani University, Thailand with scholarship from Thai government, "Science Achievement Scholarship of Thailand, SAST"
2009-2012 M. Sc. (Chemistry), Suranaree University of Technology, Thailand with scholarship from Thai government, "Science Achievement Scholarship of Thailand, SAST"

Publication

M. Pimsuta, A. Neramittagapong, S. Prayoonpokarach, and J. Wittayakun, Desilication of NaZSM-5 and utilization as support of Fe for phenol hydroxylation, International Journal of Chemical Engineering and Applications, 3 (2012) 86-91.